Superconductivity in narrow-band systems with local nonretarded attractive interactions

R. Micnas

Institute of Physics, A. Mickiewicz University, 60-769 Poznań, Poland

J. Ranninger

Centre National de la Recherche Scientifique, Centre de Recherches sur les Très Basses Températures, Boîte Postale 166X, 38042 Grenoble-CEDEX, France

S. Robaszkiewicz

Institute of Physics, A. Mickiewicz University, 60-780 Poznań, Poland

In narrow-band systems electrons can interact with each other via a short-range nonretarded attractive potential. The origin of such an effective local attraction can be polaronic or it can be due to a coupling between electrons and excitons or plasmons. It can also result from purely chemical (electronic) mechanisms, especially in compounds with elements favoring disproportionation of valent states. These mechanisms are discussed and an exhaustive list of materials in which such local electron pairing occurs is given. The authors review the thermodynamic and electromagnetic properties of such systems in several limiting scenarios: (i) Systems with on-site pairing which can be described by the extended negative-U Hubbard model. The strong-attraction limit of this model, at which it reduces to a system of tightly bound electron pairs (bipolarons) on a lattice, is extensively discussed. These electron pairs behaving as hard-core charged bosons can exhibit a superconducting state analogous to that of superfluid ^{4}He II. The change-over from weak-attraction BCS-like superconductivity to the superfluidity of charged hard-core bosons is examined. (ii) Systems with intersite pairing described by an extended Hubbard model with $U>0$ and nearest-neighbor attraction and/or nearest-neighbor spin exchange as well as correlated hopping. (iii) A mixture of local pairs and itinerant electrons interacting via a charge-exchange mechanism giving rise to a mutually induced superconductivity in both subsystems. The authors discuss to what extent the picture of local pairing, and in particular superfluidity of hard-core charged bosons on a lattice, can be an explanation for the superconducting and normal-state properties of the high-T_c oxides: doped $BaBiO_3$ and the cuprates.

CONTENTS

I. INTRODUCTION

Since the discovery of high-T_c superconductivity in La-Ba-Cu-O compounds by Bednorz and Müller (1986), a great variety of different pairing mechanisms has been proposed. Many of these proposals contain the concept of pairing in real space.

In this paper we shall review the thermodynamic and electrodynamic properties of superconductivity in narrow-band systems due to local, short-range attractive interaction. This subject is sometimes referred to as local pair superconductivity or pairing in real space or "bipolaronic superconductivity."

A. Mechanisms for local electron pairing

We shall start with a discussion of the possible physical mechanisms that under certain conditions, can lead to the formation of local electron pairs in solids, solutions, and chemical complexes. The microscopic mechanisms leading to an effective short-range attraction of electrons (holes) can be of various origins.

(i) The most obvious is strong electron-lattice coupling which gives rise to the formation of small polarons (electrons surrounded by their local deformation). Two polarons attract each other via the induced lattice deformation, and they can form small bipolarons provided that attraction overcomes the Coulomb repulsion. In particular, such an effective attraction can be realized in the case of coupling between narrow-band electrons and local phonon modes, like high-frequency intramolecular vibrations or cation-ligand vibrations. The derivation of such a local attractive interaction, initially developed by Anderson (1975,1979) for amorphous materials, was subsequently examined by many authors (Alexandrov and Ranninger, 1981a; Cohen *et al.*, 1984a, 1984b; Fradkin and Hirsch, 1983; Klinger, 1985; Nasu, 1985, 1987; Alexandrov *et al.*, 1986b; Micnas, Ranninger, and Robaszkiewicz, 1987a; Robaszkiewicz, Micnas, and Ranninger, 1987 and references therein; see also Sec. V.B.3).

(ii) Short-range attraction in a definite electronic subsystem can result from coupling between electrons and quasibosonic excitations of *electronic origin* such as excitons or plasmons (Ginzburg, 1964, 1976; Little, 1964, 1981; Beni *et al.*, 1974; Hirsch and Scalapino, 1985a). The approaches developed for the problem of strong electron-phonon coupling can be extended to this case; however, the energy scale for the characteristic frequencies will be much larger, and the coupling constants will be different.

(iii) Yet another possibility is a purely electronic mechanism resulting from coupling between electrons and other electronic subsystems in solid or chemical complexes (this coupling cannot in general be reduced to electron-quasiboson coupling). Several electronic mechanisms leading to nonretarded, static attraction due to the strong polarizability of anions have been considered by the Russian school (Ionova *et al.*, 1977; Ionov *et al.*, 1981, 1985; Moizhes and Drabkin, 1983). Some of these proposed mechanisms can also be referred to as chemical mechanisms (Khomskii and Zvezdin, 1988; Wilson, 1987, 1988; Micnas, Ranninger, and Robaszkiewicz, 1988b; Ranninger *et al.*, 1988, 1989). It has been shown (Hirsch and Scalapino, 1985b) that under specific conditions concerning the electronic levels on the cations and the surrounding ligand anions, as well as the various Hubbard repulsion terms, the Coulomb repulsion acting in a particular electronic subsystem can be overscreened. This would give rise to an effective attraction of the electrons in this subsystem. Other possible mechanisms for local attraction of "chemical or electronic" origin are discussed in Secs. V.B.3 and V.C.

(iv) Finally, the existence of "internal coordinates," such as dangling bonds or abnormal bond configurations, has also been proposed as a factor favoring local pairing in certain classes of systems referred to as nonsimple metals (Ting *et al.*, 1980).

These mechanisms giving rise to an attraction between charged carriers have to compete with the Coulomb repulsion. If the induced attractive potential partially overcomes the Coulomb repulsion (at some distance) and the attraction is strong enough, local pair formation can take place. Two carriers will form a real bound state either on a given site (on-site local pairs or Anderson bipolarons; Anderson, 1975, 1979; Robaszkiewicz *et al.*, 1981a, 1981b, 1981c, 1981d, 1982) or an adjacent site (intersite local pairs or Heitler-London bipolarons; Chakraverty, 1979; Alexandrov and Ranninger, 1981a, 1981b; Chao *et al.*, 1983; Chakraverty and Ranninger, 1985). The local pairs can be of singlet type with paired electron spins or of triplet type with parallel electron spins (Kulik, 1984; Alexandrov, Ranninger, and Robaszkiewicz, 1986a).

The concept of local electron pairing is interesting from various points of view and covers several areas of solid-state physics. It can be of importance for the following.

(i) Superconductivity, i.e., the search for high-T_c materials and for an explanation of "non-BCS" (Bardeen-Cooper-Schrieffer) properties of certain superconducting materials (Alexandrov and Ranninger, 1981b; Ionov *et al.*, 1981; Moizhes and Drabkin, 1983; Kulik, 1984; Alexandrov, Ranninger, and Robaszkiewicz, 1986a, 1986b; Micnas, Ranninger, and Robaszkiewicz, 1987a, 1988b; Robaszkiewicz *et al.*, 1987 and references therein).

(ii) Charge-density wave (CDW) formation in narrow-band systems (Ionov *et al.*, 1975, 1981; Robaszkiewicz, 1979, 1984; Rice and Sneddon, 1981; Micnas *et al.*, 1984). The static attractive interaction may favor electronic charge ordering, as indeed has been found in several inorganic compounds (Ionov *et al.*, 1975; Keller, 1981).

(iii) Amorphous semiconductors like chalcogenide glasses, with so-called $U<0$ centers (Anderson, 1975, 1979; Watkins, 1984; Klinger, 1985).

(iv) Conducting polymers (Scott *et al.*, 1983; Chung *et al.*, 1984; Brazovskii *et al.*, 1985).

(v) Heavy-fermion systems (Miyake *et al.*, 1984; Ohkawa, 1984; Ohkawa and Fukuyama, 1984; Ranninger *et al.*, 1987; Bastide and Lacroix, 1988a, 1988b).

B. Materials with local electron pairing

In a great number of experimental systems, real-space pairing plays a dominant role. These systems comprise several distinct groups of materials:

The *alternating-valence* group is made up of compounds that contain ions in two valence states differing by $2e$ (on-site pairs) and can exhibit charge ordering (Ionov *et al.*, 1975, 1981, 1985; Miller and Epstein, 1976; Robaszkiewicz, 1979, 1984; Day, 1980; Keller, 1981). Examples of such systems are (a) diamagnetic compounds of Sb^{4+} like M_2SbX_6 (M=Cs, Rb; X=Cl, Br), which exhibit alternate ordering of s-electron pairs s^2-s^0 (Sb^{3+}, Sb^{5+}), e.g., Cs_2SbCl_6; (b) TlF_2 with s^2-s^0 (Tl^{1+}, Tl^{3+}); (c) divalent compounds of Ag^{2+}, Au^{2+}, and trivalent compounds of Pd^{3+} and Pt^{3+}; for example, $CsAgCl_3$ ($d_{z^2}^2 - d_{z^2}^0$).

These systems can exhibit phase transitions with increasing temperature or pressure from a charge-ordered to a nonordered state, like Cs_2SbCl_6 (T_{CO}=70–75 K) or $BaBiO_3$ (Bi^{3+}-Bi^{5+}) with $T_{CO} \simeq 760$ K.

For a detailed discussion of the experiments supporting electron-density disproportionation in the above materials, as well as in many others, we refer the reader to the review articles of Ionov *et al.* (1975, 1981, 1985); Robin and Day (1967); Miller and Epstein (1976); and Day, (1980) and to the references cited therein. The evidence for alternating valence states in these materials comes from several supplementary types of measurements, both direct ones like ESR, NMR, Mössbauer and optical spectroscopy, and indirect ones such as x-ray absorption, magnetic measurements, etc. For example, the presence of alternating valence states in Cs_2SbCl_6 (Sb^{3+}, Sb^{5+}), suggested, among other indicators, by the absence of Sb^{4+} in solutions, was first supported by x-ray diffraction, electronic reflectance studies (Robin and Day, 1967), and magnetic and ESR measurements showing diamagnetism (Atkinson and Day, 1969). Later on it was confirmed by more direct microscopic probes, i.e., on the basis of x-ray electron spectra (Tricker *et al.*, 1972) and the study of the Mössbauer effect on Sb^{121} nuclei (Alexandrov *et al.*, 1971; Ionov *et al.*, 1975). By the latter method the existence of a smooth transition from the charge-ordered state with periodically alternating valences to the disordered state has also been established. The transition begins at about 70 K, and more than 30% of the Sb ions are in the Sb^{4+} oxidation state at 130 K. The disordered state is characterized by a two-electron exchange between $(SbCl_6)^-$ and $(SbCl_6)^{-3}$ complexes, while the compound remains diamagnetic (Ionov *et al.*, 1975).

The second group of materials are *transition-metal oxides* showing intersite bipolarons, sometimes called *Grenoble bipolarons* (Lakkis *et al.*, 1977; Schirmer and Salje, 1980; Onoda and Nagasawa, 1983; Salje and Güttler, 1984; Schlenker, 1985). The most famous of these are Ti_4O_7 and $Ti_{4-x}V_xO_7$, showing bound pairs of electrons on neighboring sites (Ti^{4+}-Ti^{4+}), (Ti^{3+}-Ti^{3+}) [see Fig. 1(a)-(c)], as well as $Na_xV_2O_5$ with (V^{4+}-V^{4+})-(V^{5+}-V^{5+}).

A great deal of insight into Ti_4O_7 and its vanadium alloys has been obtained from detailed structural studies, optical transmission, EPR, specific heat, and magnetic susceptibility measurements, as well as from transport data. These studies show very clearly that bond formation between neighboring Ti^{3+} (d^1-d^1) ions occurs along the chain concomitant with shortened Ti-Ti distances in the low-temperature phase, and that these intersite electron pairs remain unbroken and active in the intermediate phase until they break up at around 150 K. Around 150 K the material shows a semiconductor-to-metal transition. Thus there is a sequence of phase transitions in Ti_4O_7 and its vanadium alloys, first from the commensurate CDW ordering of two-electron pairs to a phase of nonordered pairs and finally to a metallic phase (Fig. 1; Lakkis *et al.*, 1976; Schlenker *et al.*, 1979; Schlenker and Marezio, 1980; Schlenker, 1985).

Convincing experimental evidence for the formation of bipolarons is also found in sodium vanadium oxide $Na_xV_2O_5$-β (V^{4+}-V^{4+}), from studies of NMR, EPR, specific-heat data, x-ray diffusive scattering, and transport properties (Chakraverty *et al.*, 1978; Kanai *et al.*, 1980; Onoda *et al.*, 1982, Erata and Nagasawa, 1983; Onoda and Nagasawa, 1984; Schlenker, 1985). This compound at low temperatures also exhibits commensurate CDW ordering of two-electron pairs. With increasing temperature at around 200 K there is a transition to a phase of nonordered pairs, which remains semiconducting up to 500 K. We notice that WO_{3-x} and other Magnelli phases of Ti and V probably also belong to this group (Schlenker, 1985 and references therein).

The third group consists of *superconducting materials* for which the concept of local pairing has been envisaged for some time. Representative examples of such materials are $BaPb_{1-x}Bi_xO_3$ (Sleight *et al.*, 1975; Groznov *et al.*, 1984; Kitazawa *et al.*, 1985a, 1985b; Tajima *et al.*, 1987; Uchida, Kitazawa, and Tanaka, 1987), PbTe⟨Tl⟩ (Chernik *et al.*, 1982), $SrTiO_3$:Zr (Eagles, 1969a, 1969b; 1985), PdH_x (Moizhes and Drabkin, 1983), and $Li_{1+x}Ti_{2-x}O_4$ (Harrison *et al.*, 1985; Ng *et al.*, 1985). These materials have superconducting properties that are quite different from those of BCS superconductors and for which there is considerable experimental evidence for local pairing. Among them is $BaPb_{1-x}Bi_xO_3$, which shows charge ordering in the insulating composition for $x > 0.35$ and superconductivity for $x < 0.35$ (see Fig. 2). For a discussion of experimental findings suggesting charge disproportionation of Bi, i.e., the existence of Bi^{3+}, Bi^{5+} in $BaBiO_3$ and doped $BaBiO_3$, see Sec. V.C.1.

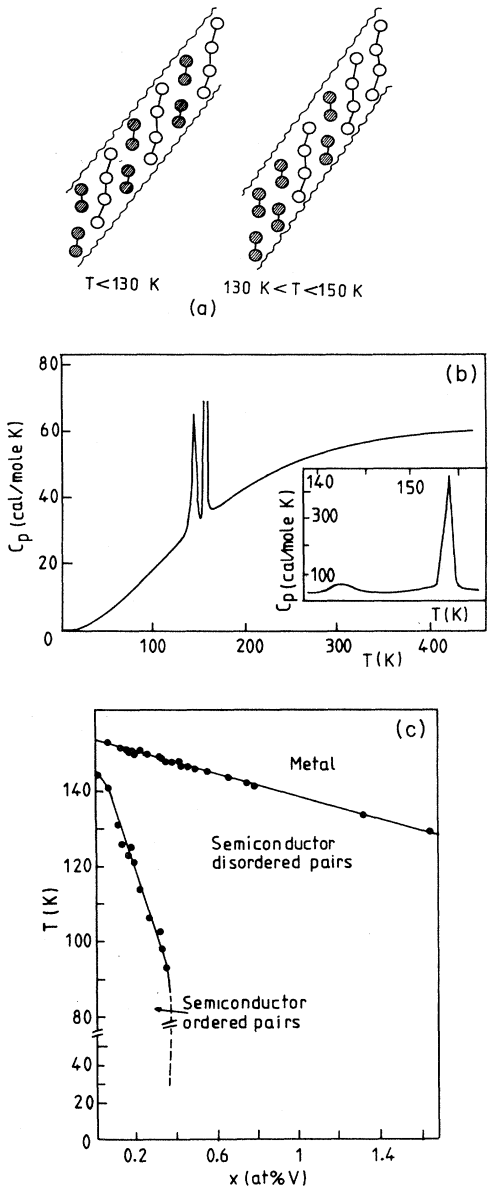

FIG. 1. (a) A cross section of the bidimensional slabs that constitute Ti_4O_7: The solid circles correspond to Ti^{3+} ions; and the open circles to Ti^{4+} ions. Notice the strong binding between pairs of Ti^{3+} ions forming the local pairs. Below 130 K the pairs are well ordered in a charge-ordered state. Between 130 K and 150 K the pairs are dynamically disordered. (b) Specific heat of Ti_4O_7 (after Lakkis *et al.*, 1976). Below the first transition the system is in a charge-ordered state, as depicted in (a) for $T<130$ K. Between the two phase transitions the system keeps its local pair character—the pairs being dynamically disordered as shown in (a) for $130\ \text{K}<T<150$ K. Above the second phase transition the pairs have broken up, and the system is an electron metal. The inset shows the details of specific heat c_p near the two phase transitions. (c) Experimental phase diagram for $(Ti_{1-x}V_x)_4O_7$, obtained by electrical resistivity measurements and corroborated by calorimetric, magnetic susceptibility, and EPR studies (after Schlenker *et al.*, 1979), which shows the increase in the stability region of the disordered local pair state upon doping.

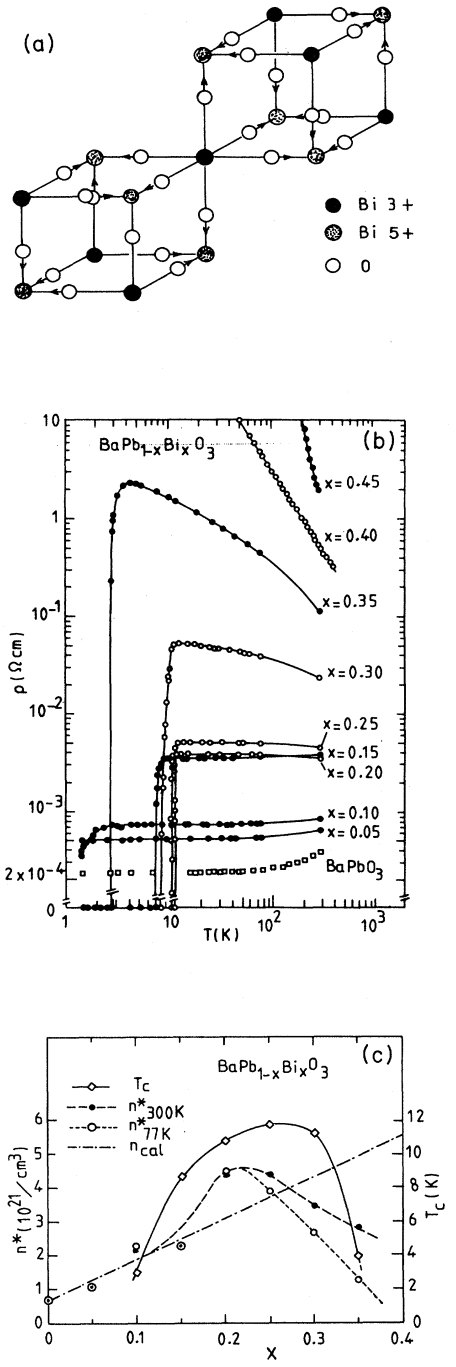

FIG. 2. (a) The crystal structure of $BaBiO_3$ showing the Bi ions in two valence states, Bi^{3+} and Bi^{5+} (after Uchida *et al.*, 1985). (b) Temperature dependence of the electrical resistivity of $BaPb_{1-x}Bi_xO_3$ for various values of x (after Thanh *et al.*, 1980). Notice the changeover in the normal-state resistivity from superconducting samples ($x \lesssim 0.35$) to samples exhibiting charge order ($x>0.3$). (c) Superconducting critical temperature T_c (solid line) and the number of carriers (deduced from the Hall coefficient) as a function of doping (after Thanh *et al.*, 1980); dot-dashed curve, carrier concentration calculated by assuming that one electron is introduced by one Bi atom (n_{cal}); dashed curve, observed carrier concentration n^*.

Both $BaPb_{1-x}Bi_xO_3$ and $Li_{1+x}Ti_{2-x}O_4$ exhibit superconductivity that does not follow the BCS characteristics. In our opinion they belong to the same group as the newly discovered high-T_c oxides, as they have several features in common: structure, low density of carriers, closeness to the metal-nonmetal transition, and relatively high T_c (see also Robaszkiewicz *et al.*, 1982; Alexandrov, Ranninger, and Robaszkiewicz, 1986b; Micnas *et al.*, 1988b).

Initially, superconducting properties and charge-density waves in $BaBi_{1-x}Pb_xO_3$ were interpreted in terms of on-site electron pairs caused by strong electron-lattice coupling (Robaszkiewicz *et al.*, 1982; Alexandrov, Ranninger, and Robaszkiewicz, 1986b). With the discovery of the new superconducting material $Ba_{1-x}K_xBiO_3$ (Cava *et al.*, 1988; Mattheiss *et al.*, 1988), with a $T_c \sim 30$ K, it appeared unlikely that electron-lattice interaction alone was the main cause for this pair formation. We believe that the origin of pairing lies in a purely electronic mechanism [mechanism (iii) discussed at the beginning of this section], which leads to stable ionic valence states differing by $2e$ (as Sb^{3+}-Sb^{5+}, Tl^{1+}-Tl^{3+}, etc.). The properties of these materials can be described in terms of the negative-U Hubbard model with intersite repulsion (Micnas, Ranninger, and Robaszkiewicz, 1988b; Ranninger *et al.*, 1989), as will be discussed in this review.

Let us also mention that $SrTiO_3$:Zr is another example of a semiconductor with very low density of carriers. Its superconductivity ($T_c \sim 1$ K) has been interpreted by Eagles (1969a, 1969b, 1985) in terms of Bose condensation of tightly bound pairs. In Table I we summarize the data concerning the superconducting oxides, including the newly discovered ones.

Superconductivity due to local pairing rather than Cooper pairing has been envisaged for many other so-called exotic superconductors, i.e., those that do not fit the pattern of BCS superconductivity (Moizhes and Drabkin, 1983; Anderson and Yu, 1985), such as $A15$, $C15$, Chevrel phases, the carbides, nitrides, and transition-metal dichalcogenides (Ting *et al.*, 1980; Kulik, 1984; Alexandrov, Ranninger, and Robaszkiewicz, 1986b; Robaszkiewicz *et al.*, 1987). As specific examples we mention V_3Si, Nb_3Ge and Nb_3Al, $PbMo_6S_8$ and $Eu_xMo_6S_8$, NbC and TaC, and $2HTaS_2$. All of these materials have narrow electron bands and large electron-phonon coupling values, which result in poor metallic properties in the normal state but rather high values of the superconducting critical temperature.

Finally, we should mention *heavy-fermion superconductors* and low-dimensional organic superconductors. Local (intersite) attractive interaction between heavy quasiparticles as the origin for exotic heavy-fermion superconductivity is at present one of the bases for theoretical investigations of these materials (Miyake *et al.*, 1984; Ohkawa, 1984; Ohkawa, and Fukuyama, 1984), although it has not yet been determined whether the source of this attraction is electron-phonon coupling (Miyake *et al.*, 1983; Ohkawa, 1984) or a purely electronic mechanism (Bastide and Lacroix, 1988a, 1988b). The anisotropic superconductivity of organic materials like those of the $(TMTSF)_2X$ family has also been considered in the same spirit (Hasegawa and Fukuyama, 1986; Mazumdar, 1988).

The fourth group consists of numerous *amorphous semiconductors* (Anderson, 1979; Watkins, 1984; Klinger, 1985), such as chalcogenide glasses (e.g., As_2Se_3 and As_2S_3), $GeSe_2$ films, silicon inversion layers, and amor-

TABLE I. Properties of superconducting oxides. Listed are superconducting transition temperature T_c, the carrier density and type, the Debye temperature Θ_D, and the coefficient of the specific-heat linear term γ.

Compound	T_c (K)	Carrier density (cm^{-3})	Carrier type	Θ_D (K)	γ (mJ/mol K^2)	Lattice type
$BaPb_{1-x}Bi_xO_3$	13	4×10^{21}	n	195	1.6	Perovskite
	(11)	(2.5×10^{21})		(173)	(1.0)	(Bi^{3+}-Bi^{5+})
$Ba_{1-x}K_xBiO_3$	25-34	$\sim10^{21}$		$\sim$200	1.5–2.6	Perovskite
$BaPbO_{3-\delta}$	0.4	2×10^{20}	n	166	0.6	Perovskite
$SrTiO_{3-\delta}$	0.4	1.4×10^{20}	n	453	1.6	Perovskite
	(0.2)	(4×10^{19})			(1.0)	
Na_xWO_3	6	$\sim10^{21}$				Perovskite
$Li_{1+x}Ti_{2-x}O_4$	12	1.3×10^{22}	n	660	20	Spinel
	(9.6)	(8×10^{21})		(600)	(11)	
$La_{2-x}Sr_xCuO_4$	40	1.5×10^{21}	p	400–500	1.7–10	Oxygen-deficient perovskites (CuO_2 layers)
$YBa_2Cu_3O_{6,7}$	60	1.5×10^{21}	p	300–400		
$YBa_2Cu_3O_7$	90	3×10^{21}	p		3–10	layers+chains
$Bi_2Sr_2Ca_{n-1}Cu_nO_y$	10, 85, 100	$\sim10^{21}$	p	230–290	$\sim$10	layers
$Tl_2Ba_2Ca_{n-1}Cu_nO_y$ $n=1,2,3$	20, 108, 125	$\sim10^{21}$	p			layers

phous silicon, in which the localization of electron pairs on impurity centers (negative-U centers) was initially invoked in order to explain their electrical, magnetic, and optical properties, and in particular the absence of paramagnetism and the stabilization (pinning) of the electronic Fermi level near the center of the gap. Recently, pressure-induced superconductivity discovered in As_2Te_3 and α $Ge_{33}As_{12}Se_{55}$ has been interpreted on the basis of local pair theory (Savransky, 1986).

The idea of negative-U centers was also introduced to explain the increase in T_c upon doping certain superconductors with impurities such as Fe and Ti (acting as impurity electron pairs; see Ganguli *et al.*, 1966), superconductivity at interfaces such as Al-Ge and Al-Si (Simanek, 1979), and the superconducting properties of nonsimple metals like carbides and nitrides, e.g., NbC (Ting *et al.*, 1980).

A quite separate group consists of several conjugated polymers with nondegenerate ground states, in which the stable defect states formed upon doping are bipolarons: doubly charged, spinless bound states of two holes with associated deformation of the molecule. Evidence for such bipolaron formation (from ESR, transport, photoelectron spectroscopy, and optical absorption data) has been found in, among others, *cis*-polyacetylene, polypyrrole, polythiophene, and polyparaphenylene (Scott *et al.*, 1983; Chung *et al.*, 1984). Recently, the possibility of bipolaronic superconductivity in such systems was pointed out by Brazovskii *et al.* (1985).

C. Theoretical models for systems with local electron pairing

The theoretical models of local pairing either start with a microscopic derivation of a local attractive interaction or postulate some effective Hamiltonian. In the following we consider the properties of the extended Hubbard model with on-site or intersite attraction, which can be thought of as a useful parametrization of the problem. The Hamiltonian is given by

$$H=\sum_{i,j,\sigma} t_{ij}c_{i\sigma}^{\dagger}c_{j\sigma}+U\sum_i n_{i\uparrow}n_{i\downarrow} +\tfrac{1}{2}\sum_{i,j} W_{ij}n_i n_j-\sum_i(\mu-E_i)n_i \ , \qquad (1.1)$$

$$n_i=n_{i\uparrow}+n_{i\downarrow}, \quad n_{i\sigma}=c_{i\sigma}^{\dagger}c_{i\sigma} \ ,$$

where t_{ij} denotes the transfer integral, U is the on-site interaction and W_{ij} the intersite interaction between tight-binding electrons, μ is the chemical potential, and E_i is a (random) site energy. The model (1.1) can be considered as generally resulting from a system of narrow-band electrons strongly coupled to a bosonic field, which they polarize and which in turn acts upon the electrons, thereby forming entirely new entities. These new entities are described by the correlated motion of the electrons and their surrounding polarization field and by an induced short-range attraction which competes with the Coulomb repulsion. The bosonic modes can be phonons, excitons, acoustic plasmons, etc. The parameters of Eq. (1.1), t_{ij}, U, and W_{ij}, are effective ones (renormalized from their bare values). An effective Hamiltonian such as this can also describe models introducing purely electronic ("chemical") mechanism of local attraction.

In the next two sections we shall present results for the following two cases.

(i) $U_{\rm eff}<0$, $W_{\rm eff}>0$, when the induced local attraction outweighs the on-site repulsion. This is the case of *on-site attraction* (or *the negative-U Hubbard model*) and the problem of formation of on-site electronic pairs in the strong $U<0$ limit. In Sec. II.A the general properties of this model are discussed. In Sec. II.B an extensive analysis of the thermodynamic and electromagnetic properties of a superconductor with preformed local on-site pairs is presented. The properties of the negative-U extended Hubbard model in the weak-attraction limit and the transition between BCS-like superconductivity and superfluidity of charge bosons are examined in Sec. II.C.

(ii) $W_{\rm eff}<0$ but $U_{\rm eff}>0$. This is the case of *intersite attraction,* when the induced attraction is strong enough to dominate over the intersite Coulomb repulsion (Sec. III). We study the various superconducting solutions of the model within a mean-field-type treatment, for the cases of both weak and strong on-site correlations (Secs. III.A and III.C, respectively); we also examine the conditions for real-space pair formation (Sec. III.B).

We should point out that, in certain cases, it is possible to introduce effective sites, and the intersite attraction can still be mapped onto a negative-U extended Hubbard model. This is, for example, the case with a model of bipolaronic superconductivity proposed by Alexandrov and Ranninger (1981b); the model begins with intersite attraction, but is mapped onto a $U<0$ problem in the strong-attraction limit.

Of course, such simple one-band models [Hamiltonian (1.1)] are highly simplified as regards real materials. There are several possible realistic extensions. Recently a model involving a mixture of narrow-band electrons strongly coupled to bosonic-field and wide-band electrons has been proposed by us (Micnas, Ranninger, and Robaszkiewicz, 1987a; Robaszkiewicz *et al.*, 1987). It will be discussed in Sec. IV.

In Sec. V.A, we summarize the major theoretical results given in this review and conclude with a list of the main physical features that distinguish systems with local pairing from standard BCS superconductors.

Most of the results regarding the model systems presented in this review are derived on the basis of self-consistent mean-field or random-phase-approximation approaches, which in many cases give a correct physical picture of the properties discussed here. Whenever possible, we also present the results of more rigorous treatments.

Finally, in Sec. V.C, we discuss at some length the possible relevance of local pairing concepts for high-T_c su-

perconducting oxides, including both doped $BaBiO_3$ and the Cu-O based perovskites.

The attraction-repulsion canonical transformation for the negative-U extended Hubbard model is summarized in the Appendix.

II. THERMODYNAMIC AND ELECTRODYNAMIC PROPERTIES OF SYSTEMS WITH ON-SITE ATTRACTION

A. Extended Hubbard model with $U<0$

The extended Hubbard model with on-site attraction has been intensively studied in the last few years, and many of its properties have been established. Thermodynamic properties of Eq. (1.1) for $U<0$ depend crucially on the lattice dimensionality d and the number of electrons n per lattice site:

$$n=\frac{1}{N}\sum_i \langle n_i \rangle, \quad n\in[0,2] . \tag{2.1}$$

Exact results are known for the ground state for $n=1$ ($E_i=E_0$) in one dimension (Shiba, 1972). For arbitrary electron density the one-dimensional attractive Hubbard model has been solved by the Bethe ansatz method (Krivnov and Ovchinnikov, 1974; Haldane, 1980; Bahder and Woynarovich, 1986; Gusmão, 1987). Krivnov and Ovchinnikov have shown that the single-electron excitation spectrum has a gap for arbitrary n, in contrast to the case of $U>0$, where such a gap exists only for $n=1$ (Lieb and Wu, 1968). It has been concluded that for $n=1$, the magnetic susceptibility is strongly suppressed by the attractive interaction, and $\chi\to 0$ as $T\to 0$ (Takahashi, 1969; Shiba, 1972; Pincus *et al.*, 1973).

An extended Hubbard model (for both $U>0$ and $U<0$) has also been analyzed for the case of weakly coupled chains (Efetov and Larkin, 1975; Emery, 1976, 1977). In the limit of strong attraction it has been shown by degenerate perturbation theory that the model is equivalent to a weakly coupled interacting array of anisotropic Heisenberg chains (Emery, 1976). Based on this equivalence, the electronic correlation functions for the half-filled extended Hubbard model have been determined from the known functions for the one-dimensional pseudospin system, and the phase transitions leading to a singlet-superconducting state and charge-density waves in coupled chains have been studied (Emery, 1976, 1977).

In the strong-coupling limit $k_BT, t, W \ll |U|$, in $d=2,3$, and *for arbitrary n,* the properties of Eq. (1.1) have been studied by perturbation theory (Robaszkiewicz *et al.*, 1981a, 1981b), and the possible phase diagrams have been determined in the mean-field-approximation (MFA) and random-phase approximation (RPA) (Kulik and Pedan, 1980; Robaszkiewicz *et al.*, 1981a, 1981b; Alexandrov and Ranninger, 1981b; Kubo and Takada, 1983; Alexandrov, Ranninger, and Robaszkiewicz, 1986b; Micnas and Robaszkiewicz, 1988a, 1988b).

The case of weak attraction has been studied by the broken-symmetry Hartreee approach (Robaszkiewicz *et al.*, 1981c, 1981d, 1982; A. R. Bishop *et al.*, 1988, Micnas *et al.*, 1988d) and the RPA method (Kostyrko, 1987). The Gutzwiller method has been applied to the 3D half-filled negative-U Hubbard model by Chao *et al.* (1979), while Olés *et al.* (1984) have studied the ground-state phase diagram of the extended Hubbard model with negative U for $n=1$, using modification of the Gutzwiller approach for weak and intermediate electron correlations (so-called local approach). The problem of transition from weak-coupling to strong-coupling superconductivity within a $U<0$ Hubbard model has been dealt with too (Robaszkiewicz *et al.*, 1981d, 1982; Nozières and Schmitt-Rink, 1985). Other studies include the zero-bandwidth limit ($t_{ij}=0$; Micnas *et al.*, 1984), the high-temperature limit $k_BT>t$ (Micnas *et al.*, 1983), and the effects of diagonal disorder (Kulik and Pedan, 1980; Pedan and Kulik, 1982; Micnas *et al.*, 1985a, 1985b; Nagaosa, 1989). Quantum Monte Carlo studies of $d=2$ and $d=3$ $U<0$ Hubbard models (Hirsch, 1985a, 1987a; Hirsch and Scalapino, 1985a, 1985b, 1986; Scalettar, Loh, *et al.*, 1989; Scalettar, Scalapino, *et al.*, 1989a) have also been reported, as well as the quasi-one-dimensional extended Hubbard model in the limit of strong on-site attraction (Imada and Scalapino, 1986; Nagasawa and Hida, 1988).

There exists a canonical transformation (attraction-repulsion transformation; see the Appendix),

$$c_{i\downarrow}^{\dagger}=\exp(i\mathbf{Q}\cdot\mathbf{R}_i)b_{i\downarrow}, \quad c_{i\uparrow}^{\dagger}=b_{i\uparrow}^{\dagger} ,$$

with the reciprocal vector $\mathbf{Q}$ satisfying the condition $\exp(i\mathbf{Q}\cdot\mathbf{R})=-1$ for any translation $\mathbf{R}$ that transforms one sublattice into another, which maps the Hubbard model with intrasite attraction and intersite Coulomb interaction and arbitrary electron density ($0\le n\le 2$) onto the half-filled Hubbard model with intrasite Coulomb repulsion and intersite exchange interaction (Robaszkiewicz *et al.*, 1981a, 1981b). The number condition (2.1) is transformed to the requirement that the magnetization have a fixed value along the z direction and be equal to $\frac{1}{2}(n-1)$. Consequently, the magnetic long-range orderings (along the z axis and in the XY plane) in the model with $U>0$ are equivalent to electronic diagonal (charge density wave—CDW) and off-diagonal (singlet superconducting—SS) orderings in the $U<0$ case.

For $n=1$ and in the absence of an intersite Coulomb interaction, the CDW and SS states are strictly degenerate. Moreover, the physical quantities determined by one-particle correlation functions like the specific heat and the entropy are independent of the sign of U. However, the two-particle correlation functions may be different. For example, magnetic susceptibility is evidently suppressed by an attractive interaction. The degeneracy will be removed by the intersite interaction W (or by deviation from half-filling, which will stabilize the SS phase). $W>0$ stabilizes the CDW ordering, while $W<0$ will stabilize the SS state.

The canonical transformation can also be used to map the phase diagram for $n=1$ of the ordinary Hubbard model onto that of the attractive Hubbard model. In

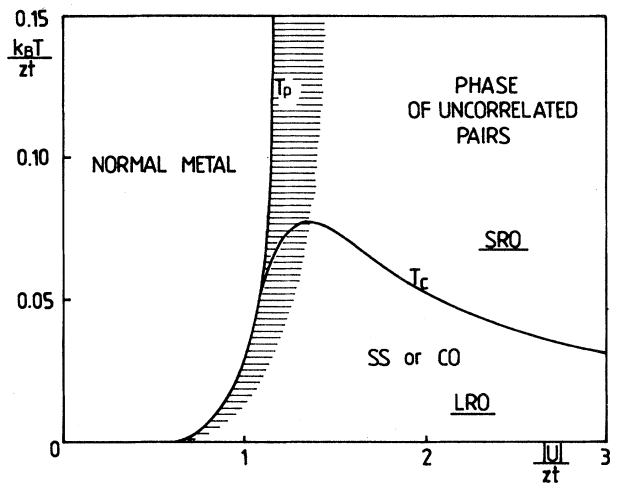

FIG. 3. Phase diagram of the half-filled Hubbard model with intra-atomic attraction ($|U| \gg W$), for a simple cubic lattice (after Robaszkiewicz *et al.*, 1981a). T_c and T_p denote the critical temperatures for the onset of long-range ordering and for the breaking of electronic pairs, respectively. SRO is short-range ordering in the region of uncorrelated pairs, which is semiconducting and diamagnetic. $2zt$ is the bandwidth.

Fig. 3 we show the phase diagram of the half-filled attractive Hubbard model for a simple cubic lattice, obtained via this mapping by the use of the earlier results of Economou and co-workers (De Marco *et al.*, 1978; Economou *et al.*, 1978; White and Economou, 1978) for the repulsive Hubbard model for $n=1$. There are two characteristic temperatures on the diagram, T_c and T_p, denoting the critical temperatures for the onset of long-range ordering (LRO) and for the breaking of electronic pairs, respectively. In the region with LRO the two-electron excitations from the SS state will be gapless, whereas the excitations from the CDW state have a gap. In the region of uncorrelated pairs, there is short-range order (SRO), and this phase is diamagnetic with a gap of order $\sim|U|$ in a one-electron excitation spectrum.

For weak attraction the superconducting critical temperature T_c follows the BCS theory, increasing with $|U|/t$ (although the form of this increase depends on the density of states used), while in the strong-attraction limit it decreases as $t^2/|U|$. Let us also note that, in the strong-attraction limit, the pairs exist above T_c and they condense below it, in contrast to the BCS-dominated regime, in which electronic pairs are created and condensed at the same temperature. The determination of a possible maximal T_c is a challenging problem (Hirsch, 1985a, 1987a; Hirsch and Scalapino, 1985b, 1986; Nozières and Schmitt-Rink, 1985; Scalettar, Scalapino, *et al.*, 1989). It is also clear that this problem is at least as difficult to solve as that of determining the Néel temperature for the ordinary half-filled band, $d=3$ Hubbard model for arbitrary U.

Recently Scalettar, Loh, *et al.* (1989) have studied the phase diagram of the negative-U Hubbard model ($W=0$) on a two-dimensional square lattice by the quantum Monte Carlo simulation technique. They concluded that there was (i) a vanishing transition temperature at half-filling but with a ground state having both SS and CDW long-range orderings, and (ii) a Kosterlitz-Thouless phase transition at finite temperature into a SS state with power-law decay of the pairing correlations away from half-filling.

B. Limit of strong attraction and properties of systems with preformed on-site local pairs

The phase diagram of the extended Hubbard model for arbitrary band filling, lattice dimensionality, and $W\neq 0$ poses a problem of considerable complexity. In the strong-attraction limit $|U| \gg t, W$, a large gap of order $|U|$ exists in the singe-particle excitation spectrum for any n, which is equivalent to the statement that the Fermi level is pinned for $U<0$, close to its value at $n=1$ ($\mu=-|U|/2+W_0+E_0$). Due to that fact, standard degenerate perturbation theory can be applied for the model (1.1) to derive an effective pseudospin Hamiltonian valid for *any band filling*. In the case without site disorder one can put $E_i=E_0=0$, and to second order in $t_{ij}/|U|$ one obtains (Robaszkiewicz *et al.*, 1981a, 1981b)

$$\bar{H}=-\sum_{i,j} J_{ij}\rho_i^+\rho_j^- +\sum_{i,j} K_{ij}\rho_i^z\rho_j^z -\bar{\mu}\sum_i(2\rho_i^z+1)-\frac{N}{4}(J_0+2W_0)\ , \tag{2.2}$$

and

$$n=\frac{1}{N}\sum_i \langle 2\rho_i^z+1\rangle\ . \tag{2.3}$$

Here,

$$J_{ij}=2t_{ij}^2/|U|,\quad K_{ij}=J_{ij}+2W_{ij}\ ,$$
$$\bar{\mu}=\mu+\tfrac{1}{2}|U|-W_0\ ,$$

and

$$W_0=\sum_j W_{ij},\quad J_0=\sum_j J_{ij}\ . \tag{2.4}$$

The charge operators are

$$\rho_i^+=c_{i\uparrow}^\dagger c_{i\downarrow}^\dagger,\quad \rho_i^-=c_{i\downarrow}c_{i\uparrow}\ ,$$
$$\rho_i^z=\tfrac{1}{2}(n_{i\uparrow}+n_{i\downarrow}-1)$$

and, in the subspace excluding single occupancy of sites, they satisfy the commutation rules of $s=\frac{1}{2}$ operators. This effective pseudospin Hamiltonian (2.2) with the auxiliary condition (2.3) has the form of an anisotropic Heisenberg model ($s=1/2$), with an effective external field $\bar{\mu}$ in the z direction, such that the average magnetization has a fixed value equal to $\frac{1}{2}(n-1)$.

On the other hand, due to the well-known properties of $s=\frac{1}{2}$ operators, one has

$$\rho_i^+=b_i,\quad \rho_i^-=b_i^\dagger,\quad \rho_i^z=\tfrac{1}{2}-b_i^\dagger b_i\ , \tag{2.5}$$

where b_i, $b_i^\dagger$ are commuting (Bose-like) operators for different sites but $b_i^2=b_i^{\dagger 2}=0$, $[b_i,b_i^\dagger]=1-2n_i$, $n_i=b_i^\dagger b_i$

TABLE II. Correspondence between electronic orderings and types of pseudospin orderings.

Long-range order (LRO) Diagonal (DLRO)	Off-diagonal (ODLRO)	Type of ordered state in extended Hubbard model with $U<0$	Ordering of pseudospins $\{\rho_i^\alpha\}$, $\alpha=+,-,z$
No	No	Nonordered phase (NO) Phase of uncorrelated local pairs, diamagnetic short-range order $n=\frac{1}{N}\sum_{i,\sigma}\langle n_{i\sigma}\rangle=\frac{1}{N}\sum_i\langle 2\rho_i^z+1\rangle$.	Ferromagnetic or paramagnetic ↑↑
Yes	No	Charge order (CO) $\Delta_Q=\frac{1}{N}\sum_{i,\sigma}\langle n_{i\sigma}\rangle e^{iQ\cdot R_i}=\langle\rho_A^z-\rho_B^z\rangle\neq 0$	Antiferromagnetic ↑↓ or more complicated orderings along z axis
No	Yes	Singlet (on-site) superconductivity (SS) $x_0=\frac{1}{N}\sum_i\langle c_{i\uparrow}^\dagger c_{i\downarrow}^\dagger\rangle=\frac{1}{N}\sum_i\langle\rho_i^x\rangle$ $=\langle\rho_A^x\rangle+\langle\rho_B^x\rangle\neq 0$	Spin flopped ↗ ↗
Yes	Yes	Mixed phase (M) of CO and SS $\Delta_Q\neq 0$, $x_0\neq 0$, $x_Q=\frac{1}{N}\sum_i\langle c_{i\uparrow}^\dagger c_{i\downarrow}^\dagger\rangle e^{iQ\cdot R_i}=\langle\rho_A^x\rangle-\langle\rho_B^x\rangle\neq 0$	Intermediate state ↗ ↘
Yes	No	Condensed phase of electron droplets (phase separation)	Droplets of ferromagnetic order $\cdots\uparrow\uparrow\uparrow\downarrow\downarrow\downarrow\cdots$

for the same site, which reflects their fermionic nature. Thus the system can be equally well considered as a hard-core Bose gas on a lattice.

In Table II we give the correspondence between ordered states in the extended Hubbard model with $U<0$ and the orderings of the pseudospins $\{\rho_i^\alpha\}$, $\alpha=+,-,z$. One notices a remarkable similarity as far as the LRO's are concerned between the present situation and the quantum lattice gas model of liquid ^{4}He II, for which such an equivalence was derived many years ago (Matsubara and Matsuda, 1956, 1957; Whitlock and Zilsel, 1963; Matsuda and Tsuneto, 1970; Mullin, 1971a, 1971b Liu and Fisher, 1973).[1] The thermodynamic and electromagnetic properties of Eqs. (2.3) and (2.4) have been analyzed in mean-field approximation and in the self-consistent random-phase approximation (Kulik and Pedan, 1980; Alexandrov and Ranninger, 1981b; Robaszkiewicz *et al.*, 1981a; Alexandrov *et al.*, 1986b; Micnas and Robaszkiewicz, 1988a, 1988b).

1. The phase diagrams

The ground-state phase diagram for the case of nearest-neighbor interaction as determined in the MFA and RPA is shown in Fig. 4 (Robaszkiewicz *et al.*, 1981a; Alexandrov *et al.*, 1986b). It consists of the mixed charge-ordered/singlet-superconducting (CO-SS) phase M, the superconducting phase SS, and the droplet phase. For $n=1$ the CO state is favored if $W>0$ ($K<J$). The phase transition between the M and the SS states is con-

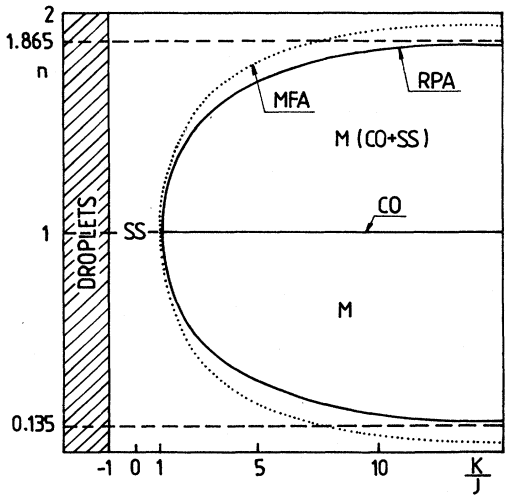

FIG. 4. Ground-state phase diagram of a local pair system: solid curves, random-phase approximation; dotted curve, mean-field approximation; SS, singlet (on-site) superconducting state; CO, charge-ordered state; M, mixed (SS-CO) state. The ground state at $n=1$ is CO without ODLRO. The dashed lines indicate critical concentrations n_c and $2-n_c$ separating the SS from the M phase for $K/J=\infty$ obtained in the random-phase approximation. $J=2t^2/|U|$, $K=J+2W$.

[1]For the quantum lattice gas model, the particular types of LRO's correspond to the following phases: ODLRO, superfluid phase; DLRO, crystalline ordering; ODLRO+DLRO, supersolid; NO, liquid phase.

tinuous.

The mean-field phase boundary is given by

$$|n_c-1|=\left[\frac{K_Q+J_0}{K_Q+J_Q}\right]^{1/2}, \tag{2.6}$$

where n_c is the critical concentration separating the SS phase from the M phase. J_0, J_Q, and K_Q are the Fourier transforms of J_{ij} and K_{ij} for $\mathbf{k}=0$ and $\mathbf{Q}$. $J_{\mathbf{k}}=\sum_j J_{ij}\exp[i\mathbf{k}\cdot(\mathbf{R}_i-\mathbf{R}_j)]$,

$$K_{\mathbf{k}}=\sum_j K_{ij}\exp[i\mathbf{k}\cdot(\mathbf{R}_i-\mathbf{R}_j)],\quad K_{\mathbf{k}}=J_{\mathbf{k}}+2W_{\mathbf{k}}\ .$$

For finite temperatures the resulting phase diagrams determined within the MFA are given in Figs. 5(a)–5(c) for different $W\geq 0$. For $W=0$, the SS, the CO, and the M states are degenerate at $n=1$. For $W>0$ all the phases can occur, and transitions among them are second order. The transition temperature between the NO and the CO phases is

$$T_{CO}=n(2-n)K_0/2k_B\ , \tag{2.7}$$

while the transition temperature between the NO and the SS phases is given by

$$T_{SS}=(n-1)J_0/k_B\ln[n/(2-n)]\ . \tag{2.8}$$

The equation determining the boundaries between the M and SS phases, as well as those between the M and CO phases, can be derived by the use of the Landau expansion; these boundaries are given in Robaszkiewicz *et al.* (1981a).

The four critical lines meet at a multicritical point MP corresponding to a tetracritical point in the B-T phase diagram of an anisotropic antiferromagnet (Liu and Fisher, 1973; Bruce and Aharony, 1975; Kosterlitz *et al.*, 1976). We should stress the nonmonotonic dependence of the superconducting transition temperature on electron concentration and the fact that T_{SS} attains its maximum at the border with the CO phase. For $n\neq 1$ and $W>0$ there are also possible successive phase transitions with varying T, such as SS→M→CO→NO and M→CO→NO.

We should like to emphasize the important difference in thermodynamic behavior between an ordinary anisotropic antiferromagnet in an external field with nearest-neighbor interactions and our pseudospin model in the effective field. For the former there are only three phases [see (Fig. (5d)], namely, the paramagnetic (P), the antiferromagnetic (AF), and the spin-flopped (SF) phases. While the transitions AF→P and SF→P are second order, the transition AF→SF is first order (Fisher and Nelson, 1974; Bruce and Aharony, 1975; Kosterlitz *et al.*, 1976). For the pseudospin Hamiltonian (2.2), due to the constraint of Eq. (2.3) on the magnetization, the first-order boundary for SF-AF splits into two second-order boundaries together with the emergence of an intermediate (M) phase and the tetracritical point.

Let us also mention that, in general, if J_{ij} and K_{ij} are

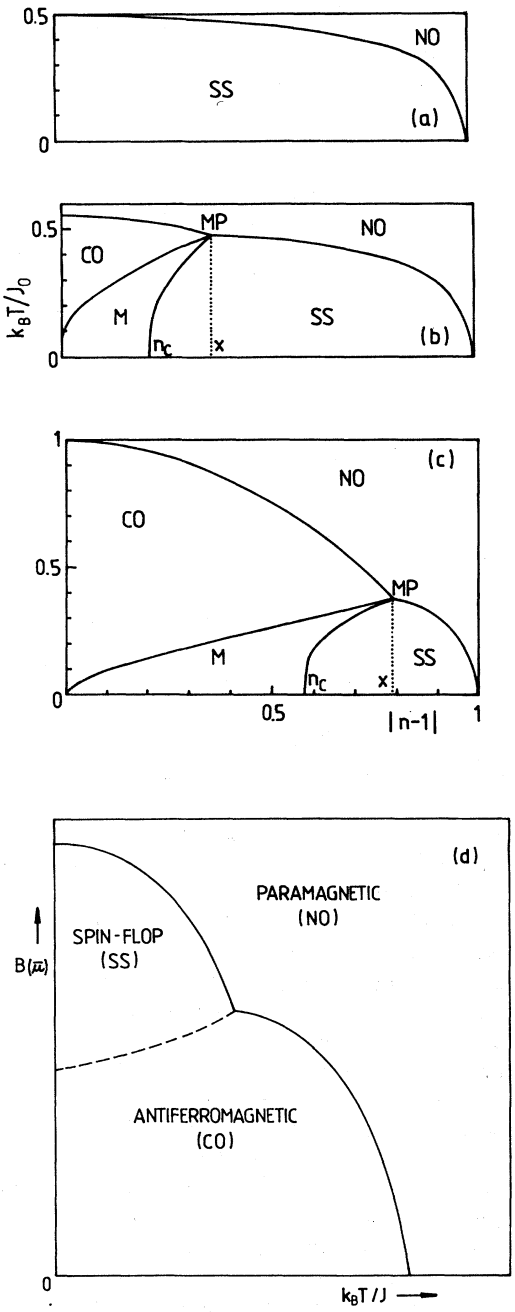

FIG. 5. MFA phase diagrams of a local pair system as a function of temperature and electron concentration: (a) $K/J=1$; (b) $K/J=1.1$; (c) $K/J=2$. MP is the multicritical point at which four phases meet. n_c is the critical electron concentration beyond which the M phase is stable at $T=0$ K. X is the position of the MP. (d) Schematic phase diagram of an ordinary anisotropic Heisenberg model with nearest-neighbor interactions in a magnetic field B along the z axis, for a fixed value $K/J>1$. The model could describe a local pair system if the chemical potential $\bar{\mu}$ were taken as an independent variable, with the following correspondences between the phases: spin-flop–singlet-superconducting (SS); antiferromagnetic–charge-order (CO); paramagnetic–nonordered (NO).

not restricted to nearest neighbors, the mixed CO-SS state can have a periodicity characterized by a vector **Q** different from half the smallest reciprocal lattice vector. Moreover, **Q** can be commensurate or incommensurate with the lattice periodicity depending on the range of the repulsive interaction K_{ij}, its strength, and the concentration of local pairs $n/2$. A preliminary discussion of this problem has been given by Kubo and Takada (1983).

2. The excitation spectra

The four different phases making up the phase diagram of a local pair system have quite distinct excitation spectra. They arise from single-particle excitations (the local pair transfer) and collective oscillations (the density fluctuations of local pairs). These two excitations couple with each other in the phases with ODLRO, i.e., the mixed phase M and the pure superconducting phase SS. All these excitations can be considered as pseudospin waves in the various MFS states. The average direction of the pseudospins changes due to thermal and quantum fluctuations.

In order to take these effects into account, two methods have been used.

(i) RPA-MFA using the standard basis operators (Robaszkiewicz *et al.*, 1981a), spin-wave approximation (Alexandrov and Ranninger, 1981b), and a memory-function approach (Kubo and Takada, 1983);

(ii) the self-consistent RPA (Alexandrov *et al.*, 1986b; Micnas and Robaszkiewicz, 1988a, 1988b). Here we shall simply give the results and discuss their physical implications.

a. Pure superconducting phase

For the pure superconducting phase the excitation spectrum corresponds to fluctuations of the phase φ_i of the local pair wave function, which, as in ^{4}He II, is coupled to the density fluctuations. The spectrum is given by

$$\omega_{\mathbf{k}}^{(\mathrm{SS})}=2M\{[(J_0-J_{\mathbf{k}})+V_{\mathbf{k}}\sin^2\Theta](J_0-J_{\mathbf{k}})\}^{1/2}\ , \tag{2.9}$$

where

$$V_{\mathbf{k}}=J_{\mathbf{k}}+K_{\mathbf{k}},\quad M^2=\langle\rho^x\rangle^2+\langle\rho^z\rangle^2\ ,$$
$$\langle\rho^x\rangle=M\sin\Theta,\quad \langle\rho^z\rangle=\tfrac{1}{2}(n-1)=M\cos\Theta\ . \tag{2.10}$$

In Eq. (2.10) $J_{\mathbf{k}}$ and $K_{\mathbf{k}}$ are the Fourier transforms of J_{ij} and K_{ij}, respectively. The length of the pseudospin M within the mean-field approximation satisfies the equation

$$M=\tfrac{1}{2}\tanh(\beta J_0 M),\quad \beta=1/k_B T\ , \tag{2.11}$$

whereas within the framework of the self-consistent RPA

$$\frac{1}{2M}=\frac{2M}{N}\sum_{\mathbf{k}}\frac{J_0-J_{\mathbf{k}}+\frac{1}{2}V_{\mathbf{k}}\sin^2\Theta}{\omega_{\mathbf{k}}^{(\mathrm{SS})}}\coth\left[\frac{\beta\omega_{\mathbf{k}}^{(\mathrm{SS})}}{2}\right]\ . \tag{2.12}$$

Notice that in the long-wave limit the spectrum (2.9) is sound-wave like:

$$\omega_{\mathbf{k}}^{(\mathrm{SS})}=s|\mathbf{k}|+O(\mathbf{k}^2)\quad(\mathbf{k}\to 0)\ , \tag{2.13}$$

where

$$s=2\langle\rho^x\rangle\delta J_0\sqrt{1+K_0/J_0}\ , \tag{2.14}$$

$$\delta^2=\frac{1}{z^2}\sum_{|\mathbf{m}|=a}\left[\frac{|\mathbf{k}\cdot\mathbf{m}|}{|\mathbf{k}|}\right]^2\ . \tag{2.15}$$

The sound velocity s is proportional to $\langle\rho^x\rangle$, which measures the fraction of local pairs in the condensate (being equal to $n_0=\langle\rho^x\rangle^2$).

As n approaches the critical density n_c separating the SS phase from the M phase, the spectrum (2.9) becomes soft at the zone boundary ($\omega_{\mathbf{Q}}^{(\mathrm{SS})}\to 0$), thus indicating the instability of the homogeneous SS phase to the symmetry-broken M phase, which doubles the lattice periodicity. As $T\to T_{\mathrm{SS}}$, $\langle\rho^x\rangle\to 0$, and hence the spectrum (2.9) becomes

$$\omega_{\mathbf{k}}^{(\mathrm{SS})}=|n-1|(J_0-J_{\mathbf{k}})\ , \tag{2.16}$$

which has a free-particle-like dispersion $\sim k^2$ reflecting the *nonordered local pair state.*

We should mention that the sound velocity (2.14) becomes imaginary for $K_0/J_0<-1$, which indicates that at $K_0/J_0=-1$ the system becomes unstable toward a phase of local pair droplets, which corresponds to the creation of two domains of ferromagnetic order along the z direction, in pseudospin language, or to a liquid-gas phase separation, in quantum lattice gas language.[2]

The linear, sound-wave-like dispersion for excitations in the SS phase is the complete equivalent of the situation in ^{4}He II and satisfies the Landau criterion for superfluidity, i.e., $V_{\mathrm{crit}}=\hbar^{-1}(\partial\omega_k/\partial k)_{\mathrm{min}}>0$.

It is interesting that hard-core bosons on a lattice rather than in continuum have a temperature-dependent sound velocity, which goes to zero upon approaching T_{SS}. The disappearance of sound-wave-like behavior when the temperature is increased above T_{SS} gives rise to the appearance of a quadratic dispersion law with a temperature-dependent gap

$$\omega_{\mathbf{k}}^{(\mathrm{NO})}=\left[k_B T\ln\left[\frac{n}{2-n}\right]-(n-1)J_0\right]+(n-1)(J_0-J_{\mathbf{k}})\ . \tag{2.17}$$

The first **k**-independent term of $\omega_{\mathbf{k}}^{(\mathrm{NO})}$ represents simply

[2]However, such a phase of droplets (of sufficiently large or even macroscopic volume) would not necessarily be stable if one takes into account the long-range Coulomb repulsion between charged local pairs, which gives rise to a droplet energy contribution proportional to the square of the droplet volume. See also the discussion of the condensation–phase-separation transition in Sec. III.A.

the T-dependent chemical potential of quasifree bosons (local pairs) which have quadratic dispersion in the long-wave limit.

b. Mixed charge-ordered/singlet-superconducting phase

Let us turn next to the mixed CO-SS phase. In this case the excitation spectrum has two branches—one corresponding to local pairs oscillating in phase and one resulting from local pairs oscillating with opposite phases. At $n=n_c$ and $n=2-n_c$ (where n_c is the critical concentration separating the SS and the M phases for $n<1$), these two branches are degenerate, while for $2-n_c>n>n_c$ they split into two separate branches having a gap at the Brillouin zone, which is now reduced due to the doubling of lattice periodicity. The lower branch of the spectrum is gapless and sound-wave-like in the long-wave limit. As in the pure superconducting phase, this behavior is due to the Goldstone mode arising from the rotational invariance of the pseudospin Hamiltonian in the basal plane. General expressions determining the spectrum in the M phase are rather involved, and for these we refer the reader to Robaszkiewicz *et al.* (1981a) and Kubo and Takada (1983). In contrast, when the temperature is increased beyond $T_c(\mathrm{M}\rightarrow\mathrm{CO})$, the dispersion in the CDW state again becomes rather simple,

$$\omega_{\mathbf{k}}^{\pm(\mathrm{CDW})}=2B-K_0(n-1)\pm A_{\mathbf{k}} , \tag{2.18}$$

where

$$A_{\mathbf{k}}=\{K_0^2\eta^2+[(n-1)^2-\eta^2]J_{\mathbf{k}}^2\}^{1/2} . \tag{2.19}$$

Within the RPA-MFA (Robaszkiewicz *et al.*, 1981a; Kubo and Takada, 1983) the effective field (chemical potential) $B=\bar{\mu}$ and the charge-order parameter $\eta=\langle\rho_A^z\rangle-\langle\rho_B^z\rangle$ are given by

$$\begin{aligned}\eta&=\tfrac{1}{2}\tanh\{\beta[B-\tfrac{1}{2}(n-\eta-1)K_0]\}\\&\quad-\tfrac{1}{2}\tanh\{\beta[B-\tfrac{1}{2}(n+\eta-1)K_0]\} ,\\ n-1&=\tfrac{1}{2}\tanh\{\beta[B-\tfrac{1}{2}(n-\eta-1)K_0]\}\\&\quad+\tfrac{1}{2}\tanh\{\beta[B-\tfrac{1}{2}(n-\eta+1)K_0]\} ,\end{aligned} \tag{2.20}$$

whereas the self-consistent RPA provides the following equations (Micnas and Robaszkiewicz, 1988a, 1988b):

$$\begin{aligned}\eta&=[\eta^2-(n-1)^2]\frac{1}{N}\sum_{\mathbf{k}}\frac{\eta K_0}{A_{\mathbf{k}}}\left[\coth\left[\frac{\beta\omega_{\mathbf{k}}^+}{2}\right]-\coth\left[\frac{\beta\omega_{\mathbf{k}}^-}{2}\right]\right] ,\\ n-1&=[\eta^2-(n-1)^2]\frac{1}{N}\sum_{\mathbf{k}}\left[\coth\left[\frac{\beta\omega_{\mathbf{k}}^+}{2}\right]+\coth\left[\frac{\beta\omega_{\mathbf{k}}^-}{2}\right]\right] .\end{aligned} \tag{2.21}$$

Along the phase boundary between the CO and NO phases ($\eta\rightarrow 0$) Eqs. (2.18) and (2.19) become (within the RPA-MFA)

$$\omega_{\mathbf{k}}^{\pm}=n(1-\tfrac{1}{2}n)K_0\ln\left[\frac{n}{2-n}\right]\pm(n-1)J_{\mathbf{k}} , \tag{2.22}$$

and, upon approaching the multicritical point MP defined by $T_{\mathrm{SS}}=T_{\mathrm{CO}}$ we obtain

$$\omega_{\mathbf{k}}^{\pm}=(n-1)(J_0\pm J_{\mathbf{k}}) . \tag{2.23}$$

Thus the two branches, one gapless and one with a gap existing in the M phase, evolve into two branches that both have a gap when the temperature is increased upon entering the CO phase.

In Fig. 6 we present collective excitation spectra for the four phases discussed above (Robaszkiewicz *et al.*, 1981a).

c. Effects of long-range Coulomb interactions

So far we have considered the short-range density-density interaction K_{ij} corresponding to a screened Coulomb interaction W_{ij}. Such screening can be due to the presence of a separate electronic subsystem of wide-band electrons (Alexandrov and Khmelinin, 1986; Beloborod'ko and Kulik, 1986; Micnas *et al.*, 1987a; Robaszkiewicz *et al.*, 1987). It is interesting to examine

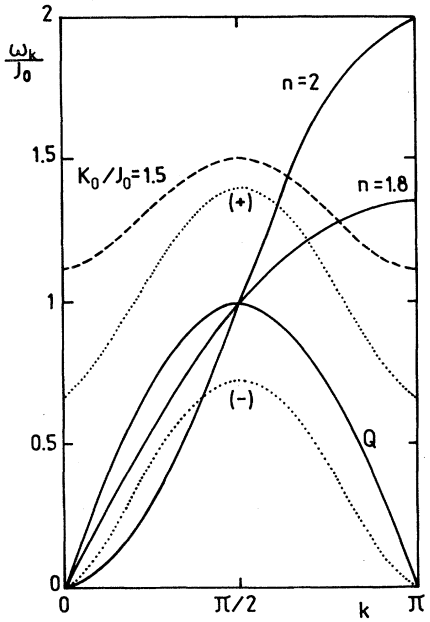

FIG. 6. Collective excitation spectrum of a local pair system at $T=0$ K: solid curves, excitations from the SS state for $K/J=2$, and for $n=1.8$ and 2; dotted curves, the two collective modes from the M state, for $K/J=1.1$ and $n=1.1$; solid curve Q, the mode at the boundary between the M and the SS phases, for $K/J=1.1$ and $n=1.218$; dashed curve, the spectrum from the CO state for $K/J=1.5$ and $n=1$.

the effect of long-range Coulomb forces. In such a case, $W_{\mathbf{k}\to 0}=4\pi e^2/\epsilon_0 k^2$ for a 3D lattice, and $W_{\mathbf{k}\to 0}=2\pi e^2/\epsilon_0 k$ for a 2D lattice, where ϵ_0 denotes the dielectric constant and where we set the lattice constant $a=1$. In the superconducting phases the sound-wave-like mode (in the case of a screened Coulomb interaction) is turned into a plasma-like mode if the Coulomb interaction is long ranged. For the 3D case in the long-wave limit one obtains (Micnas and Robaszkiewicz, 1988a, 1988b)

$$\omega_{\mathbf{k}}=[(\hbar\Omega_0^*)^2+Ak^2+Bk^4]^{1/2} \approx \hbar\Omega_0^*+\frac{1}{2\hbar\Omega_0^*}(Ak^2+Bk^4)\ , \tag{2.24}$$

where

$$(\Omega_0^*)^2=\frac{4\pi q^2\langle\rho^x\rangle^2}{\epsilon_0 m^*},\quad q=2e\ ; \tag{2.25}$$

$$A=\frac{\hbar^2 J_0\langle\rho^x\rangle^2}{m^*}\ , \qquad B=\frac{\hbar^4}{(2m^*)^2}(4M^2-8\langle\rho^x\rangle^2)\ ; \tag{2.26}$$

and where $m^*=\hbar^2/2J$ denotes the effective mass of the local pair. Taking into account the fact that $\langle\rho^x\rangle^2$ determines the number of condensed local pairs ($\langle\rho^x\rangle^2_{T=0}\approx\frac{1}{2}n$, $n\ll 1$), $\Omega_0^*(T=0)$ can be called the plasma frequency of local pairs. The spectrum (2.24) can be compared with that derived by Foldy (1961, 1962) and Fetter (1970) for a standard 3D charged Bose gas at $T=0$ K, which for the case of doubly charged bosons ($q=2e$) has the form

$$\omega_k^{(\mathrm{BG})}=[(\hbar\Omega_0)^2+(\varepsilon_{\mathbf{k}}^0)^2]^{1/2}\underset{\mathbf{k}\to 0}{\approx}\hbar\Omega_0+\frac{1}{2\hbar\Omega_0}(\varepsilon_{\mathbf{k}}^0)^2\ , \tag{2.27}$$

where

$$\Omega_0^2=\frac{4\pi q^2\bar{n}_0}{\epsilon_0 m},\quad \varepsilon_k^0=\frac{\hbar^2k^2}{2m}\ ,$$

and $\bar{n}_0$ is the density of condensed bosons.

An extra term Ak^2 appearing in Eq. (2.24) and absent from Eq. (2.27) follows from the short-range part of the density-density interaction, for both kinematic (hard-core effects) and dynamic interactions, resulting from J_{ij} [$V_{\mathbf{k}}=J_{\mathbf{k}}+K_{\mathbf{k}}=2J_{\mathbf{k}}+2W_{\mathbf{k}}$; compare Eqs. (2.9) and (2.5)]. Notice that the k^4 term in Eq. (2.24) tends to $(\varepsilon_{\mathbf{k}}^0)^2$ in the low-density limit only [$Bk^2\approx(\varepsilon_{\mathbf{k}}^0)^2(1-4n)$]. The form of $\omega_{\mathbf{k}}$ for larger $\mathbf{k}$ is influenced by hard-core effects (except for $n\ll 1$) and by the effects of a discrete lattice and moreover depends on the local pair density ($n/2$). In particular, for $\hbar\Omega_0^*\ll J_0$ ($n\ll 1$) with increasing k, $\omega_{\mathbf{k}}$ steadily increases and merges with the spectrum for the short-range Coulomb forces in the region near the zone boundary ($\omega_{\mathbf{k}}\to\varepsilon_{\mathbf{k}}^0=J_0-J_{\mathbf{k}}$). For $\hbar\Omega_0^*>J_0$ the spectrum is more complicated, having a minimum for some definite value of $\mathbf{k}\neq 0$ (min $\omega_{\mathbf{k}}=\Delta<J_0<\hbar\Omega_0^*$). In contrast to the 3D case, the collective excitation spectrum for a two-dimensional local pair system with long-range Coulomb forces is gapless. In the long-wave limit, RPA calculations yield (Micnas and Robaszkiewicz, 1988a, 1988b)

$$\omega_{\mathbf{k}}^{(2\mathrm{D})}=\left[\frac{2\pi\hbar^2q^2}{\epsilon_0 m^*}\langle\rho^x\rangle^2|\mathbf{k}|+A|\mathbf{k}|^2+B|\mathbf{k}|^4\right]^{1/2} \cong\left[\frac{2\pi\hbar^2q^2\langle\rho^x\rangle^2}{\epsilon_0 m^*}\right]^{1/2}|\mathbf{k}|^{1/2} +\frac{1}{2\left[\frac{2\pi\hbar^2q^2\langle\rho^x\rangle^2}{\epsilon_0 m^*}\right]^{1/2}}(A|\mathbf{k}|^{3/2}+B|\mathbf{k}|^{7/2})\ , \tag{2.28}$$

with A and B given by Eq. (2.26).

The spectrum (2.28) can again be compared with the RPA energy spectrum at $T=0$ K, for a standard 2D charged Bose gas derived by Hines and Frankel (1975) in the low-density limit, which for $q=2e$ takes the form

$$\frac{\omega_{\mathbf{k}}^{(2\mathrm{D})}}{\hbar}=\left[\frac{2\pi q^2\bar{n}}{m}|\mathbf{k}|+\frac{\hbar^2|\mathbf{k}|^4}{4m^2}\right]^{1/2}. \tag{2.29}$$

The differences between Eqs. (2.28) and (2.29) have the same origin as in the 3D case [see comments below Eq. (2.27)].

3. Thermodynamic properties, especially transition temperature

The existence of sound-wave-like collective excitations for sufficiently screened Coulomb interactions changes qualitatively the thermodynamic and electromagnetic properties of the local pair system from those predicted by the mean-field approximation. (Alexandrov and Ranninger, 1981b; Robaszkiewicz *et al.*, 1981a; Kubo and Takada, 1983; Alexandrov *et al.*, 1986b; Micnas and Robaszkiewicz, 1988a, 1988b). The ground-state phase boundary between the M and SS phases is modified (Fig. 4), and the concentration dependence of the superconducting order parameter $\langle\rho^x\rangle$ is changed (Fig. 7) (Alexandrov *et al.*, 1986b). The zero-point fluctuations extend the region of stability of the homogeneous SS phase and suppress charge order. Thus the SS phase exists even in the $K/J=\infty$ limit if $n<n_c\neq 0$, in contrast to the MFA, which yields $n_c=0$ in this limit. For $K/J=\infty$ and for various lattices, n_c is calculated within the RPA and the spin-wave approximation and is given in Table III (Micnas and Robaszkiewicz, 1988a). Due to the gapless nature of the spectrum, the order parameter, the internal energy, and the specific heat acquire *power-law characteristics* in the SS and M phases at low temperatures. In particular, at low enough temperatures, where the linear-in-k term dominates, the specific heat varies as T^d and $\langle\rho^x(0)\rangle-\langle\rho^x(T)\rangle\sim T^{d-1}$, where d is the lattice dimensionality. It is also important to note that in the

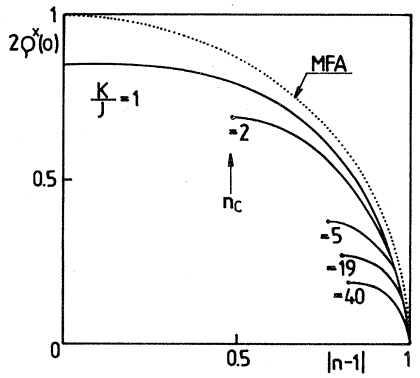

FIG. 7. Concentration dependence of the order parameter at $T=0$ K for a local pair superconductor, for different values of K/J determined within the random-phase approximation. For $n > n_c$ the M phase exists.

low-density limit the k^2 term in the spectrum (2.9) becomes dominant at higher temperatures, and for the SS phase this gives rise to $c_v \sim T^{d/2}$ and $\langle \rho^x(0) \rangle - \langle \rho^x(T) \rangle \sim T^{d/2}$ characteristics that are valid for $T_c > T > T^*$ [T^* being the crossover temperature, $T^* \sim (J_0 + K_0) n_0$, $n_0 = \langle \rho^x(0) \rangle^2$].

The critical temperature for the superconducting transition within the RPA is given by (Alexandrov *et al.*, 1986b)

$$(n-1)^{-1} = \frac{1}{N} \sum_{\mathbf{k}} \coth \left[\frac{(n-1)(J_0 - J_{\mathbf{k}})}{2k_B T_C} \right] . \quad (2.30)$$

If $J_{\mathbf{k}} = 0$, Eq. (2.30) reduces to Eq. (2.8), yielding the MFA transition temperature. In the low-density limit $n \ll 1$, T_c becomes

$$k_B T_C = \frac{3.31 (n a^{-3}/2)^{2/3}}{m^*} [1 - 0.54 (n a^{-3}/2)^{2/3} + \cdots] , \quad (2.31)$$

where $m^* = (2Ja^2)^{-1}$ is the effective mass of the local pair for the simple cubic lattice ($\hbar \equiv 1$).

In the high-density limit $|n-1| \ll 1$, Eq. (2.30) yields

$$k_B T_c = \tfrac{1}{2} J_0 [C^{-1} - \tfrac{1}{3} (n-1)^2] , \quad (2.32)$$

where C is the Watson integral $= 1.5164$, 1.393, and 1.345 for simple cubic, body-centered-cubic, and face-centered-cubic lattices, respectively. The superconducting T_c for the local pair system versus electron concentration is given in Fig. 8. Two facts concerning T_c should be noted. First, the MFA overestimates T_c and yields incorrect concentration dependences of T_c for low densities. Secondly, for $n < 0.1$, T_c is practically the same as for an ideal Bose gas on a lattice, with the density being equal to the density of electron pairs in the system.

TABLE III. Critical electron concentration (n_c) separating the SS phase from the M phase, calculated in the spin-wave approximation (SWA) and in the random-phase approximation (RPA) for various lattices and $K/J = \infty$.

Lattice types	SWA	RPA
sc	0.156	0.135
bcc	0.1186	0.106
Quadratic layer	0.394	0.283

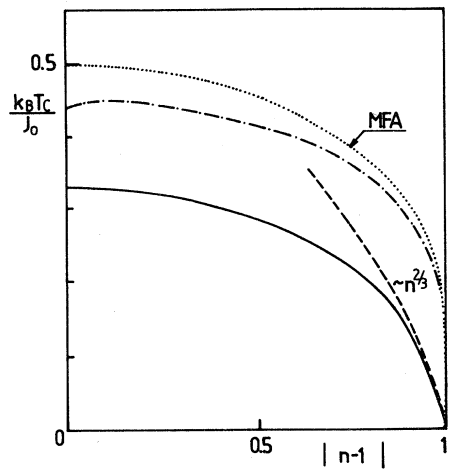

FIG. 8. Critical temperature of a local pair superconductor vs concentration n for $K/J = 1$ ($W = 0$): solid curve, RPA for a simple cubic lattice; dotted curve, MFA; dot-dashed curve, result of the cluster variation method; dashed curve, the T_c for an ideal Bose gas.

As has already been mentioned, superconductivity in a local pair system can also be considered as a condensation of charged bosons. Using Eq. (2.5), we can rewrite the Hamiltonian (2.2) as

$$\bar{H} = -\sum_{i,j} J_{ij} b_i^\dagger b_j + \sum_{i,j} K_{ij} n_i n_j - \bar{\mu} \sum_i n_i + \text{const} , \quad (2.33)$$

where $\bar{\mu}$ is the chemical potential for bosons. The first term in Eq. (2.33) describes the boson hopping, whereas the second term describes the boson interaction. These lattice bosons have a hard-core interaction that prevents two bosons from occupying the same site. This hard-core condition can be modeled by adding the term $U' \sum_i n_i n_i$ to Eq. (2.33) and by taking the limit $U' \to \infty$ excluding double occupancy; i.e., Eq. (2.33) is a kind of Hubbard model for the lattice bosons.

In the very dilute limit, the hard-core interaction is not relevant and $[b_i, b_i^\dagger] = 1 - 2n_i \approx 1$ ($n \ll 1$). Thus, in that limit, one can consider Eq. (2.33) as a weakly nonideal Bose gas. The Bose-Einstein condensation temperature is readily determined in $d = 3$ to be $k_B T_0 = (3.31/m^* a^2)(n/2)^{2/3}$, which is just the first term in the expansion (2.31). In the dilute limit, the boson interaction (including the hard-core effects) changes T_c as (Micnas, 1988a)

$$(T_c - T_0)/T_0 = -(1 + K/J) n , \quad (2.34)$$

where T_0 is the Bose-Einstein condensation temperature.

An important, experimentally measured quantity is the

jump of the specific heat at T_c: Δc. Within the MFA one obtains $\Delta c/k_B n \sim (J_0/k_B T_c)^2 > 1$, where T_c is given by Eq. (2.8). In the low-concentration limit, where the MFA is not realistic, Δ_c can be estimated by means of the standard formulas of the Landau quasiparticle theory, with the quasiparticle spectrum given by Eq. (2.9), which in a dilute limit reduces to that of a weakly nonideal Bose gas. In this way one gets $\Delta c/k_B n \sim 0-1$, depending on the strength of the interparticle potential and the particle (local pair) density (Micnas and Robaszkiewicz, 1988a, 1988b; Sobyanin, 1988).

Let us now consider the *quasi-two-dimensional case* for the superconductivity of local pair systems (Micnas and Robaszkiewicz, 1988a). In order to obtain T_c we use the self-consistent RPA equation (2.30) for a simple tetragonal lattice with

$$J_{\mathbf{k}} = 2J_{\parallel}(\cos k_x a + \cos k_y a) + 2J_{\perp}\cos k_z d \ .$$

The quantities a and d denote the intralayer and interlayer lattice spacings, respectively. In the high-density limit, T_c versus n is again given by Eq. (2.32), with C now being the Watson integral for anisotropic lattices and

$$J_0 = 4J_{\parallel} + 2J_{\perp} \ ,$$

$$C = \frac{2+\alpha}{N}\sum_k (2+\alpha-\cos k_x a - \cos k_y a - \alpha\cos k_z d)^{-1} \ ,$$

$$\alpha = J_{\perp}/J_{\parallel} \ .$$

The region of density for which Eq. (2.32) is valid diminishes with decreasing α.

On the other hand, in the low-density limit ($n \ll 1$), the concentration dependence of T_c changes with the ratio α. For $\alpha < 1$, T_c is well described by

$$k_B T_c = 4.17 J_{\parallel}\alpha^{1/3} n^{2/3} = \frac{3.31(n^*)^{2/3}}{m^*} \ , \qquad (2.35a)$$

which is just the formula for the $d=3$ (anisotropic) free Bose gas with an effective mass $m^* = (m_{\perp}^2 m_{\parallel})^{1/3}$, $m_{\parallel} = (2J_{\parallel}a^2)^{-1}$, $m_{\perp} = (2J_{\perp}d^2)^{-1}$, and with a density equal to the density of electron pairs in the system $n^* = \frac{1}{2}n(a^2 d)^{-1}$. However, for $\alpha \ll 1$, T_c is governed by the expression

$$k_B T_c = J_{\parallel}\frac{2\pi(1-|n-1|)}{\ln\left[\dfrac{k_B T_c}{J_{\perp}|n-1|}\right]} \cong \frac{2\pi n^* d}{m_{\parallel}\ln(2k_B T_c m_{\perp} d^2)} \ , \qquad (2.35b)$$

which shows linear-in-n behavior and reduces to the formula for a noninteracting Bose gas with a quasi-two-dimensional spectrum,

$$E_k = \frac{1}{2m_{\parallel}}(p_x^2 + p_y^2) + \frac{1}{m_{\perp}d^2}(1-\cos k_z d) \ , \qquad (2.35c)$$

where the bandwidth in the k_z direction $m_{\perp}^{-1}d^{-2} \ll k_B T_c$, and where the density is n^*. The crossover of T_c-versus-n behavior from that of a Bose gas with anisotropic mass ($T_c \sim n^{2/3}$) to that of a quasi-two-dimensional (or $d=2+\varepsilon$) Bose gas ($T_c \sim n$) takes place at $\alpha \sim 10^{-2}$. In Fig. 9 we give full numerical solutions of T_c versus n for several different ratios α. We also observe that the range of electron concentration for which T_c exhibits linear-in-n dependence strongly extends with decreasing α.

To close this subsection, let us discuss briefly the effects of *long-range Coulomb forces* on the thermodynamic properties of the SS phase. As was pointed out in Sec. II.B.2, if the long-range Coulomb interaction between local pairs is not screened by other carriers, pseudomagnon collective excitations in the SS phase will acquire a plasmalike gap in three dimensions [cf. Eq. (2.24)]. Due to this fact the leading thermodynamic characteristics at low temperatures will be exponential rather than power-law like. In particular, for $\hbar\Omega_0^* \ll J_0$, the specific heat and the order parameter for $T \to 0$ calculated in the RPA are given by (Micnas and Robaszkiewicz, 1988b)

$$c_v \sim T^{-1/2}\exp\left[-\frac{\hbar\Omega_0^*}{k_B T}\right] , \qquad (2.36a)$$

$$\langle\rho^x(0)\rangle - \langle\rho^x(T)\rangle \sim T^{1/2}\exp\left[-\frac{\hbar\Omega_0^*}{k_B T}\right] , \qquad (2.36b)$$

whereas for $\hbar\Omega_0^* > J_0$ one gets

$$c_v \sim T^{-1/2}\exp\left[-\frac{\Delta}{k_B T}\right] , \qquad (2.37)$$

$$\langle\rho^x(0)\rangle - \langle\rho^x(T)\rangle \sim T^{1/2}\exp\left[-\frac{\Delta}{k_B T}\right] , \qquad (2.38)$$

where

$$\Delta = \min\omega_k < \hbar\Omega_0^* \ .$$

In both cases the power-law temperature dependences $c_v \sim T^{3/2}$, $\langle\rho^x(0)\rangle - \langle\rho^x(T)\rangle \sim T^{3/2}$ can be recovered at higher T, i.e., if $k_B T_c > k_B T > \hbar\Omega_0^*$ (or Δ). In the case of a standard $d=3$ charged Bose gas, the calculation of $c_v(T)$ and the density of condensed bosons $n_0(T)$ performed within the Bogoliubov approximation yields at $T \to 0$ (Fetter, 1970)

$$c_v \sim T^{-5/4}\exp\left[-\frac{\hbar\Omega_0}{k_B T}\right] , \qquad (2.39)$$

$$\bar{n}_0(0) - \bar{n}_0(T) \sim T^{1/4}\exp\left[-\frac{\hbar\Omega_0}{k_B T}\right] , \qquad (2.40)$$

where Ω_0 is given by Eq. (2.27). The differences between the preexponential factors in Eqs. (2.35), (2.36) and (2.39), (2.40) result from a difference between the excitation spectra of the two models [compare Eqs. (2.24) and (2.27)] and in particular from the fact that the Ak^2 term in Eq. (2.24) is generated by the short-range interaction

J_{ij}. At higher temperatures a crossover to power-law characteristics, $c_v \sim T^{d/2}$, $\langle \rho^x(0) - \rho^x(T) \rangle \sim T^{d/2}$, can take place for $\hbar\Omega_0^* < J_0$.

The effects of unscreened long-range Coulomb interactions on the critical temperature T_c, as well as the nature of the phase transition and critical behavior in such a case (see Sec. II.B.5), have not been fully explored to date. Estimates of T_c for a model based on a semimicroscopic approach analogous to the Landau theory of ^{4}He II yield $T_c \leq T_0$ (Micnas and Robaszkiewicz, 1988b; Sobyanin, 1988). A similar result has been obtained for a standard d-dimensional dense charged Bose gas by means of a self-consistent Hartree-Fock theory with a static screened interparticle potential; this theory estimates the shift in the transition temperature as (Fetter, 1971; R. F. Bishop, 1974)

$$(T_c - T_0)/T_0 \sim r_s^{(d-2)/3} \quad \text{for } d > 2 , \tag{2.41}$$

where $r_s = (q^2 m/\hbar^2)(4\pi\bar{n}/3)^{-1/3}$ is the ratio of the interparticle spacing to the Bohr radius.

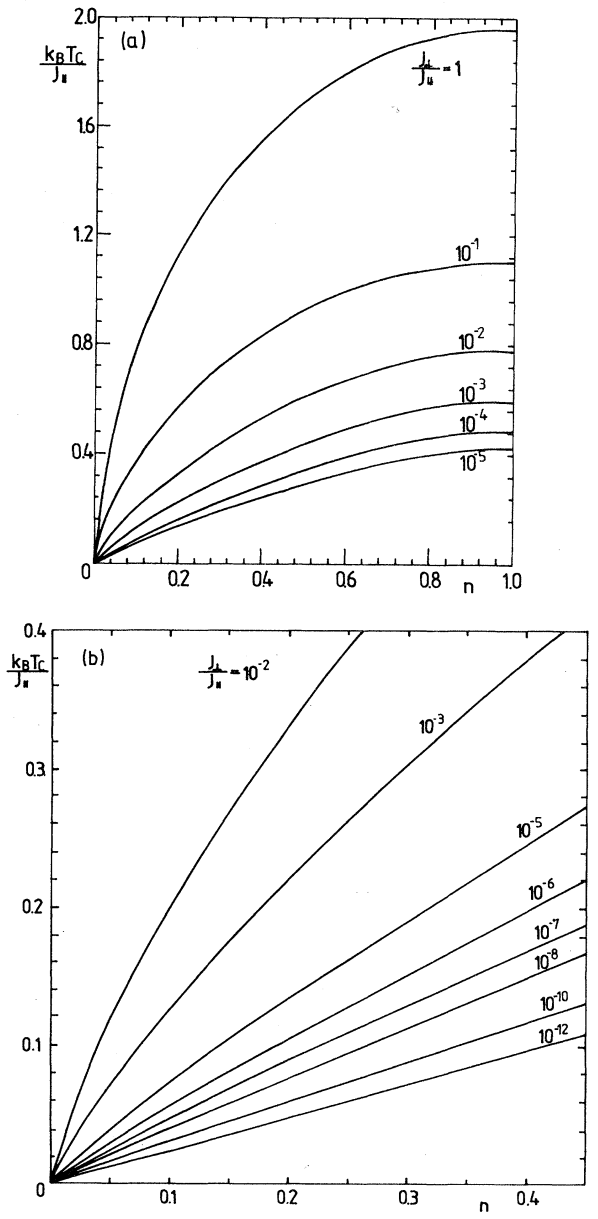

FIG. 9. (a) Critical temperature of a local pair superconductor vs concentration n, for a quasi-two-dimensional lattice, determined within the self-consistent RPA method. $K_\parallel/J_\parallel = K_\perp/J_\perp = 1$. For $\alpha \lesssim 10^{-2}$ and low n, there is a crossover of T_c from that of a Bose gas with anisotropic mass to that of a Bose gas in $d = 2+\varepsilon$, showing linear-in-n behavior. (b) As in (a). Notice the expansion of the concentration region with a linear-in-n behavior of T_c with decreasing $\alpha = J_\perp/J_\parallel$.

4. Electrodynamic properties: the penetration depth, H_c, H_{c_1} and H_{c_2}

The electrodynamic properties of local pair superconductors have been analyzed within the mean-field approach for the Ginzburg-Landau functional, and we refer the reader to the work by Bulaevskii *et al.* (1984) for details. Their analysis shows that the superconductivity of local pairs is of extreme type II with very short coherence length, substantial penetration depth, small H_{c_1}, and extremely large H_{c_2}. However, mean-field-type analysis may be insufficient to describe the electrodynamics, due to the equivalence of this problem to that of a hard-core charged Bose gas on a lattice. In particular, in the low-density limit, one clearly is dealing with the problem of an interacting charged Bose gas in an electromagnetic field. We should point out that, while the electromagnetic properties of a charged Fermi gas are well understood, this is not the case for a charged Bose gas. The dielectric properties and the excitation spectrum of a charged Bose gas, both with and without magnetic field, have been investigated repeatedly (Foldy, 1961, 1962; Hore and Frankel, 1975, 1976). On the other hand, not much is known about various critical fields H_{c_1} (lower), H_{c_2} (upper), H_c (thermodynamic) and the vortex structure of the charged Bose superfluid. Before the Bardeen-Cooper-Schrieffer (1957) theory (BCS), Schafroth showed that an ideal charged Bose gas exhibits the Meissner effect and has an upper critical field H_{c_2} identically zero, i.e., there is no condensation at any temperature in the noninteracting charged Bose gas for arbitrarily small applied magnetic field (Schafroth, 1955; Schafroth *et al.*, 1957; Blatt, 1964).

The problem to which we address ourselves is essentially that of a charged interacting hard-core Bose gas on a lattice. For arbitrary density of bosons, the electrodynamics of this gas is at present only accessible within the mean-field theory (Bulaevskii *et al.*, 1984), but a rather complete picture begins to emerge for the low-density limit (Alexandrov *et al.*, 1986b; Alexandrov, Samarchenko, and Traven, 1987).

a. Interacting charged hard-core Bose gas in the dilute limit

For the following discussion of the penetration depth H_{c_1} and H_c we shall closely follow the description given by Alexandrov *et al.* (1986b) and Alexandrov, Samarchenko, and Traven (1987). We shall start from our microscopic Hamiltonian (2.1) for on-site pairs and derive phenomenological equations of the Ginzburg-Pitaevskii type for a weakly interacting Bose gas. This is possible in the low-density limit, where the $s=\frac{1}{2}$ Pauli operators $\rho_i^{\pm}$ can be replaced by the boson operators $b_i, b_i^{\dagger}$, since $[\rho_i^{+},\rho_i^{-}]=1-2n_i\approx 1$ in this limit. In order to make the link with the well-known derivation of the Ginzburg-Pitaevskii equations for a neutral Bose gas, let us introduce the field operators $\psi^{\dagger}(\mathbf{r})$, $\psi(\mathbf{r})$ defined by

$$b_i^{(\dagger)}=\sqrt{V/N}\int d^3r\,\psi(\mathbf{r})^{(\dagger)}\delta(\mathbf{r}-\mathbf{R}_i)\ ,$$
$$\psi(\mathbf{r})^{(\dagger)}=\sqrt{V/N}\sum_i \delta(\mathbf{r}-\mathbf{R}_i)b_i^{(\dagger)}\ , \tag{2.42}$$

where V is the volume of the system and N is the number of sites. The Hamiltonian (2.33) then becomes

$$\mathcal{H}=-\int d^3r\int d^3r' J(\mathbf{r}-\mathbf{r}')\psi^{\dagger}(r)\psi(\mathbf{r}')$$
$$+\int d^3r\int^3 r' K(\mathbf{r}-\mathbf{r}')\psi^{\dagger}(\mathbf{r})\psi^{\dagger}(\mathbf{r}')\psi(\mathbf{r})\psi(\mathbf{r}')$$
$$-\bar{\mu}\int d^3r\,\psi^{\dagger}(\mathbf{r})\psi(\mathbf{r})\ , \tag{2.43}$$

where

$$J(\mathbf{r}-\mathbf{r}')=\frac{V}{N}\sum_{i,j}J_{ij}\delta(\mathbf{r}-\mathbf{R}_i)\delta(\mathbf{r}'-\mathbf{R}_j)\ ,$$
$$K(\mathbf{r}-\mathbf{r}')=\left[\frac{V}{N}\right]^2\sum_{i,j}K_{ij}\delta(\mathbf{r}-\mathbf{R}_i)\delta(\mathbf{r}'-\mathbf{R}_j)\ . \tag{2.44}$$

An external magnetic field can now be easily incorporated in this Hamiltonian. There are in general two contributions. One couples the magnetic field H to the spin degrees of freedom, i.e.,

$$-g\mu_B H\sum_i (c_{i\uparrow}^{\dagger}c_{i\uparrow}-c_{i\downarrow}^{\dagger}c_{i\downarrow})\ ,$$

where g is the gyromagnetic factor and μ_B is the Bohr magneton. This contribution is negligible for the case of singlet on-site pairs. The second contribution of an external magnetic field is due to its coupling to the orbital motion of the local pairs. This coupling can be taken into account in the same fashion as for fermions by making use of the replacement

$$J_{ij}\rightarrow J_{ij}\exp\left[-\frac{2ei}{\hbar c}\int_{\mathbf{R}_i}^{\mathbf{R}_j}\mathbf{A}(\mathbf{r})d\mathbf{r}\right]\ . \tag{2.45}$$

where $\mathbf{A}(\mathbf{r})$ denotes the vector potential. Notice that the charge $2e$ enters because of the bosons' being made up of two electrons. Considering only slow variations of $\mathbf{A}(\mathbf{r})$ on the scale of a few lattice constants, we can write

$$J(\mathbf{r}-\mathbf{r}')=\frac{1}{V}\sum_{\mathbf{k}}e^{i\mathbf{k}\cdot(\mathbf{r}-\mathbf{r}')}J_{\mathbf{k}+(2e/\hbar c)\mathbf{A}}\ . \tag{2.46}$$

In order to get the continuum limit we expand $J_{\mathbf{k}+(2e/\hbar c)\mathbf{A}}$ near $\mathbf{k}=0$, yielding the expression for a free Bose gas in the continuum

$$J(\mathbf{r}-\mathbf{r}')=\left[J_0+\frac{\hbar^2}{2m^*}\left[\nabla-\frac{2ie}{\hbar c}\mathbf{A}(\mathbf{r})\right]^2\right]\delta(\mathbf{r}-\mathbf{r}')\ , \tag{2.47}$$

where the effective mass is given by

$$m^*=-\hbar^2\left[\frac{\partial^2 J_k}{\partial k^2}\right]^{-1}\Bigg|_{k=0}=\frac{\hbar^2}{2Ja^2}\ .$$

Therefore the Hamiltonian (2.43) reads

$$\mathcal{H}=-\frac{\hbar^2}{2m^*}\int d^3r\,\psi^{\dagger}(\mathbf{r})\left[\nabla-\frac{2ie}{\hbar c}\mathbf{A}(\mathbf{r})\right]^2\psi(\mathbf{r})$$
$$+\int d^3r\int d^3r' K(\mathbf{r}-\mathbf{r}')\psi^{\dagger}(\mathbf{r})\psi^{\dagger}(\mathbf{r}')\psi(\mathbf{r})\psi(\mathbf{r}')$$
$$-\tilde{\mu}\int d^3r\,\psi^{\dagger}(\mathbf{r})\psi(r)\ , \tag{2.48}$$

where $\tilde{\mu}=\bar{\mu}+J_0$.

The Ginzburg-Landau-Pitaevskii equation can now be derived in standard fashion. The time evolution of the field operator $\psi(\mathbf{r},t)$ in the Heisenberg representation is given by

$$i\hbar\frac{\partial\psi(\mathbf{r},t)}{\partial t}=-\left[\tilde{\mu}+\frac{\hbar^2\left[\nabla-\frac{2ie}{\hbar c}\mathbf{A}(\mathbf{r})\right]^2}{2m^*}\right]\psi(\mathbf{r},t)$$
$$+2\int d^3r'\psi^{\dagger}(\mathbf{r}',t)K(\mathbf{r}-\mathbf{r}')\psi(\mathbf{r}',t)\psi(\mathbf{r},t)\ . \tag{2.49}$$

We approximate $K(\mathbf{r}-\mathbf{r}')$ by a weak, short-range (contact) interaction $K(\mathbf{r}-\mathbf{r}')=\bar{K}_0\delta(\mathbf{r}-\mathbf{r}')$, $\bar{K}_0=K_0a^3$ and assume the conditions for the dilute gas limit

$$n^{1/3}l\ll 1,\quad l=\frac{m^*}{4\pi\hbar^2}\int d^3r\ K(r)=\frac{m^*}{4\pi\hbar^2}\bar{K}_0$$

to be satisfied, where l denotes the scattering length in the Born approximation. Let us now decompose the field operator $\psi(r,t)$ in the form

$$\psi(\mathbf{r},t)=\psi_0(\mathbf{r},t)+\bar{\psi}(\mathbf{r},t)\ , \tag{2.50}$$

where we take

$$\psi_0(\mathbf{r},t)=\lim_{\substack{N\rightarrow\infty\\ V\rightarrow\infty}}\langle\bar{N}|\psi(r,t)|\bar{N}+1\rangle,\ \bar{N}/V=\text{const}\ , \tag{2.51}$$

which is a c number giving the macroscopic wave function of the condensate. $\bar{N}$ denotes the total number of particles. The average density of particles in the condensed phase is given by

$$\bar{n}_0=\frac{1}{V}\int d^3r|\psi_0(r,t)|^2 . \tag{2.52}$$

$\bar{\psi}(r,t)$ describes the part of $\psi(r,t)$ that is not in the condensed phase. Provided we are at low temperatures (well below the Bose condensation temperature), we can neglect the contribution from noncondensed bosons and obtain the following equation for ψ_0:

$$i\hbar\frac{\partial\psi_0(\mathbf{r},t)}{\partial t}=-\left[\tilde{\mu}+\frac{\hbar^2}{2m^*}\left[\nabla-\frac{2ie}{\hbar c}\mathbf{A}(\mathbf{r})\right]^2\right]\psi_0(\mathbf{r},t)$$
$$+2\bar{K}_0|\psi_0(\mathbf{r},t)|^2\psi_0(\mathbf{r},t) . \tag{2.53}$$

This is a direct generalization of the Ginzburg-Pitaevskii equation for a neutral Bose gas.

Within the same approximation one gets for the supercurrent

$$\mathbf{j}_s(\mathbf{r},t)=\frac{\hbar e}{m^*i}[\Psi_0^*(\mathbf{r},t)\nabla\Psi_0(r,t)-\Psi_0(r,t)\nabla\Psi_0^*(r,t)]$$
$$-\frac{4e^2}{m^*c}|\Psi_0|^2\mathbf{A}(\mathbf{r}) , \tag{2.54}$$

which is related to the vector potential by the Maxwell equation

$$\text{rot rot}\,\mathbf{A}(\mathbf{r},t)=\frac{4\pi}{c}\mathbf{j}_s(\mathbf{r},t) . \tag{2.55}$$

Therefore the London equation follows,

$$\text{rot}\mathbf{J}=-\frac{4\bar{n}_0e^2}{m^*c}\mathbf{H} . \tag{2.56}$$

It should be pointed out that the existence of the London equation for the weakly nonideal charged Bose gas has also been demonstrated by Ranninger and Thirring (1963) on the basis of a gauge-invariant formulation of linear-response-function theory. Moreover, the $(\mathbf{q},\omega)$-dependent magnetic susceptibility was calculated by Ranninger and Thirring (1963), yielding the following contribution from condensed bosons:

$$\chi_s(\mathbf{q},\omega)=-\frac{4e^2n_0}{m}\frac{\omega_q^2}{q^2(\omega_q^2-\omega^2)} , \tag{2.57}$$

where $\omega_q=[(\varepsilon_q^0)^2+2n_0\varepsilon_q^0K_q]^{1/2}$, $\varepsilon_q^0=\hbar^2q^2/2m$ is the excitation spectrum of the weakly nonideal Bose gas, with K_q being the Fourier transform of K_{ij}.

Equations (2.53), (2.54), and (2.55) are obviously equivalent to the Ginzburg-Landau equations, and the penetration depth is given by

$$\lambda_H=\left[\frac{m^*c^2}{16\pi\bar{n}_0e^2}\right]^{1/2} . \tag{2.58}$$

The coherence length determined from the spatial variation of $\psi_0(r)$ is given by

$$\xi_0=\left[\frac{\hbar^2}{4m^*\bar{n}_0\bar{K}_0}\right]^{1/2} , \tag{2.59}$$

where we inserted the low-temperature relation for the chemical potential $\bar{\mu}=2\bar{n}_0\bar{K}_0$, with $\bar{n}_0$ being the density of condensed bosons. The Ginzburg-Landau parameter $\kappa=\lambda_H/\xi_0$ then becomes

$$\kappa=\frac{m^*c}{\hbar}\left[\frac{K_0a^3}{4\pi e^2}\right]^{1/2} , \tag{2.60}$$

where a is the intersite distance. Taking the effective radius of the interaction K_{ij} to be of order of a few lattice constants and $m^*>m_e$, we find that we are dealing with an extreme type-II superconductor. The thermodynamic critical field is given by

$$H_c^2/8\pi=F_s(H=0)-F_s(H_c)$$
$$=F_s(H=0)-F_N(H_c) ,$$

which near $T=0$ becomes

$$H_c=\bar{n}_0(8\pi\bar{K}_0)^{1/2} . \tag{2.61}$$

The lower critical field H_{c_1} is given by

$$H_{c_1}\simeq\frac{H_c}{\sqrt{2}\kappa}\ln\kappa=\frac{4\pi\hbar e\bar{n}_0}{m^*c}\ln\left[\frac{m^*c}{\hbar}\left[\frac{\bar{K}_0}{4\pi e^2}\right]^{1/2}\right] . \tag{2.62}$$

The upper critical field is formally given by

$$H_{c_2}=\sqrt{2}\kappa H_c . \tag{2.63}$$

We notice that in the dilute limit, inclusion of hard core effects in a first approximation amounts to a change $K_0\to J_0+K_0$ in Eqs. (2.59)–(2.63) (Micnas and Robaszkiewicz, 1988a).

b. Upper critical field and dimensionality

Let us now consider the question of the upper critical field H_{c_2} in more detail. Schafroth (1955) has already demonstrated that this critical field for an ideal charged Bose gas is zero. This is due to the fact that in the presence of a magnetic field an ideal charged 3D Bose gas has the dispersion $\omega_k=\sum_n\omega_n+k_z^2/2m$, where $\omega_n=\omega_0(n+\frac{1}{2})$, with

$$\omega_0=\frac{2eH}{mc}$$

being the cyclotron frequency. As a result the particle motion is effectively one dimensional, and no Bose condensation can occur at any temperature. The three-dimensional character of the system can be reestablished either by introducing boson-impurity scattering (Alexandrov *et al.*, 1986b) or by an interaction between the bosons (Alexandrov, Samarchenko, and Traven, 1987). The effect is to round off the one-dimensional singularities in the density of states at the bottom of the boson band, which leads to an effective three-dimensional problem. H_{c_2} is determined as that value of the external magnetic field H at which, at a given temperature $T\le T_c$, the Bose

condensation is suppressed. This happens when the chemical potential $\mu(H,T)$ coincides with the lowest eigenvalue of the charged Bose gas in a magnetic field:

$$\mu(H_{c_2},T)=\frac{eH_{c_2}}{mc}+\Sigma_{H_{c_2}}(\mathbf{k}=0,\omega=0)\ . \tag{2.64}$$

$\Sigma_{H_{c_2}}(\mathbf{k},\omega)$ denotes the self-energy of bosons with wave vector $\mathbf{k}$ and frequency ω evaluated in the normal state in the presence of a magnetic field. This self-energy has been evaluated for boson-impurity scattering (Alexandrov *et al.*, 1986b) and for a weakly interacting Bose gas (Alexandrov, Samarchenko, and Traven, 1987). For the latter case it yields a renormalized boson energy dispersion for the lowest Landau level of the form (Alexandrov, Samarchenko, and Traven, 1987)

$$\bar{\varepsilon}_0(k_z)=\frac{k_z^2}{2m^*}+\left[\frac{K_0}{4\pi^3}\right]^{1/4}(m^*\omega_0)^{1/2}T^2\sqrt{|k_z|}\ . \tag{2.65}$$

H_{c_2} as a function of T and the boson density $\bar{n}$ is then determined by the expression

$$\bar{n}=\frac{eH_{c_2}}{\pi^2 h}\sum_n\int_{-\infty}^{+\infty}dk_z\frac{1}{e^{\beta[\bar{\varepsilon}_n(k)-\mu(H_c,T)]}-1}\ , \tag{2.66}$$

together with Eq. (2.64).

$\bar{\varepsilon}_n(k_z)$ is the renormalized eigenfrequency of the nth Landau level for $H=H_{c_2}$ in the normal state. Since the dominant contribution to the sum in Eq. (2.66) comes from the lowest Landau level, i.e., $n=0$, all the other Landau orbitals can be neglected and, for $n\geq 1$, $\varepsilon_n(k)$ can be replaced by the boson dispersion in the absence of magnetic field. This finally yields (Alexandrov, Samarchenko, and Traven, 1987)

$$\bar{n}\left[1-\left[\frac{T}{T_0}\right]^{3/2}\right]=\frac{eH_{c_2}}{\pi^2 h}\int_{-\infty}^{+\infty}\frac{dk_z}{\beta\bar{\varepsilon}_0(k_z)}\ , \tag{2.67}$$

from which H_{c_2} has been determined to be

$$H_{c_2}\approx 3.74\frac{\phi_0}{2\pi}\left[\frac{\bar{n}}{l}\right]^{1/2}\frac{T_0}{T}\left\{\left[1-\left[\frac{T}{T_0}\right]^{3/2}\right]\right\}^{3/2} \tag{2.68}$$

for weakly interacting bosons. Here $\phi_0=hc/2e$ is the flux quantum, T_0 is the Bose-Einstein condensation temperature, and l denotes the scattering length.

A similar result is obtained for a system with boson-impurity scattering (Alexandrov *et al.*, 1986b),

$$H_{c_2}(T)=0.64\frac{\phi_0}{2\pi}\left[\frac{\bar{n}}{l_{\rm imp}}\right]^{1/2}\left\{\frac{T_0}{T}\left[1-\left[\frac{T}{T_0}\right]^{3/2}\right]\right\}^{3/2}\ , \tag{2.69}$$

where $l_{\rm imp}=(4\pi n_{\rm imp}f^2)^{-1}$ is the mean free path of the bosons, $n_{\rm imp}$ the impurity concentration, and f the boson-impurity scattering amplitude. The expressions for H_{c_2} show a temperature behavior

$$\left[1-\left[\frac{T}{T_c}\right]^{3/2}\right]^{3/2}$$

near T_c with a positive curvature for H_{c_2}. This is a *characteristic feature* of charged bosons. With decreasing temperature, H_{c_2} as given by Eqs. (2.68) and (2.69) formally diverges. This divergency results from the assumption in the derivation of H_{c_2} that $T>\omega$. In any case, for charged bosons we expect very high values of H_{c_2} and saturation towards $H_{c_2}(T=0)=\phi_0/2\pi\xi_0^2$ as $T\to 0$, with ξ_0 given by Eq. (2.59). In Fig. 10 the temperature dependence of H_{c_2} is shown.

Finally we should mention the interesting case of the quasi-two-dimensional charged Bose gas; the electromagnetic properties of this system have been analyzed by Wen and Kan (1988).

5. Critical behavior

As has been shown above, the $U<0$ Hubbard model in the $|U|\gg t$ limit can be described by an effective pseudospin Hamiltonian [Eq. (2.2)], and the superconducting state corresponds to an ordering of "spins" in the XY plane. In view of this equivalence one expects the critical behavior to be very different from that of the BCS model. The symmetry of a superconducting local pair system is equivalent to that of the XY model, and hence its universality class should be the same as that of the quantum $S=\frac{1}{2}$ XY model. Moreover, according to the universality, its critical behavior should also be equivalent to that of ^{4}He II, i.e., the critical properties are of the same nature as those near the λ transition in helium.

Such a system with short coherence length will exhibit

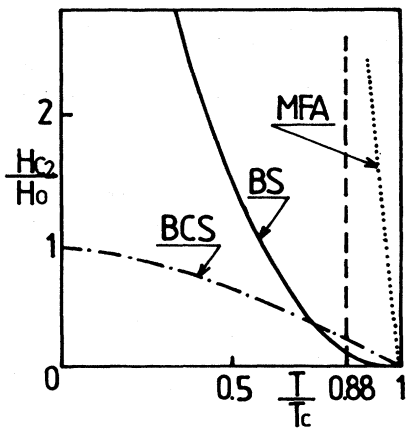

FIG. 10. Temperature dependence of the upper critical field H_{c_2} for a local pair superconductor: dotted curve, the MFA result of Bulaevskii *et al.* (1984); solid curve (BS), upper critical field for a charged Bose gas (with impurity scattering); dot-dashed line, H_{c_2} for a BCS type-II superconductor.

a wide critical regime, and its true critical behavior should be observable. This is in contrast to the weak-coupling BCS model, in which the width of the critical regime can be as narrow as $10^{-15}T_c$ and is usually experimentally inaccessible, so that the Ginzburg-Landau critical exponents apply. One therefore expects that the specific heat of a local pair system in $d=3$ will exhibit a λ anomaly (Fig. 11), the correlation length will vary as $\xi \sim |\tau|^{-\nu}$ with $\nu \approx \frac{2}{3}$, and the order parameter as $n_0 \sim |\tau|^{2\beta}$ with $\beta \approx \frac{1}{3}$ [$\tau=(T-T_c)/T_c$].

In Table IV we summarize critical exponents for local pair superconductors and compare them with the Ginzburg-Landau critical exponents. They follow from general considerations based on the Ginzburg-Landau functional and dimensional analysis (Bulaevskii *et al.*, 1984; Lobb, 1987; Kapitulnik *et al.*, 1988). The penetration depth $\lambda_H \sim (n_0)^{-1/2}$ has an exponent ($\sim \frac{1}{3}$) that is different from that of the correlation length ($\sim \frac{2}{3}$), and consequently the Ginzburg-Landau ratio $\kappa=\lambda_H/\xi$ will be temperature dependent ($\kappa \sim |\tau|^{1/3}$). One therefore expects a crossover near T_c from type-II to type-I superconductivity. Such behavior also allows for the possibility of a weakly first-order phase transition due to intrinsic fluctuations of the vector potential A (Halperin *et al.*, 1974; Chen *et al.*, 1978; Dasgupta and Halperin, 1981; Doniach, 1984).

The critical exponents for H_c, H_{c_1}, H_{c_2} are also different from those of the BCS model, and H_{c_2} will have an exponent $2\nu \sim \frac{4}{3}$, since $H_{c_2}=\phi_0/2\pi\xi^2$. Furthermore, as was pointed out by Bulaevskii *et al.* (1984) and Lobb (1987), the dynamical phenomena for $T > T_c$ should display behavior different from that of the BCS theory, in particular, as concerns the fluctuation component of the conductivity and the diamagnetism.

Some of these predictions seem to have been observed in the new high-T_c materials of the Y-Ba-Cu-O family, namely, the positive curvature of H_{c_2} and the critical behavior of H_{c_2} with an exponent $\nu \sim 0.65$ (Oh *et al.*, 1988), the fluctuation excess of the conductivity for $T > T_c$ (Vidal *et al.*, 1988), and a logarithmic singularity in the specific heat (Butera, 1988; Ishikawa *et al.*, 1988; Voronel *et al.*, 1988).

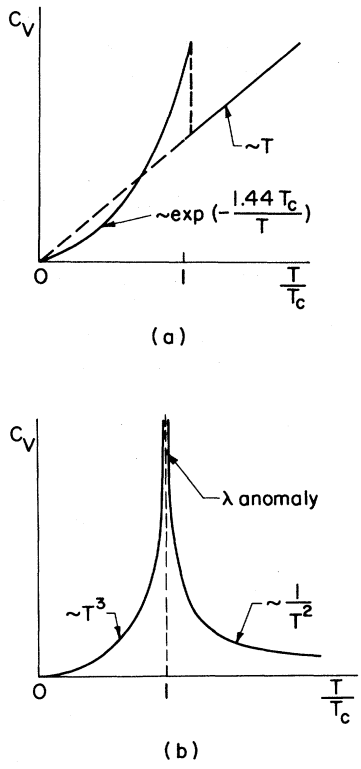

FIG. 11. Specific heat for (a) BCS and (b) local pair superconductors. $\Delta C_v/\gamma T_c=1.43$ in the BCS theory, with γ being the Sommerfeld constant.

Although many of these predictions are universally correct, a full description of critical phenomena in charged superfluids is at present not completely worked out. For example, for a charged Bose gas with Coulomb forces, Ma (1972) has argued that the critical exponents ν and η should be the same as for a neutral Bose gas, but that there will be differences in the correlation functions. It should also be stressed that in the presence of a long-

TABLE IV. Critical exponents for Bardeen-Cooper-Schrieffer (BCS) and local pair (LP) superconductors in $d=3$. n_0 is the density of superconducting electrons, σ_s is the fluctuation component of the conductivity, and $\tau=(T-T_c)/T_c$.

	$c_v \sim \tau^{-\alpha}$	$\xi \sim \lvert\tau\rvert^{-\nu}$	$n_0 \sim \lvert\tau\rvert^{2\beta}$	$\lambda_H \sim \lvert\tau\rvert^{-l}$	$\kappa \sim \lvert\tau\rvert^{-\bar{m}}$	$H_c \sim (-\tau)^{1-\alpha/2}$	$H_{c_1} \sim (-\tau)^{2\beta}$	$H_{c_2} \sim (-\tau)^{2\nu}$	$\sigma_s \sim \tau^{-\bar{s}}$
BCS superconductor Ginzburg-Landau critical exponent	$\alpha=0$ discontinuity	$\nu=\frac{1}{2}$	$\beta=\frac{1}{2}$	$l=\frac{1}{2}$	$\bar{m}=0$	$=1$	$=1$	$=1$	$\bar{s}=\frac{1}{2}$
Local pair Superconductor critical exponent	$\lvert\alpha\rvert \le 10^{-2}$ or $\ln\lvert\tau\rvert$	$\nu \simeq \frac{2}{3}$	$\beta \simeq \frac{1}{3}$	$l \simeq \frac{1}{3}$	$\bar{m} \simeq \frac{1}{3}$	$\simeq 1$	$\simeq \frac{2}{3}$	$\simeq \frac{4}{3}$	$\bar{s} \simeq \frac{1}{3}$

range unscreened Coulomb interaction, Wigner crystallization may compete with the superconducting state for the low-density limit of the hard-core charged Bose gas.

6. Disorder effects

To close this subsection we shall discuss the effects of disorder on the properties of a local pair system. In fact, the very first ideas about $U<0$ centers dealt with amorphous semiconductors, disordered interfaces, and the possibility of "superconducting glasses," i.e., superconducting systems sensitive to structural disorder (Anderson, 1979; Šimanek, 1979; Kulik and Pedan, 1980; Pedan and Kulik, 1982; Kulik, 1984; Micnas *et al.*, 1985a).

Within the framework of the attractive Hubbard model the effects of structural disorder can be modeled by adding the random site energy term $\sum_i E_i n_i$ with random E_i. For $|U| \gg t$, perturbation theory yields (Micnas *et al.*, 1985a)

$$\tilde{H} = -\sum_{i,j} J_{ij}\rho_i^+\rho_j^- + \sum_{i,j} K_{ij}\rho_i^z\rho_j^z - \sum_i (\bar{\mu}-E_i)(2\rho_i^z+1)+\text{const} , \tag{2.70}$$

and the electron concentration n is given (we assume quenched disorder) by

$$\left\langle \frac{1}{N}\sum \langle \rho_i^z \rangle \right\rangle_{\text{av}} = \tfrac{1}{2}(n-1) , \tag{2.71}$$

where $\langle\ \rangle_{\text{av}}$ denotes a configurational average over the probability distribution of E_i. Equation (2.70) is an $s=\frac{1}{2}$ anisotropic antiferromagnet in a random longitudinal magnetic field with the constraint (2.71) on the magnetization. The random E_i is coupled with the CO parameter in the same way as the longitudinal magnetic field is coupled with the antiferromagnetic order parameter. Thus we are dealing with a form of the random-field problem, and it is well known that random E_i will drastically change the critical behavior. On the other hand, SS is a transverse ordering that *is not directly coupled* to random E_i.

Mean-field and renormalization-group (RG) studies have been performed for this problem in the half-filled band case (Micnas *et al.*, 1985a, 1985b). It was found that the CDW ordering is strongly suppressed by diagonal disorder. T_{SS}^c is reduced with increasing degree of disorder (so the Anderson theorem may not be satisfied). Moreover, a stronger suppression of the diagonal correlations than of the transverse ones by random E_i makes possible *disorder-induced superconductivity.* In particular, for $W>0$, increasing disorder can induce a transition from the CO to the SS phase. There is also a rich multicritical behavior depending on the probability distribution of E_i (for details, see Micnas *et al.*, 1985a, 1985b).

The Hubbard model with large negative U, the special case of Eq. (2.70) with $K=J$ ($W=0$), has also been proposed by Kulik and Pedan (1980) as a model of a superconducting glass. Both our results (Micnas *et al.*, 1985a) and those of Kulik and Pedan (1980) reach the same conclusion that the SS phase in local pair superconductors is rather sensitive to diagonal disorder effects, contrary to the standard BCS theory. It is reasonable to assume that the general qualitative features of the model derived from mean-field-type calculations and the renormalization group are correct. However, the mean-field and standard RG analyses are not sufficient to resolve the thermodynamics below dimensionality 4, in view of strong fluctuation effects caused by the randomness. One of the questions to be answered concerning the superconductivity of a local pair system is whether the system will prefer electron pairs localized by disorder or superfluidity of charged pairs. The problem is that of a hard-core charged Bose gas on a lattice in a random potential. In the dilute limit, the simplest model approximating the original one [Eq. (2.70)] is that of a free (or weakly interacting) Bose gas in a random chemical potential,

$$\mathcal{H} = \sum_{i,j} \tilde{t}_{ij} b_i^\dagger b_j - \sum_i (\bar{\mu}-E_i) b_i^\dagger b_i . \tag{2.72}$$

There are several important points to be resolved.

(i) Can free bosons condense in a random potential? (Kac and Luttinger, 1973, 1974.)

(ii) Does an interacting Bose gas undergo a phase transition below $d=4$ or does it form a Bose glass? (Hertz *et al.*, 1979; Bray and Moore, 1982.)

(iii) How is superfluidity destroyed with increasing disorder?

These questions are of general relevance for strongly disordered superconductors and superfluids (Kapitulnik and Kotliar, 1985; Ma and Lee, 1985; Kotliar and Kapitulnik, 1986) and remain to a large extent unresolved. In the dilute limit the considered local pair system will be much similar to that of ^{4}He II in a porous medium (like vycor), which is known to preserve superfluidity (Crooker *et al.*, 1983; Weichmann *et al.*, 1986; Weichmann and Fisher, 1986). The superfluidity (superconductivity) can be destroyed by an interplay of disorder, interaction, and quantum effects. One of the challenging problems is to identify the universality class of this onset transition (Ma *et al.*, 1986; Micnas, 1988b; Fisher and Fisher, 1989). In one dimension, the system (2.70) for $K=0$ reduces to one of free spinless fermions, so that all states will be localized by disorder and no transition is allowed at the ground state (Schneider and Politi, 1986). Recently, Fisher and Fisher (1988) have argued that d-dimensional, repulsively interacting bosons in a random potential undergo a $T=0$ K onset transition from the superfluid to the Bose glass state. The associated quantum critical behavior is characterized by the exponents $\nu \geq 2/d$, η, and a dynamic exponent z; $z=d$ in neutral cases and $z=1$ (for all d) in charged cases.

C. Weak-attraction limit and transition from Bardeen-Cooper-Schrieffer superconductivity to charged-boson superfluidity

The $U<0$ extended Hubbard model has also been analyzed in the weak-attraction limit ($|U|<2zt$) within the broken-symmetry Hartree approach (BCS-like for superconductivity) for arbitrary electron density in $d=3$ [with the use of square density of states (DOS)] and in $d=2$ (Robaszkiewicz *et al.*, 1981c, 1981d, 1982; Micnas *et al.*, 1988a; Micnas, Ranninger, Robaszkiewicz, and Tabor, 1988), as well as within the local approach for electron correlation (Oleś *et al.*, 1984).

1. The broken-symmetry Hartree approach

Within the broken-symmetry Hartree approach the ground-state phase diagram of the negative-U extended Hubbard model shows for $n=1$ the CO phase if $W>0$ and the SS phase if $W<0$. For a non-half-filled band the ground state is always ordered exhibiting either the SS or the M (mixed CO-SS) state, and the phase boundary between them is continuous, being dependent on the parameters of the model and the electron concentration (Robaszkiewicz *et al.*, 1981c, 1981d).

At finite temperatures the same type of analysis indicates the four main phases, CO, SS, M, and the nonordered phase (NO), which is, however, metallic, i.e., without preformed pairs. For a half-filled band, if the CO phase is stable, the system remains nonmetallic, and at T_{CO} the insulator-to-metal phase transition occurs. For the SS state there is a single continuous phase transition at T_{SS} to the normal metallic phase. For a non-half-filled band the CO phase is still characterized by an energy gap, but at the Fermi level one finds a finite number of carriers that can support the current. This is due to the fact that for $n\neq 1$ the wave vector **Q** of the two-sublattice charge order is different from $2k_F$. This CO phase is stabilized by intersite repulsion W, i.e., with increasing W both the energy gap and T_{CO} increase and the CO phase expands toward higher values of $|n-1|$. For the SS phase and $n\neq 1$, the energy gap and T_{SS} were found to be functions of electron density (Robaszkiewicz *et al.* 1981d, 1982; Micnas, Ranninger, Robaszkiewicz and Tabor, 1988), and it was established that the SS phase could be stable even for arbitrarily small n. However, T_{SS} signals only a BCS-type transition to the metallic phase, and if it is continued to very large values of $|U|$ it goes over to $\frac{1}{4}|U|$, i.e., to the pair-breaking temperature.

The competition between the CO and the SS states results in the M phase, as in the strong-attraction limit discussed previously. It was concluded that the weight of the SS component in the M phase increases as the temperature gets lower, and that one expects the appearance of superconducting features while going from the metallic CO phase ($n\neq 1$) to the M phase with decreasing temperature (Robaszkiewicz *et al.*, 1982).

In Fig. 12 we give the finite-temperature phase diagram of the extended Hubbard model for arbitrary n, obtained within the Hartree approximation for two values of zW/D and several values of $-U/D$ (D is the half-bandwidth). All the phase transitions are continuous, and the phase boundaries intersect at a multicritical point between SS, M, CO, and NO phases in a way analogous to the strong-attraction limit [cf. Figs. 5(a)–5(c)]. The essential difference between the strong- and weak-attraction regimes emerges in the form of the *heat charge order* in the Hartree theory. This reentrance behavior, characterized by a sequence of phase transitions SS→NO →CO→NO with increasing temperature, occurs near the multicritical point when zW/D is comparable to or greater than $-U/D$ (Robaszkiewicz *et al.*, 1982).

2. Transition from Bardeen-Cooper-Schrieffer superconductivity to charged-boson superfluidity

From the Hartree analysis (which reduces to the BCS theory as far as the SS phase is concerned), it has been found that ground-state characteristics, such as order parameter, energy gap, and chemical potential, change continuously with increasing $|U|$ for $n\in[0,2]$ and that the

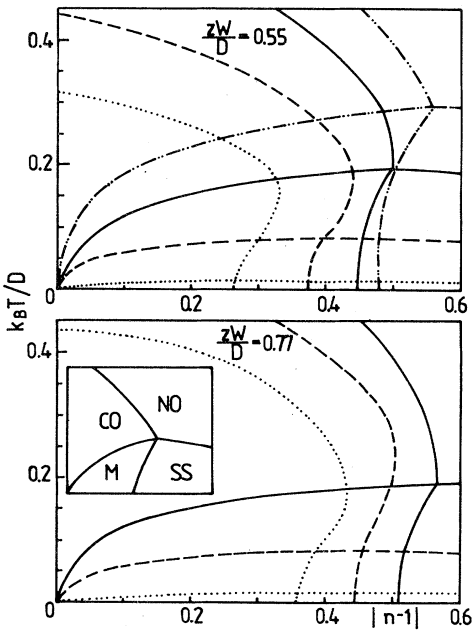

FIG. 12. Finite-temperature phase diagrams of the extended Hubbard model with $U<0$ and $W>0$ for the square density of states. D is the half-bandwidth. The upper and lower figures are for $zW/D=0.55$ and 0.77, respectively, each for several values of U/D: dotted curves, $U/D=-0.4$; dashed curve, -0.8; solid curves, -1.2; dot-dashed curve, -1.6. Relative positions of the four phases (CO,M,SS,NO) are illustrated by the inset in the panel for $zW/D=0.77$. For any given set of zW/D and U/D, four lines intersect at a multicritical point in a way analogous to that in Fig. 5(b),(c).

BCS wave function can give reasonable results not only for $|U|<2zt$ but also for $|U|\gg t$. Moreover, the finite-T phase diagrams determined in the weak-attraction limit (although different) preserve many similarities to those of strong coupling (compare Figs. 12 and 5) (Robaszkiewicz *et al.*, 1981a, 1981b, 1981d, 1982).

Analogous results were obtained by Nozières and Schmitt-Rink (1985) in their analysis of the continuum model of a Fermi gas with attractive potential and the attractive Hubbard model. That paper offered an illuminating physical discussion of the problem of transition from weak-coupling to strong-coupling superconductivity, a problem first addressed by Leggett (1980a, 1980b), and concluded that at the ground state this transition is smooth (i.e., there is no sharp distinction between superconductivity and pair Bose condensation), though the properties of these two limiting cases are in many aspects quite different.

a. Zero temperature

Let us consider the Hartree equations describing the SS state at $T=0$ for the negative-U Hubbard model (Robaszkiewicz *et al.*, 1981d; Nozières and Schmitt-Rink, 1985):

$$1=\frac{|U|}{2N}\sum_{\mathbf{k}}\frac{1}{[(\varepsilon_{\mathbf{k}}-\bar{\mu})^2+\Delta^2]^{1/2}}\ , \tag{2.73a}$$

$$n-1=-\frac{1}{N}\sum_{\mathbf{k}}\frac{\varepsilon_{\mathbf{k}}-\bar{\mu}}{[(\varepsilon_{\mathbf{k}}-\bar{\mu})^2+\Delta^2]^{1/2}}\ , \tag{2.73b}$$

where $\bar{\mu}=\mu+n|U|/2$ and Δ is the superconducting order parameter $\Delta=|U|\langle c_{i\downarrow}c_{i\uparrow}\rangle$.

In the very-weak-coupling limit, $|U|\ll zt$, Δ is exponentially small and we recover the usual BCS picture: the fact that the fermions are confined to a lattice is not essential, since the radius of the Cooper pair is much larger than the lattice spacing ($\Delta\ll zt$). In the opposite strong-coupling limit, however, the physics is different. The fermions form local singlet pairs on a given lattice site, being composite bosons, with binding energy $\sim|U|$. As was extensively discussed in Sec. II.B, these bosons can move via virtual ionization, with the effective hopping amplitude $-2t^2/|U|$ and with near-neighbor repulsion $2t^2/|U|$. Superfluidity then corresponds to condensation of these hard-core bosons. At low density, one has essentially a weakly interacting Bose gas, whereas for higher densities the hard-core correlations are important, and overlap of the bound pairs severely restricts their motion.

In the large-$|U|$ limit it readily follows from Eqs. (2.73a) and (2.73b) that

$$\bar{\mu}=\tfrac{1}{2}|U|(n-1),\quad \Delta=\tfrac{1}{2}|U|\sqrt{n(2-n)}\ , \tag{2.74}$$

and the minimum energy to break a pair is

$$\varepsilon_m=2\sqrt{\bar{\mu}^2+\Delta^2}=|U|\ , \tag{2.75}$$

which is the binding energy of the pair. Let us notice that calculation of $\bar{\mu}$ to the $t^2/|U|$ order yields

$$\bar{\mu}=\frac{|U|}{2}(n-1)+\frac{2zt^2}{|U|}(n-1)\ ,$$

which exactly reproduces the strong-attraction-limit result (Robaszkiewicz *et al.*, 1981a).

In the dilute limit $\bar{\mu}\to-\frac{1}{2}|U|$, $\Delta=|U|\sqrt{n_p}$, where $n_p=n/2$ is the number of pairs per site. In this limit one can also readily show that the BCS equation reduces to a Schrödinger equation for a single bound pair. The superconducting gap parameter Δ can be written as

$$\Delta=\frac{|U|}{N}\sum_{\mathbf{k}}\frac{\Delta}{2\bar{\varepsilon}_{\mathbf{k}}}(1-2n_{\mathbf{k}})\ , \tag{2.76}$$

where

$$n_{\mathbf{k}}=\frac{1}{2}\left[1-\frac{\bar{\varepsilon}_{\mathbf{k}}}{(\bar{\varepsilon}_{\mathbf{k}}^2+\Delta^2)^{1/2}}\right]$$

is the ground-state fermion distribution function, $n=(2/N)\sum_{\mathbf{k}}n_{\mathbf{k}}$, and $\bar{\varepsilon}_{\mathbf{k}}=\varepsilon_{\mathbf{k}}-\bar{\mu}$. Upon introducing the function $\phi_{\mathbf{k}}=\Delta/(\bar{\varepsilon}_{\mathbf{k}}^2+\Delta^2)^{1/2}$, we find that Eq. (2.76) takes the form

$$\begin{aligned}&(2\varepsilon_{\mathbf{k}}-2\bar{\mu})\phi_{\mathbf{k}}=(1-2n_{\mathbf{k}})\frac{|U|}{N}\sum_{\mathbf{k}'}\phi_{\mathbf{k}'}\ ,\\ &n_{\mathbf{k}}=\tfrac{1}{2}[1-\mathrm{sgn}(\bar{\varepsilon}_{\mathbf{k}})(1-|\phi_{\mathbf{k}}|^2)^{1/2}]\ .\end{aligned} \tag{2.77}$$

In the dilute limit $\phi_{\mathbf{k}}\ll 1$, hence Eq. (2.77) reduces in leading order to

$$(2\bar{\varepsilon}_{\mathbf{k}}-2\bar{\mu})\phi_{\mathbf{k}}=\frac{|U|}{N}\sum_{\mathbf{k}'}\phi_{\mathbf{k}'}\ , \tag{2.78}$$

which is just the Schrödinger equation for a single bound pair, with $2\bar{\mu}$ playing the role of the eigenvalue.[3] In that order $\bar{\mu}(<0)$ is essentially given by half of a binding energy of the pair and $n_p=(1/4N)\sum_{\mathbf{k}}|\phi_{\mathbf{k}}|^2$, as expected for an ideal Bose gas.

Thus the BCS wave function contains the right physics in both the weak- and the strong-coupling limits, and it may be used to describe progressive building of pairing correlations in the ground state. The evolution of the particle distribution function $n_{\mathbf{k}}$ is smooth. In the weak-coupling limit it is close to the normal-state step function, while in the strong-coupling limit it remains practically constant, reflecting the Fourier transform of a point internal wave function. Similarly one finds that $\Delta(n,|U|)$, $\mu(n,|U|)$, and $\varepsilon_m(n,|U|)$ evolve smoothly with increasing $|U|$ from weak- to strong-coupling regimes, for a given n. For example, ε_m goes continuously from twice the small cooperative BCS gap in weak coupling to

[3]This procedure applies generally in the dilute limit to any form of the attractive potential $V_{\mathbf{k},\mathbf{k}'}$ (Nozières and Schmitt-Rink, 1985). For solutions of the Schrödinger equation for on-site and intersite pairs versus dimensionality, see Sec. III.B.

the atomic binding $|U|$ in strong coupling.

In conclusion, there is no sharp distinction between superconductivity and pair Bose condensation at $T=0$ K.

b. Finite temperature

The question is now whether we can have similar continuous evolution from BCS-like superconductivity to charged-boson superfluidity at finite temperatures. In weak coupling, T_c is controlled by pair breaking and increases exponentially with the coupling constant. In the opposite limit of strong coupling, the pairs are strongly bound, and T_c is determined by their center-of-mass motion, decreasing with increasing coupling constant as $2t^2/|U|$. However, the Hartree approximation is valid only for $|U|<2zt$, where T_c results from single-particle excitations. If $|U|\gg t$, T_c is determined by the thermal excitation of collective modes; these cannot be treated by the Hartree-Fock method, which only includes pairing via the average static order parameters.

Let us point out that the negative-U Hubbard model, even in the weak-coupling limit, retains some essential differences from the standard BCS model. As electron pairing takes place in the whole Brillouin zone, the effective half-bandwidth (instead of ω_D) will play the role of the energy scale. In consequence, for example

$$k_B T_c = 1.14 D\sqrt{n(2-n)}\exp(-2D/|U|)\ ,$$

and

$$\Delta(T=0) = D\sqrt{n(2-n)}/\sinh(2D/|U|)$$

for the square DOS (Robaszkiewicz *et al.*, 1982). Other differences will appear if the true DOS for a given lattice is used, including the ratio $\Delta(T=0)/k_B T_c$, which will deviate from the BCS value 1.76.

The problem of continuation from BCS-like superconductivity to the superfluidity of charged bosons at finite T for the $U<0$ Hubbard model is at present unresolved. We should stress that an analogous question arises in itinerant magnetism: is T_c determined by a rearrangement of single-particle distributions or by thermally excited spin fluctuations? Available computer simulations for the $U>0$ $d=3$ half-filled Hubbard model (Hirsch, 1985a; Scalettar, Scalapino, *et al.*, 1989), which by the repulsion-attraction transformation can be used for the $U<0$ case, indicate that the evolution of T_c with increasing $|U|$ is smooth, despite the fact that the mechanism of T_c changes [compare Figs. 3 and 13(a)].[4] In the numerical simulations for lattices ranging from 4^3 to 10^3 sites, maximum T_c is reached around $U/t\sim 10$ with $T_c\sim 0.55t$.

[4]However, the possibility has been suggested that the transition is weakly first order at small-to-intermediate values of U and that it changes to a second-order transition at some critical value of U/t (De Marco *et al.*, 1978; Hirsch, 1985a; Scallettar, Scalapino, *et al.*, 1989).

Nozières and Schmitt-Rink (1985) have analyzed these intriguing questions for a *continuum model of a Fermi gas* with fictitious separable attractive potential $V_{\mathbf{k},\mathbf{k}'}$. They asked whether the onset of BCS-type superconductivity and that of Bose condensation were manifestations of a common instability mechanism, which *a priori* is not clear. For weak coupling the onset of a BCS state is controlled by a divergence of the t matrix—the Thouless criterion (Thouless, 1960). For strong coupling, on the contrary, it is controlled by a Bose condensation. Nozières and Schmitt-Rink (1985) could show that indeed the thermodynamic potential evaluated in the BCS approximation but including pair fluctuations could lead to critical temperatures as one would expect in both of the two extreme limits, i.e., $T_c\sim\varepsilon_F\exp[-1/N(0)V_{k_F,k_F}]$ for weak coupling and T_c saturating towards a constant in the strong-coupling (ideal Bose gas) limit. V_{k_F,k_F} denotes the strength of the attractive potential at k_F and $N(0)$ is the density of states at the Fermi level. T_c as a function of coupling strength evaluated numerically for a given density interpolates smoothly between weak- and strong-coupling regimes (Nozières and Schmitt-Rink, 1985).

We note that the saturation of T_c towards its ideal Bose gas value in the strong-coupling limit is a characteristic feature of the continuums model such as the attractive Fermi gas. For a discrete model like the attractive Hubbard model, T_c decreases with increasing coupling constant in the strong-coupling limit.

In Fig. 13(a) we plot schematically the expected phase diagram of the 3D attractive Hubbard model for a simple cubic lattice, illustrating the transition from BCS-type superconductivity to superfluidity of charged hard-core bosons. This changeover is realized by increasing $|U|$ for any fixed density.

c. Two-dimensional case

Let us now conclude with the two-dimensional case. For the 2D continuum model of a dilute gas of fermions at $T=0$, interacting via a given two-body potential, Randeira *et al.* (1989) have recently shown that the many-body ground state is unstable to s-wave pairing if and only if a two-body bound state exists. This result noticeably differs from the 3D case, where the sharpness of the Fermi surface is sufficient to induce the Cooper instability of the normal metallic state for every attraction (and thus in the absence of a true bound state). Moreover, Randeira *et al.* (see also Miyake, 1983), using the standard BCS route, found very simple expressions for the ground-state energy gap Δ and the chemical potential μ, varying continuously as

$$\Delta=\sqrt{2\varepsilon_F E_a},\quad \mu=\varepsilon_F-\tfrac{1}{2}E_a \tag{2.79}$$

upon going from weak to strong coupling. E_a denotes the binding energy in the two-body problem, and $\varepsilon_F=(\pi\hbar^2/m)n$. The BCS results follow if $E_a\ll\varepsilon_F$; then $\mu\approx\varepsilon_F$ and $\Delta/\varepsilon_F\sim(\xi_0 k_F)^{-1}\ll 1$, i.e., the pair size is much larger than the interparticle spacing k_F^{-1}. In the

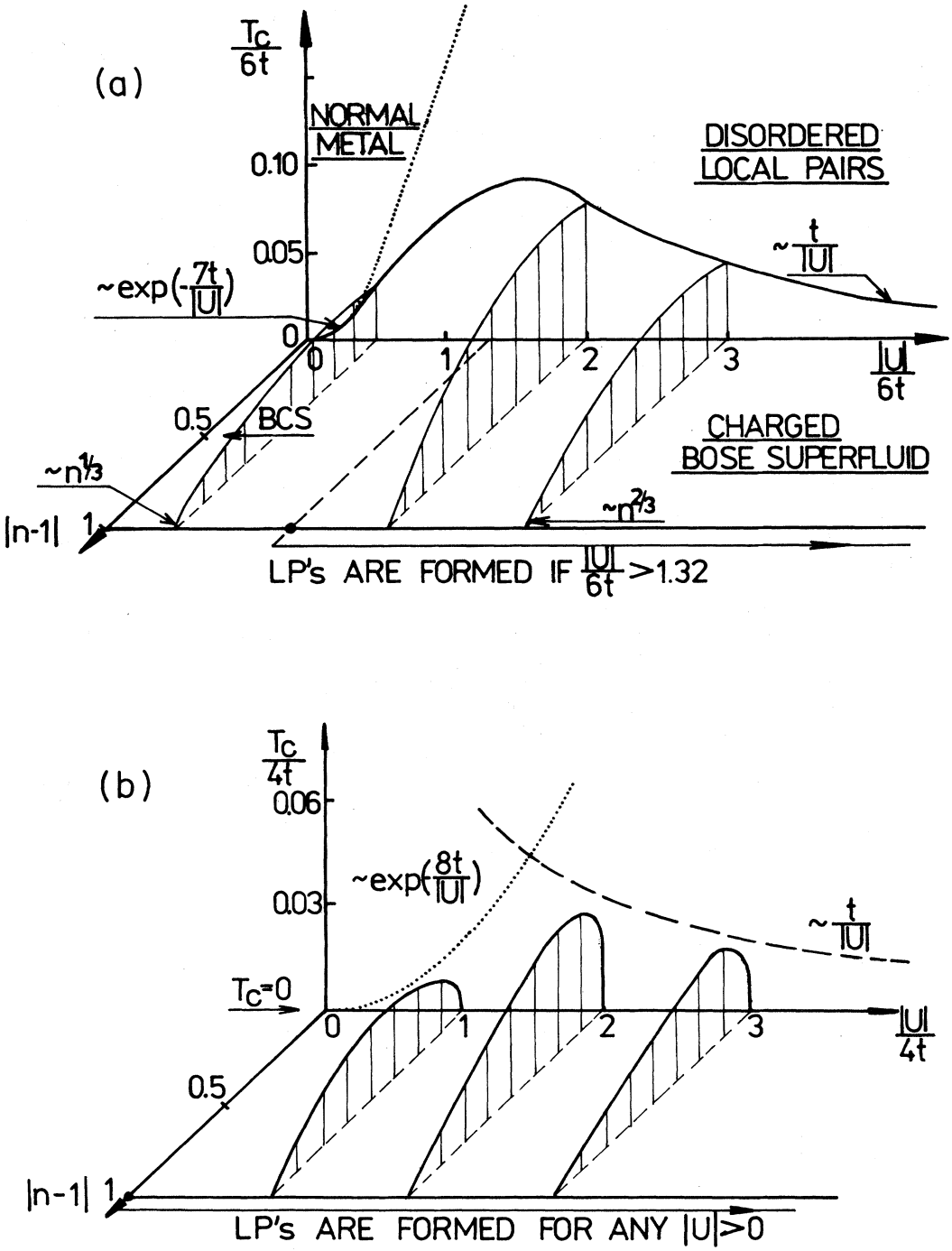

FIG. 13. (a) Schematic phase diagram for the $d=3$ attractive Hubbard model for a simple cubic lattice, illustrating the transition from BCS type superconductivity to superfluidity of charged bosons: solid curve, the T_c vs $|U|$ curve for $n=1$, plotted using the Monte Carlo results of Scalettar, Scalapino, *et al.* (1989) for $U>0$ and the repulsion-attraction transformation (Appendix); dotted curve, the weak-coupling (Hartree theory) prediction. (b) Schematic $T_c/4t$ vs $|U|/4t$ and $|n-1|$ for the $d=2$ attractive Hubbard model on a square lattice (after Scalettar, Loh, *et al.*, 1989): dotted curve, the weak-coupling (Hartree theory) prediction for T_c away from half-filling [$\sim\exp(-8t/|U|)$]; dashed curve, the strong-coupling energy $t^2/|U|$ divided by $4t$. The sections depict the slices of a superconducting phase that has a Kosterlitz-Thouless power-law decay of the pairing correlations.

TABLE V. Comparison of local pair and BCS superconductors.

	Local pair (on-site) superconductor	BCS (weak-coupling) superconductor
1.	All electrons are paired via short-range static attraction (real-space pairing). Radius of local pair ~radius of an effective site. Pairs move via virtual ionization with amplitude $\sim t^2/\|U\|$.	Only a small number of electrons near ε_F participate in the Cooper pairing.
2.	Non-ordered pairs can exist above T_c, and at T_c they undergo a Bose condensation, $T_c \sim (t^2/\|U\|) f(n)$; $f(n) \sim n^{2/3}$ in $d=3$ and $f(n) \sim n$ in $d=2+\varepsilon$, for $n \ll 1$. T_c decreases with increasing $\|U\|$.	The Cooper pairs are formed and condensed at T_c; $T_c \sim \exp[-1/N(0)V_{\mathrm{BCS}}]$ increases with increasing V_{BCS}.
3.	Energy gap in the single-particle spectrum $E_g \sim \|U\|$ (binding energy of local pair). E_g exists above T_c; at T_c, SS→nonmetal or local pair metal, $1.76 k_B T_c / E_g(0) \sim 2t^2/U^2 \ll 1$.	$E_g^{\mathrm{BCS}}(0)$ decreases monotonically with increasing T; at T_c SS→metal transition. $1.76 k_B T_c / E_g(0) \simeq 1$.
4.	Critical behavior can deviate from the Ginzburg-Landau type. Universality class of $s=\frac{1}{2}$ quantum XY model (λ-type anomaly in the specific heat). Similarly with ^{4}He II. Large critical regime and breakdown of mean-field behavior (Table IV).	Classical Ginzburg-Landau type critical behavior. Critical region very narrow and usually inaccessible.
5.	Low-temperature thermodynamics and collective excitations. (a) Without long-range Coulomb interactions: SS, gapless branch $\omega_{\mathbf{k}} \sim k$. SS-CDW: two branches ($\omega_{\mathbf{k}} \sim k$ and $\omega_{\mathbf{k}} = a + bk^2$). CDW: two branches with a gap. Power-law behavior of $C_v \sim T^d$ in SS and SS-CDW phases at low T. Low-T behavior similar to the quantum lattice gas model of ^{4}He II.	Neutral Fermi liquid SS: $\omega_{\mathbf{k}} \sim k$.
	(b) With long-range Coulomb interaction: SS: $\omega_{\mathbf{k}} = \hbar\Omega_0^*(T)$ for $k \to 0$, $\Omega_0^* = \left[\frac{16\pi e^2}{\epsilon_0 m^* a^2}\langle \rho^x \rangle^2\right]^{1/2}$, $m^* = \frac{\hbar^2}{2Ja^2}$ (plasma gap). $C_v \sim \exp(-\Delta/T)$, $\Delta \sim \min\omega_{\mathbf{k}} < \hbar\Omega_0^*$.	Plasmon gap; exponential behavior determined by the single-particle excitations.
6.	Coherence length $\xi/a \gtrsim 1$ (except for $T \sim T_c$).	$\xi/a \sim t/V_{\mathrm{BCS}} \gg 1$.
7.	Penetration depth for magnetic field $\lambda_H \gtrsim (1-100)\lambda_{\mathrm{BCS}}$.	
8.	$\kappa = \lambda_H/\xi \gg 1$ (extreme type-II superconductor).	
9.	Upper critical magnetic field: (a) Paramagnetic effect ($T \ll T_c$), $k_B T_c \ll \mu_B H_{c_2} \lesssim \|U\|$.	(Usually) $\mu_B H_{c_2} \lesssim k_B T_c$ (Clogston limit).
	(b) $T \lesssim T_c$, orbital effect. Very large values of H_{c_2} and possible positive curvature, $\frac{d^2 H_{c_2}}{dT^2} > 0$, $\frac{H_{c_2}}{H_{c_1}} \gg 1$.	
10.	Effect of structural disorder (nonmagnetic impurities) is strong. A possibility of disorder-induced superconductivity and superconducting glass behavior.	Effect of structural disorder is weak.
11.	Effect of magnetic impurities is weak (large binding energy of local pairs).	Effect of magnetic impurities is strong.

opposite limit of very strong attraction (or of very low density), there is a deep two-particle bound state, $E_a \gg \varepsilon_F$, $\mu \approx -E_a/2$, indicating Bose condensation of tightly bound pairs of fermions, and the pair size is much smaller than the interparticle distance $(\xi_0 k_F)^{-1} \gg 1$. Since there is no singularity in Eq. (2.79) as a function of E_a/ε_F, there is a smooth crossover from the BCS limit to Bose condensation. Nevertheless, there is a weak singularity in the excitation spectrum at $\mu=0$, at which point the energy gap in the excitation spectrum changes from Δ to $\sqrt{\Delta^2+\mu^2}$ as μ goes from positive to negative values. The point $\mu=0$ can mark the transition between the BCS-type regime ($\mu>0$) and the Bose condensed regime ($\mu<0$) for a continuum model at $T=0$ K.

The problem of evolution from weak- to strong-coupling superconductivity at finite temperatures is more involved than in the 3D case, due to the absence of Bose condensation in 2D systems for $T\neq 0$ K (Hohenberg, 1967; but superfluidity is possible even in two dimensions and is related to the excitation spectrum).[5]

For the $d=2$ negative-U Hubbard model, computer simulation studies have recently become available (Scalettar, Loh, *et al.*, 1989). They also indicate a smooth transition between weak- and strong-coupling regimes, but the superconducting phase has a Kosterlitz-Thouless power-law decay of the pairing correlations away from half-filling, and $T_c=0$ for $n=1$. In Fig. 13(b) we give a schematic plot of T_c as a function of electron concentration and strength of the Hubbard $|U|$.

In Table V we compare the main properties of local pair superconductivity with those of the BCS model. This comparison is made in order to contrast these two physically different cases.

In our opinion the question whether there is a clear-cut transition between BCS-like superconductivity and charged-boson superfluidity, and whether this can have detectable effects on the excitation spectrum, is at present unresolved.

We should also like to point out that the $U<0$ Hubbard model is the simplest model of local pairing, and that the fundamental questions regarding the transition from BCS behavior to superfluidity of charged bosons have to deal explicitly with the microscopic pairing mechanism, i.e., in electron-phonon (exciton) systems, with the electron-boson coupling constant, the Coulomb interactions, and the problem of interpolation between the adiabatic limit and the inverse-adiabatic limit (Fradkin and Hirsch, 1983; Guinea, 1983; Hirsch and Fradkin, 1983; Hirsch and Scalapino, 1985a; Nasu, 1985, 1987, 1988; Yu and Anderson, 1985)

Another question, crucial for real materials, concerns the coexistence of bound pairs and itinerant electrons and the effects resulting from interactions between these two species. We have analyzed this subject in a sequence of recent papers (Ranninger *et al.*, 1985; Micnas *et al.*, 1987a; Robaszkiewicz *et al.*, 1987; Ranninger *et al.*, 1988), and the results are summarized in Sec. IV.

III. THERMODYNAMICS OF SYSTEMS WITH INTERSITE ELECTRON PAIRING

In this section we shall summarize the recent studies of superconductivity and magnetism in the extended Hubbard model (1.1) with on-site repulsion and intersite attractive interaction, i.e., $U_{\rm eff}>0$, $W_{\rm eff}<0$ (Micnas, Ranninger, and Robaszkiewicz, 1988a, 1989; Micnas, Ranninger, Robaszkiewicz, and Tabor, 1988; and references therein). This is a simple model incorporating magnetic correlations due to $U_{\rm eff}$ and intersite pairing due to $W_{\rm eff}$. An important problem in superconductivity due to intersite attraction is the formation of intersite pairs and their eventual Bose condensation. These studies have been carried out for the $d=2$ square lattice with nearest- and next-nearest-neighbor hopping, bearing in mind that the two-dimensional aspect is relevant for the newly discovered high-T_c superconducting oxides. We shall present a mean-field analysis of anisotropic superconductivity (within a BCS-type weak-coupling approximation) and the spin-density wave (SDW) state for weak and strong on-site correlations $U_{\rm eff}$ and arbitrary electron density. In contrast to the original BCS treatment of phonon-mediated attraction, the present problem does not contain any intrinsic cutoff in either momentum or frequency. The effective short-range attraction in the considered model can be treated as essentially instantaneous on the time scale of the inverse bandwidth. Such an unretarded interaction can result either from the coupling of electrons with high-frequency bosonic modes or from purely electronic (or chemical) mechanisms, as discussed in Sec. I. The effects of exchange interaction and correlated hopping are analyzed in Sec. III.A.2. The problem of local pair formation as a function of dimensionality in the low-density limit is also discussed (Micnas, 1988c); Sec. III.B.

A. Weak-correlation limit ($U<2zt$)

In the weak (intermediate)-correlation limit $U<2zt$, upon using the broken-symmetry Hartree-Fock scheme for the Hamiltonian (1.1), one obtains the following gap equation for *singlet pairing* $\Delta_{\mathbf{k}}=(1/N)\times\sum_{\mathbf{q}}V_{\mathbf{k},\mathbf{q}}\langle c_{-\mathbf{q}\downarrow}c_{\mathbf{q}\uparrow}\rangle$:

$$\Delta_{\mathbf{k}}=\frac{1}{N}\sum_{\mathbf{q}}V_{\mathbf{k},\mathbf{q}}\frac{\Delta_{\mathbf{q}}}{2E_{\mathbf{q}}}\tanh\left[\frac{E_{\mathbf{q}}}{2k_BT}\right], \tag{3.1}$$

where $E_{\mathbf{q}}=(\bar{\varepsilon}_{\mathbf{q}}^2+|\Delta_{\mathbf{q}}|^2)^{1/2}$ is the quasiparticle energy,

[5] An extension of the Nozières and Schmitt-Rink analysis suggests that a dilute continuum 2D Fermi gas with an attractive s-wave interaction becomes unstable at all temperatures to a state of coexisting bound and ionized fermion pairs and that such a state is inaccessible by an adiabatic continuation of the $V=0$ limit, unlike the conventional Fermi-liquid theory (Schmitt-Rink *et al.*, 1989).

$$\bar{\varepsilon}_q=\varepsilon_q+p|W|\gamma_q/\gamma_0-\bar{\mu},\quad \bar{\mu}=\mu-n(U/2-|W|\gamma_0)\ ,$$
$$\varepsilon_q=-t\gamma_q,\quad V_{k,q}=-U-W_{k-q}\ ,$$

and

$$\gamma_q=2(\cos q_x+\cos q_y)\ .$$

The Fock parameter $p=(1/N)\sum_q\gamma_q\langle c^\dagger_{q\sigma}c_{q\sigma}\rangle$ and the chemical potential satisfy the equations

$$p=-\frac{1}{N}\sum_q\bar{\varepsilon}_q\gamma_qF_q,\quad n-1=-\frac{2}{N}\sum_q\bar{\varepsilon}_qF_q\ , \tag{3.2}$$

with

$$F_q=(2E_q)^{-1}\tanh\left[\frac{E_q}{2k_BT}\right]\ . \tag{3.3}$$

The free energy is given by

$$F/N=\tfrac{1}{4}(U-2|W|\gamma_0)n^2+\bar{\mu}(n-1)-|W|p^2\gamma_0+\frac{1}{N}\sum_k\frac{|\Delta_k|^2}{2E_k}\tanh(\beta E_k/2)-\frac{2}{\beta N}\sum_k\ln[2\cosh(\beta E_k/2)]\ . \tag{3.4}$$

For a $d=2$ square lattice, the pairing potential $V_{k,q}$ takes on a separable form, and Eq. (3.1) can be solved by an ansatz: $\Delta_k=\Delta_0+\Delta_\gamma\gamma_k+\Delta_\eta\eta_k$ where particular terms refer to on-site s-, extended s- and d-wave pairings. $[\eta_k=2(\cos k_x-\cos k_y)]$.

Similarly, the gap equation for *triplet (equal-spin) pairing* is given by

$$\Delta^p_\alpha=\frac{2|W|}{N}\sum_q\sin q_\alpha\Delta^p_qF_q,\quad \alpha=x,y\ , \tag{3.5}$$

where $\Delta^p_q=\Delta^p_x\sin q_x+\Delta^p_y\sin q_y$ has a p-like character. The equations for p and μ are the same as for the singlet pairing; moreover, the free energy has the form of Eq. (3.4) if Δ_k is replaced by Δ^p_k.

For the *spin-density-wave* (SDW) *state*, the order parameter

$$m_Q=\frac{1}{2N}\sum_{k,\sigma}\sigma\langle c^\dagger_{k\sigma}c_{k+Q\sigma}\rangle$$

is determined by

$$m_Q=\frac{Um_Q}{4N}\sum_q\frac{1}{x_q}[\tanh(\beta E^+_q/2)-\tanh(\beta E^-_q/2)]\ . \tag{3.6}$$

The chemical potential satisfies the equation

$$n-1=-\frac{1}{2N}\sum_q[\tanh(\beta E^+_q/2)+\tanh(\beta E^-_q/2)]\ . \tag{3.7}$$

where the quasiparticle energies are given by

$$E^\pm_q=\tfrac{1}{2}(\bar{\varepsilon}_q+\bar{\varepsilon}_{q+Q})\pm x_q\ , \tag{3.8a}$$

$$x_q=[\tfrac{1}{4}(\bar{\varepsilon}_q-\bar{\varepsilon}_{q+Q})^2+U^2m^2_Q]^{1/2}\ , \tag{3.8b}$$

and $Q=(\pi,\pi)$ for a 2D square lattice.

The Fock parameter satisfies the equation

$$p=-\frac{1}{2N}\sum_q\gamma_q[\tanh(\beta E^+_q/2)+\tanh(\beta E^-_q/2)]+\frac{1}{4N}\sum_q\frac{\gamma_q(\bar{\varepsilon}_q-\bar{\varepsilon}_{q+Q})}{x_q}[\tanh(\beta E^+_q/2)-\tanh(\beta E^-_q/2)]\ . \tag{3.9}$$

The free energy is given by

$$F/N=\tfrac{1}{4}(U-2|W|\gamma_0)n^2+\bar{\mu}(n-1)-|W|p^2/\gamma_0+Um^2_Q-\frac{1}{\beta N}\sum_q\{\ln[2\cosh(\beta E^+_q/2)]+\ln[2\cosh(\beta E^-_q/2)]\}\ . \tag{3.10}$$

In Eqs. (3.6)–(3.10), summation over $\mathbf{q}$ is not restricted to the inner half of the Brillouin zone. The transition temperature T_N is obtained upon the assumption of a continuous transition, i.e., $m_Q\to0$. For a $d=2$ lattice such a transition can have only a formal meaning within the mean-field theory, at least for finite-range hopping, since the fluctuations destroy the SDW ordering for any $T\neq0$, and no phase transition is allowed even in the Kosterlitz-Thouless sense. However, the interplanar couplings can easily stabilize the SDW state at finite temperatures. Another view is that the range of nonzero solutions for m_Q indicates the role of the spin fluctuations.

The self-consistent equations for the superconducting critical temperatures determining the onset of pure pairings, as well as for T_N, have been solved numerically. The lattice sums were performed using exact DOS in $d=2$ or by direct numerical integration, thus taking into account the Van Hove singularity (Micnas *et al.*, 1988a; Micnas, Ranninger, Robaszkiewicz and Tabor, 1988).

In the half-filled band case ($n=1,\bar{\mu}=0$), one finds that for $U\geq0$, $W<0$, d-wave pairing yields the highest T_c, while an extended s-wave pairing can occur only for $|W|/D\geq\pi^2/8$, where $D=4t$ is the half-bandwidth. For $U<0$, on-site s-wave pairing can exist for any value of $|W|/D$ (Fig. 14).

1. Relative stability of pure phases

In Fig. 15 we give a preliminary ground-state phase diagram for $n=1$, based on a comparison of critical temperatures for pure phases. For $U>0$ and $W>0$ there are only two phases possible: the CDW and the SDW, which are separated by the line $U=4W$. For $U<0$, the CDW and the singlet-superconducting (SS) state meet at $W=0$. For $W<0$ and $U<0$ one has the SS (on-site) pairing and the d-wave pairing, whereas the SDW and the d-wave pairing are possible for $W<0$ and $U>0$. We should like to point out that Fig. 15 indicates only the main pure

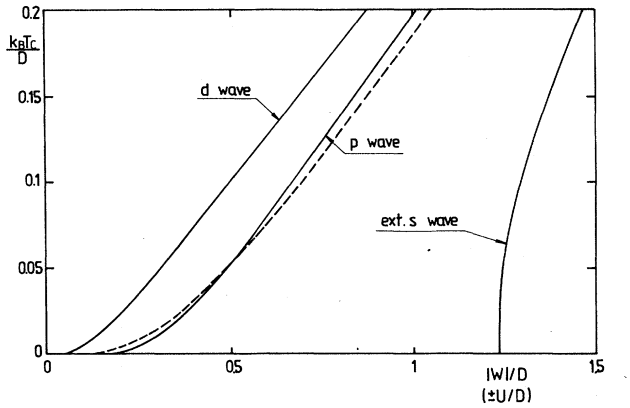

FIG. 14. T_c for d-, p-, and extended s-wave pairings on a square lattice with $n=1$ (nearest-neighbor hopping). The dashed curve indicates T_c for both on-site (s) pairing vs $-U/D$ and spin-density waves vs U/D (repulsion-attraction symmetry).

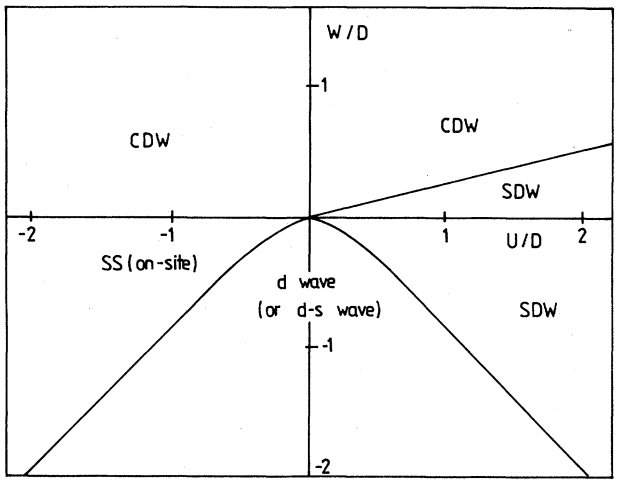

FIG. 15. A preliminary phase diagram of the extended Hubbard model in two dimensions and a square lattice and for the half-filled band: CDW, charge-density waves; SDW, spin-density waves; SS, singlet pairing (on-site); d-s wave, a possible mixed superconducting state.

phases; it does not contain a possible mixed superconducting state (d-s), neither a mixed superconducting–SDW state, nor a condensation transition.

For the non-half-filled band the nature of the pairing state strongly depends on band filling. The numerical solutions for T_c versus electron density are given in Figs. 16(a) and 16(b). These plots are symmetric with respect to $n \to 2-n$, due to electron-hole symmetry. While d-wave pairing yields the highest T_c close to $n=1$, the competing p-wave and extended s-wave pairings can be stabilized for lower electron densities. T_c for s-wave pairing shows nonmonotonic behavior with rapid increase for small n, going through a maximum upon increasing n, and then vanishing above some value of n.

Note that, in the present model, electron pairing can take place throughout the whole Brillouin zone, and there is no cutoff vector (except for a reciprocal one), in contrast to the BCS model. This is due to the fact that the pairing caused by the negative W is instantaneous and hence mediated by a frequency-independent interaction. Thus T_c and Δ_k are functions of a half-bandwidth and of the electron concentration instead of ω_D as in the BCS theory. This can be seen from the analytical expression for T_c derived for the s-wave pairing, upon making use of a square DOS and taking the weak-coupling limit,

$$k_B T_c = 1.14 D \sqrt{n(2-n)} \exp\left[-\frac{1+\lambda[3(n-1)^2-1]+\alpha\lambda(n-1)^2}{2\lambda\{(n-1)^2-\alpha/4\lambda+(\alpha/4)[1+(n-1)^2]\}} \right], \tag{3.11}$$

where $\alpha = U/D$ and $\lambda = |W|/D$. To derive (3.11) we have used $\bar{\mu} \cong D(n-1)$ at low T (see also Alexandrov and Elesin, 1982, 1985). Equation (3.11) indicates that for $U>0$ and given density n there exists some limiting value for $|W|$ in order for s-wave pairing to exist.

For other types of pairing, the above approximation based on a square DOS is no longer useful. In general, one can perform a high-T_c expansion for arbitrary values of n to determine T_c for s-, p-, and d-wave pairing in the strong-coupling regime. The weak-coupling formulas for the different pairings, with the use of exact DOS or logarithmic approximations and exploring the idea of averaging the pairing potential over the Fermi surface, are not accurate, since the model contains pairing in the entire Brillouin zone. For this reasons we are obliged to solve the equations for T_c numerically.

For $U>0$ (or small $U<0$) one can have the following sequence of transitions upon decreasing n: $d \to p \to s$. For larger values of negative U it is possible to have a $d \to s$ transition or only an s-wave state stable for any n. Figure 17 shows the relative stability of s-, p-, and d-wave pairings.

The repulsive on-site interaction U gives rise to the SDW phase and reduces the stability of s-wave pairing. The d- and p-wave pairings are independent of U. In Fig. 16 we indicate the Néel temperatures for several U/D values. Note that for $n=1$ the SDW is always most stable for sufficiently large U, but is rather quickly destroyed upon deviating from $n=1$ (even for U/D as large as 1) due to the spoiling of the Fermi-surface nesting.

We have also studied the effects of next-nearest-neighbor hopping on superconducting T_c, taking $\varepsilon_k = -t\gamma_k - 4t_2 \cos k_x \cos k_y$, where t_2 is the next-nearest-neighbor hopping integral (for details, see Micnas, Ranninger, and Robaszkiewicz, 1988a, 1989; Mic-

nas, Ranninger, Robaszkiewicz, and Tabor, 1988). The perfect nesting condition $\varepsilon_{k+Q}=-\varepsilon_k$ is no longer satisfied, and there is no electron-hole symmetry. Consequently the Van Hove singularity does not coincide with the Fermi level for $n=1$, and the maximum of T_c for d- and p-wave pairing, as well as for on-site s-wave pairing, is shifted due to the fact that the logarithmic singularity moves to $n\neq 1$. In Fig. 18 we show T_c for s-, p-, and d-wave pairings versus the band filling in the case of intersite attraction, for $t_2/t=0.3$. The cases of $t_2>0$ and $t_2<0$ are linked by the relation $T_c(n,t,t_2)=T_c(2-n,t,-t_2)$. One observes that T_c can be substantially altered even for small t_2, and both signs of t_2 are important. This is an interesting effect, since it can be responsible for the pressure dependence of T_c. This overall variation of T_c with n and t_2/t obtained for the case of intersite attraction is interesting to compare with the T_c for purely on-site attraction ($U<0$ Hubbard model with nearest- and next-nearest-neighbor hopping). Figure 19 shows T_c for the $U<0$ case and $t_2/t=0.3$, where again one can see the effect of moving the Van Hove singularity and the strong enhancement of T_c for on-site pairing.

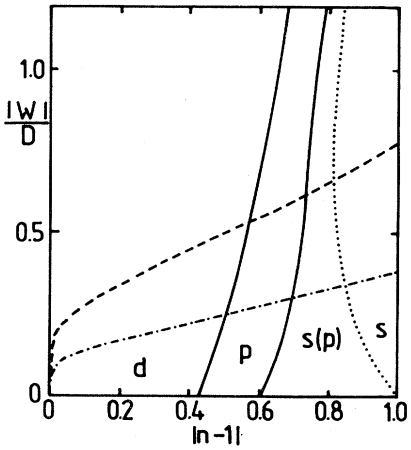

FIG. 17. Relative stability of s-, p-, and d-wave pairings for a square lattice: solid-curves, for $U=0$; dotted curve, the p-s boundary for $U/D=0.5$; dot-dashed and dashed curves, boundaries between the superconducting and the condensed (droplet) phases for $U=0$, $W_{LR}=0$, and for $|W|/D=U/4D+W_{LR}/4D$, respectively, where $W_{LR}=\sum_{n\geq 2} z_n W_n$ is the long-range part of the Coulomb interaction (the condensed phase can occur above these lines).

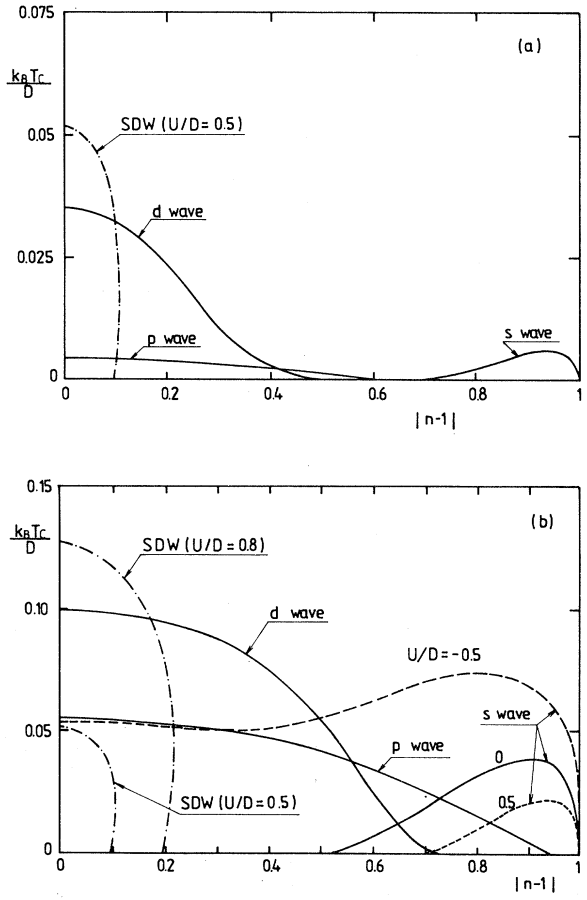

FIG. 16. T_c vs n for s-, p-, and d-wave pairings on a square lattice and with nearest-neighbor hopping. T_c for s-wave pairing is plotted for different values of U/D. Notice that T_c for p- and d-wave pairings is independent of U. (a) $|W|/D=0.25$ (T_c^s is for $U=0$), (b) $|W|/D=0.5$. The dot-dashed curves mark T_N for the spin-density wave state.

It is important to stress that for a $d=2$ square lattice the long-range SDW ordering at $T\neq 0$ is precluded; therefore interplanar coupling is necessary to stabilize the antiferromagnetism. This may not be the case for superconductivity because of the possibility of the Kosterlitz-Thouless transition. A consistent treatment of spin fluctuations within the Hartree-Fock theory would require an analysis of mixed SDW-anisotropic superconductivity solutions.

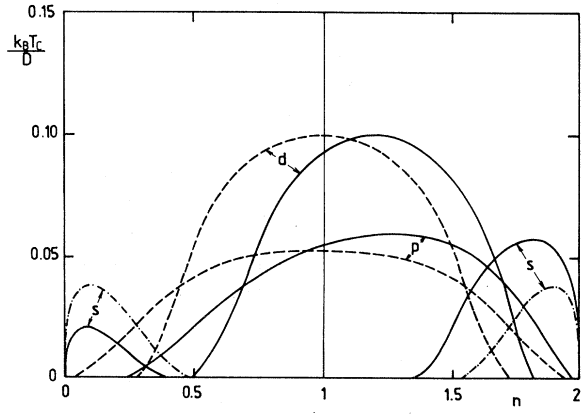

FIG. 18. T_c vs electron density for different pairings on a square lattice with nearest (t) and next-nearest-neighbor (t_2) hopping for $|W|/D=0.5$, $U=0$, and $t_2/t=0.3$; solid curves, T_c for $t_2/t=0.3$; other curves, $t_2=0$. $T_c(n,t_2/t)=T_c(2-n,-t_2/t)$.

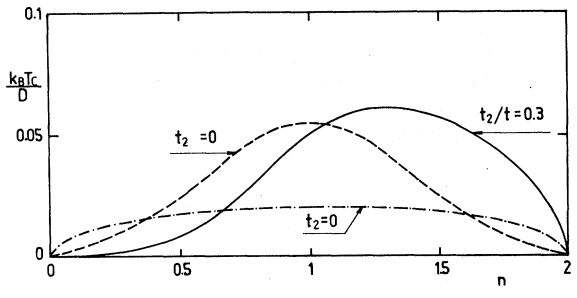

FIG. 19. Effects of next-nearest-neighbor hopping on T_c for the $U<0$ Hubbard model on a square lattice, $U/D=-0.5$, $D=4t$; solid curve, $t_2/t=0.3$; dashed curve, $t_2=0$; dot-dashed curve, T_c vs n for a square density of states and nearest-neighbor hopping.

2. Effect of exchange interaction and correlated hopping

Let us observe, however, that we can readily incorporate into the present scheme the effects of direct exchange interaction by adding to Eq. (1.1) a term of the form

$$\sum_{i,j} J_{ij}\mathbf{s}_i\cdot\mathbf{s}_j, \quad s_i^+ = c_{i\uparrow}^\dagger c_{i\downarrow}, \quad s_i^z = \tfrac{1}{2}(n_{i\uparrow}-n_{i\downarrow}) .$$

This amounts to changing the pairing potentials so that $|W|\rightarrow|W|+\frac{3}{2}J$ for the s- and d-wave pairings, $|W|-\frac{1}{2}J$ for the p-wave pairing, and the SDW is enhanced by the factor Jz. A comprehensive study of the effects of such an effective direct exchange interaction, as well as of the correlated hopping term

$$\tfrac{1}{2}\sum_{i,j,\sigma}[\tilde{K}_{ij}n_{i\sigma}(c_{i-\sigma}^\dagger c_{j-\sigma}+\text{H.c.})] ,$$

on the superconductivity of systems with intersite pairing has been carried out by Micnas, Ranninger, and Robaszkiewicz (1989). In that paper the Hamiltonian (1.1) with additional J_{ij} and $\tilde{K}_{ij}$ terms, treated as independent from U and W, has been analyzed in the broken-symmetry Hartree-Fock approach for a two-dimensional square lattice and new features, introduced by these couplings into the model (1.1), have been worked out. It should be stressed that these J_{ij} and $\tilde{K}_{ij}$ terms are of different origin (as discussed below) from those of the kinetic exchange interaction as well as of certain correlated hopping terms appearing in the derivation of the strong-correlation limit for the single-band Hubbard model (see Sec. III.C). Formally, J_{ij} and $\tilde{K}_{ij}$ are the off-diagonal terms of the Coulomb interaction $V(\mathbf{r}-\mathbf{r}')$ (Hubbard, 1963), $J_{ij}=(ii|V(r)|jj)$, $\tilde{K}_{ij}=(ii|V(r)|ij)$. These terms, involving bond charge density, result from the fact that due to translational invariance the electron density operator is not diagonal in a Wannier representation. The estimates of Hubbard (1963), Kivelson *et al.* (1987, 1988), Baeriswyl *et al.*, (1988), and Gammel and Campbell (1988) show that such terms can be of importance in narrow-band materials. The typical range of electron-electron interaction parameters arising from the Coulomb potential is $U>W>\tilde{K}>|J|$ or, for a strongly screened potential $U>\tilde{K}>W,|J|$ (Campbell *et al.*, 1988).

In the simplest derivation the sign of the "Coulomb-driven" exchange J_{ij} is typically negative, i.e., ferromagnetic, and for many systems its value can be negligibly small. However, the effective antiferromagnetic interaction $J_{ij}>0$ is also possible (Miyake *et al.*, 1983; Hirsch, 1987a; Que and Kirczenov, 1987; Bastide and Lacroix, 1988b), and in particular it can originate from the coupling of electrons with intermolecular (intersite) vibrations, via modulation of the hopping integral (Miyake *et al.*, 1983; Hirsch, 1987a) or from the on-site hybridization term in the periodic Anderson model (Bastide and Lacroix, 1988b).

This antiferromagnetic exchange interaction enhances both the d-wave and the extended s-wave pairing and suppresses the p-wave pairing, while the ferromagnetic exchange interaction does the opposite, suppressing d- and s-wave pairing and enhancing p-wave pairing. If it prevails over the intersite density-density interaction, such an effective antiferromagnetic exchange term can be the leading mechanism for superconductivity. However, its effect strongly depends on the band filling and the t_2/t ratio, giving in particular for $t_2=0$, s-wave (d-wave) pairing most favorable in the low- (high-) density limit. In Fig. 20 we show the relative stability of s and d pairings obtained for the case $J>0$, $W=0$ ($t_2=0$). The boundary between the d and s pairing states is located at

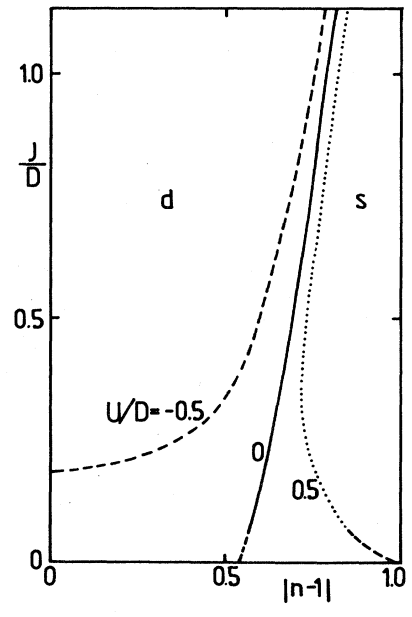

FIG. 20. Relative stability of s- and d-wave pairings for a square lattice in a plot of J/D vs $|n-1|$, where J measures the nearest-neighbor antiferromagnetic exchange interaction ($W=0$): solid curve, $U=0$; dashed curve, $U/D=-0.5$; dotted curve, $U/D=0.5$. The solid and dotted lines are extrapolated down to $J/D=0$, which is shown by the dashed parts.

$0.15 < n_c < 0.46$, for $0 < J/D < \frac{4}{3}$ and n_c decreases with increasing J. Increasing $U > 0$ shifts n_c towards lower values, whereas $U < 0$ can extend the stability region of s pairing up to $n = 1$ (cf. the case of $J = 0$, $W < 0$; Fig. 17).

The off-diagonal $\tilde{K}$ term (correlated hopping) describes the interaction between site charge density and bond charge density. This term is repulsive ($\tilde{K} > 0$) if it results from the Coulomb potential $V(r)$. An effective attractive interaction of this form ($\tilde{K} < 0$) is also possible, and in narrow-band systems it can be due to phonons, e.g., simultaneous modulation of the near-neighbor hopping and the site energy by lattice vibrations (Miyake *et al.*, 1984), or due to the coupling of electrons with other electronic subsystems (Bastide and Lacroix, 1988b). This interaction can also arise when one includes coupling to a degree of freedom describing the deformation of the outer electron cloud of the ion by the presence of the conduction hole (Hirsch, 1989b). Hirsch (1989b) has suggested that this hopping, modulated by the presence of other particles, can be particularly effective in the case of holes in unstable anions with filled shells, i.e., just in the case of high-T_c oxides.

The $\tilde{K}$ term affects mostly s-wave pairing and can modify the relative stability of superconducting states and the variation of T_c with electron density. When $\tilde{K}/D$ is increased ($\tilde{K} > 0$), T_c^s is enhanced in the regime $1 < n < 2$, and the s-wave pairing extends over a wider range of densities. For $0 < n < 1$, T_c^s is reduced, and the s-(p-) d- phase boundary is shifted towards smaller densities (see Figs. 7 and 8 in Micnas *et al.*, 1989). We stress that the $\tilde{K}$ term breaks the electron-hole symmetry, and as in the case of next-nearest-neighbor hopping, T_c^s for $\tilde{K} > 0$ and $\tilde{K} < 0$ is linked by the relation $T_c^s(n, \tilde{K}, \ldots) = T_c^s(2-n, -\tilde{K}, \ldots)$. As we have pointed out (Micnas *et al.*, 1989), there is a possibility of having s-wave pairing due to the $\tilde{K}$ term only, even if all the other pairing mechanisms ($W < 0$, $J > 0$, or $U < 0$) are absent.

The s-wave pairing generated by the modulated hopping interaction shows some characteristic features which are different not only from the usual BCS behavior but also from the extended s-wave pairing driven by the $W < 0$ and (or) $J > 0$ terms.

These characteristic features are direct consequences of the form of the interaction which has the same momentum dependence as the kinetic energy and which breaks the electron-hole symmetry.

(i) For $\tilde{K} > 0$ this interaction stabilizes the s-wave superconductivity of holes in the more than half-filled band case (i.e., $n_h = 2 - n < 1$), whereas for $\tilde{K} < 0$ it yields the s-wave superconductivity of electrons in the less than half-filled band case.

(ii) With increasing carrier concentration ($n_h = 2 - n$ for $\tilde{K} > 0$) or n for $\tilde{K} < 0$, T_c increases first, goes through a maximum, and then drops to zero. For most of the parameter space ($U > 0$, $W > 0$) T_c is restricted to low densities and increasing U shifts the maximum of T_c towards lower concentrations.

(iii) T_c increases with the bandwidth (for fixed $\tilde{K}/t$ and U) and hence with applied pressure.

(iv) The energy gap persists over the entire Fermi surface but it has strong energy dependence.

(v) The gap ratio $2\Delta/k_B T_c$ varies with concentration being higher than 3.52 at low densities and reaching the BCS value for higher n.

(vi) The tunneling DOS shows the same square root singularity as the usual BCS case. However, an inherent asymmetry in the tunneling characteristics arises due to the energy dependence of the gap (Hirsch and Marsiglio, 1989; Marsiglio and Hirsch, 1989). As the pairing induced by the $\tilde{K}$ term always consists of on-site s-wave and extended s-wave components ($\Delta_0 \neq 0$, $\Delta_\gamma \neq 0$), it will be reduced by both the on-site repulsion $U > 0$ and the intersite repulsion $W > 0$. However, in the low-concentration limit superconductivity can exist even with repulsive interactions substantially larger than $\tilde{K}$ (up to $U/\tilde{K} \simeq 10$–30, if $W = 0$) (Micnas *et al.*, 1989; Hirsch and Marsiglio, 1989). Beyond this limit (except for very special cases) the $\tilde{K}$ term alone cannot serve as the driving mechanism of superconducting pairing. Nevertheless, in the presence of other terms favoring superconductivity, its effects can be important for any concentration, and they can substantially modify the mutual stability of superconducting states and the variation of T_c with the electron concentration.

It should be noted that the effective exchange interactions and correlated hopping terms have been treated here as independent interactions (which can arise from several mechanisms discussed above), and we have not imposed any constraints on the site occupancy. This has to be contrasted with the limit of strong correlations for the single-band repulsive Hubbard model, for which antiferromagnetic (kinetic) spin exchange and certain correlated hopping terms can be derived if one eliminates from the Hilbert space (via a strong-coupling transformation) all states with either doubly occupied or unoccupied sites. This case of strong on-site correlations ($U \gg t_{ij}$) is discussed in Sec. III.C.

In the presence of an attractive density-density interaction, the electronic system can undergo (under specific conditions) a *condensation–phase-separation transition,* similar to liquid-gas condensation. This problem has recently been analyzed for the extended Hubbard model with intersite attraction [Eq. (1.1)], within the framework of the RPA, including explicitly the long-range part of the Coulomb interaction, W_{LR} (Micnas *et al.*, 1989). The stability conditions for such an electron droplet phase with respect to other types of orderings were determined as a function of the band filling. For a $d = 2$ square lattice, the most favorable condition for condensation was found to be the half-filled band case, where the Van Hove singularity coincides with the Fermi level. However, any deviation from $n = 1$ makes condensation less likely and leads to a sharp increase in the minimal value of the intersite attraction needed to stabilize the electron droplet phase. A comparison of condensation

transition temperatures and superconducting transition temperatures versus electron density yields the mutual stability phase diagram given in Fig. 17. This diagram includes an extreme case $U=0$, $W_{LR}=0$, and also shows a rapid shift of the phase separation line towards higher values of $|W|/D$ upon increasing repulsive short-range and long-range Coulomb interactions.

To close this subsection we should mention that the interesting problems to be solved are the coexistence of superconductivity and the SDW state as well as whether the presence of spin fluctuations can enhance anisotropic pairing, especially close to $n=1$ (see, for example, Miyake *et al.*, 1986; Scalapino *et al.*, 1986, 1987). The mean-field treatment presented here is justified for not too strong on-site repulsion and for not too low electron concentrations. One limitation is the Hartree-Fock approximation for the on-site repulsion term, which neglects all mass renormalization effects. (For strong on-site correlations, see Sec. III.C.). For low enough concentrations, the formation of real-space pairs can take place (Sec. III.B); such a situation is beyond the applicability of the Hartree-Fock theory at finite temperatures, either for the superconducting or for the normal state. One should also stress that for strong intersite attraction, unlike the case of on-site attraction, an exact mapping onto the pseudospin model is (apart from a very dilute limit) unknown. It is therefore important to go beyond this simple mean-field approximation scheme for both superconductivity and the SDW state, as well as to include the effects of long-range Coulomb interaction. Finally, for a square lattice, the possibility of electron pairing in the antiferromagnetic background via a spin-bag mechanism (Schrieffer *et al.*, 1988) should also be considered.

B. Low-density limit and local pair formation

In the low-density limit the formation of real bound intersite pairs is expected. For this purpose let us consider the Schrödinger equation for a single bound pair for the system described by the Hamiltonian (1.1)

$$(2\varepsilon_{\mathbf{k}}-E)\psi_{\mathbf{k}}=\frac{1}{N}\sum_{\mathbf{p}}V_{\mathbf{k},\mathbf{p}}\psi_{\mathbf{p}}\ , \tag{3.12}$$

where $V_{\mathbf{k},\mathbf{p}}=-U+|W|\gamma_{\mathbf{k}-\mathbf{p}}$, $\varepsilon_{\mathbf{k}}=-t\gamma_{\mathbf{k}}$. Equation (3.12) can be considered as the low-density limit of the BCS equations (3.1)–(3.3) for singlet pairing (Leggett, 1980a, 1980b; Nozières and Schmitt-Rink, 1985). Letting $E=2\varepsilon_0-\Delta$ where $\Delta>0$ is the binding energy, one can analyze the local pair formation for different dimensionalities (Micnas, 1988c).

For s-wave pairs an exact analysis of Eq. (3.12) can be performed in terms of the lattice Green's function. The binding energy for an s-wave pair is given by

$$\frac{2D}{U}=\frac{\frac{|W|}{2t}[(\alpha+1)G(\alpha)-1]-G(\alpha)}{1-\frac{|W|}{2t}(\alpha+1)[(\alpha+1)G(\alpha)-1]}\ , \tag{3.13}$$

where

$$G(\alpha)=\frac{1}{N}\sum_{\mathbf{k}}\frac{1}{(\alpha+1)-\gamma_{\mathbf{k}}/z},\quad \gamma_{\mathbf{k}}=2\sum_{i=1}^{d}\cos k_i\ ,$$

$\alpha=\Delta/2D$, $D=zt$, and $z=2d$ is the coordination number.

For p- and d-wave pairs an essentially exact analysis can also be carried out. The critical values of U and $|W|$ to bind an s-wave pair are given by

$$\frac{|W|}{2t}=\left[1+\frac{2D}{U}\right]^{-1}+(C+1)^{-1}\ , \tag{3.14}$$

where

$$C=\frac{1}{N}\sum_{\mathbf{k}}(1-\gamma_{\mathbf{k}}/z)^{-1}$$

is the Watson integral. If $U=0$ there will be no critical value of $|W|/2t$ to bind an s-wave pair in $d=1,2$, whereas in $d=3$ such a value always exists (for example, in a simple cubic lattice this critical value is 1.9365). If $U<0$ and $W=0$, th on-site pair is formed for any negative U in $d=1,2$; but in $d=3$ the critical value is given by $|U|/2D=C^{-1}$(0.659, 0.718, and 0.743 for simple cubic, body-centered-cubic, and face-centered-cubic lattices, respectively; (see Fig. 21).

In Fig. 22 we show local pair formation for $W<0$. In $d=1$, the bound states are s or p type, and if $U>0$ there exists a critical value. Notice that for $U=\infty$ the binding energies of s and p bound states coincide (Fig. 23). Figure 24 shows the binding energies of s-, p-, and d-wave pairs for $U=0$ and $U=\infty$ and different dimensionalities. As regards the p- and d-wave pairs, there are always critical values of $|W|$ in order to bind in $d\geq 2$, with binding energies independent of U. These critical values in the $d=2$ square lattice are $|W|/2t=\pi/(4-\pi)\approx 3.66$ for d-wave and ~ 2.75 for p-wave pairs, respectively. For a simple cubic lattice, the critical binding values for $|W|/2t$ are as follows: for extended s-wave pairs, 1.9365 for $U=0$ and 2.9365 for $U=\infty$, respectively; for p pairs, 4.766; and for d pairs, 5.398. We note that these binding

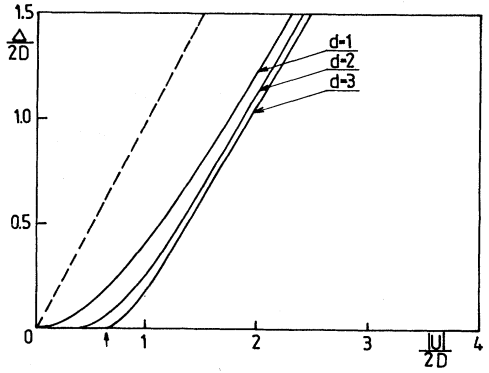

FIG. 21. Binding energies of the on-site pairs in the $U<0$ Hubbard model for different dimensionalities: dashed line, asymptotics for $|U|\to\infty$ ($\Delta=|U|$). A square lattice is assumed for the 2D results and a simple cubic lattice, for the 3D results.

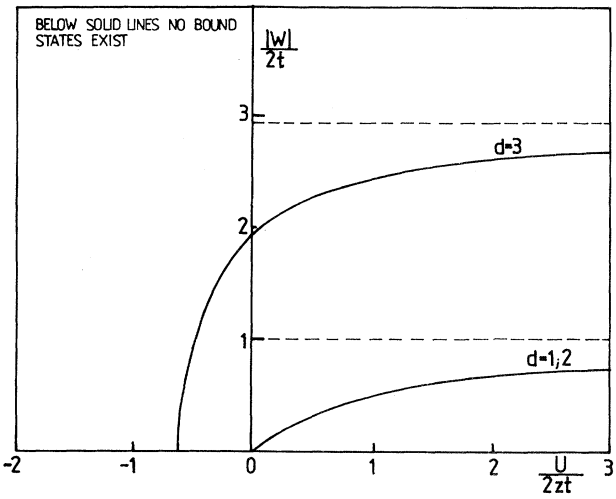

FIG. 22. Local pair formation for $W<0$ for $d=1$, 2, and 3. Below the solid curves there are no bound states. The dashed lines indicate the $U=\infty$ limit. A square lattice is assumed for the 2D results and a simple cubic lattice for the 3D results.

energies are in qualitative agreement with the stability of different pairings (in the low-density limit), analyzed in Sec. III.A on the basis of the Hartree-Fock theory for T_c in the case of nearest-neighbor hopping.

The superconducting state requires Bose condensation of such electron pairs. For low electron density the system can be characterized as a dilute gas of two-electron molecules. Correspondingly, the coherence length should be very much smaller than it is in weak-coupling superconductors. We should stress, however, that the quantitative description of a possible superfluid state of intersite pairs is not well understood, nor is its relation to a charged hard-core Bose gas on a lattice (in contrast to the case of on-site pairs).

C. Limit of strong correlations ($U \gg t, W$)

For a half-filled band and $U \gg t$, clearly no superconducting state exists (the Mott insulator limit). It is an important question whether superconductivity can be established for strong correlations away from the half-filling. Assuming $U \gg t, W$, the canonical transformation method (Harris and Lange, 1967; Chao *et al.*, 1977; Hirsch, 1985b) applied to the Hamiltonian (1.1) yields an effective Hamiltonian acting in a subspace of singly occupied states of the form (neglecting pair hopping terms)

$$H_{\text{eff}}=\sum_{i,j,\sigma} t_{ij} h_{i\sigma}^{\dagger} h_{j\sigma}+\sum_{i,j} J_{ij}(\mathbf{S}_i\cdot\mathbf{S}_j-\tfrac{1}{4}N_iN_j) +\tfrac{1}{2}\sum_{i,j} W_{ij}N_iN_j \ , \tag{3.15}$$

where $J_{ij}=2t_{ij}^2/U$, $h_{i\sigma}=c_{i\sigma}(1-n_{i-\sigma})$, $N_{i\sigma}=h_{i\sigma}^{\dagger}h_{i\sigma}$, $N_i=N_{i\uparrow}+N_{i\downarrow}$. If $n=1$ (the Mott insulator) Hamiltonian (3.15) reduces to Anderson's kinetic exchange Hamiltonian,

$$H_{\text{eff}}=\sum_{i,j} J_{ij}(\mathbf{S}_i\cdot\mathbf{S}_j-\tfrac{1}{4})+\text{const} \ . \tag{3.16}$$

Otherwise Eq. (3.15) is a generalization of the kinetic exchange Hamiltonian for the non-half-filled-band case. Such a model is similar to the resonating-valence-bond (RVB) proposals (Anderson, 1987, 1988; Baskaran *et al.*, 1987; Ruckenstein *et al.*, 1987; Wheatley *et al.*, 1988).

Anderson (1987, 1988) has suggested from the very beginning that the Cu-O-based high-T_c superconducting oxides are materials with strong electron correlations and that they can be understood within a two-dimensional, large-U, single-band Hubbard model. The model (3.15) for $W=0$, as recently proposed, can also be derived by an effective mapping of a two-band copper-oxygen 2D network model to a one-band model (the so-called t-J model, in which t and J are effectively independent parameters; Zhang and Rice, 1987; Zhang, 1989; Zhang and Rice, 1989).[6]

The nature of the ground state and excitations of the two-dimensional Heisenberg model are the objects of current interest. The numerical work shows that the quantum Néel state is the stable ground state of Eq. (3.16) for a square lattice (see, for example, Reger and Young, 1988, and references therein). The dynamics and quantum effects of 2D Heisenberg antiferromagnets have been analyzed intensively in this connection (e.g., Arovas and Auerbach, 1988; Chakravarty *et al.*, 1988) as well as with neutron scattering experiments on undoped La_2CuO_4, which demonstrated the existence of long-range Néel ordering and the exchange energy $J\approx 0.1$ eV (Shirane *et al.*, 1987; Auerbach and Arovas, 1988; Birgenau and Shirane, 1989).

Away from the half-filling, the central questions are the nature of mobile quasiparticles (holes in a nearly

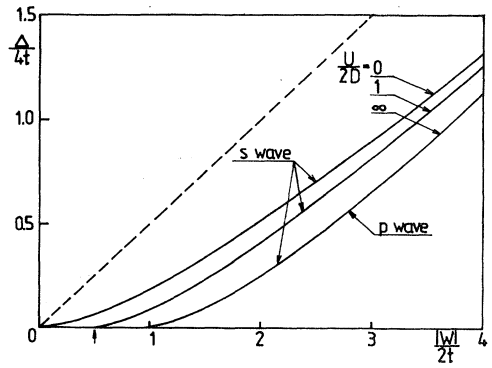

FIG. 23 Binding energies of s and p local pairs in one dimension for different values of $U/4t$. The dashed line is an asymptotic line $\Delta=|W|$.

[6]The relation of the t-J model to a more general Hamiltonian of the CuO-based high-T_c oxides containing Cu and O bands and intra- and interatomic Coulomb interactions is still under debate (Emery and Reiter, 1988a, 1988b; Stechel and Jennison, 1988; Zaanen and Oleś, 1988.)

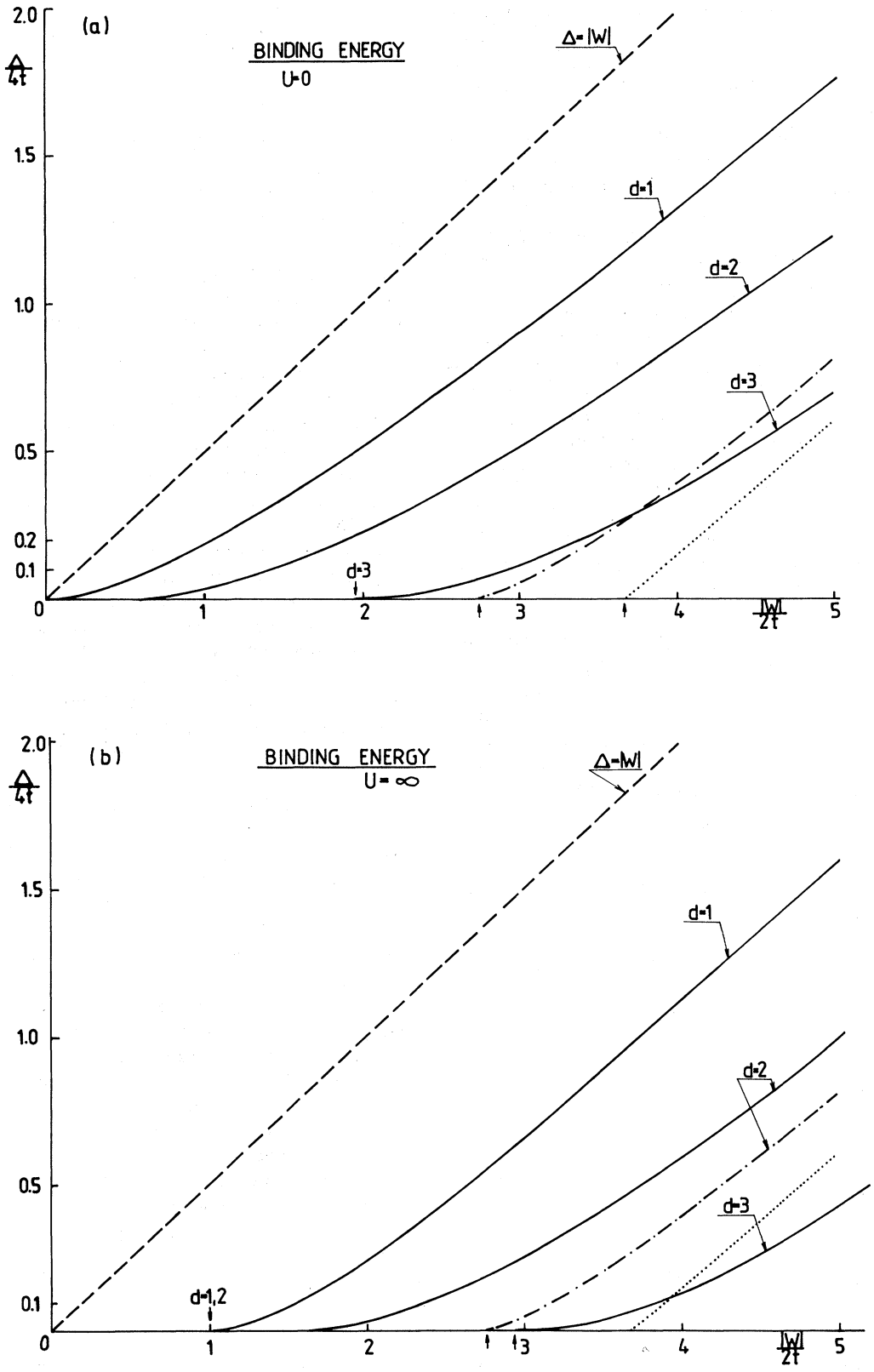

FIG. 24. Binding energies of intersite local pairs vs $|W|/2t$ for dimensionalities $d=1$, 2, 3; solid curves, s-wave pairs; dotted curve, d-wave pairs for $d=2$; dot-dashed curve, p-wave pairs for $d=2$. A square lattice is assumed for the 2D results and a simple cubic lattice for the 3D results. (a) $U=0$, (b) $U=\infty$.

half-filled Hubbard model) and the possibility of their attractive interaction leading to superconducting ordering (e.g., Loh *et al.*, 1988; Schmitt-Rink *et al.*, 1988; Shraiman and Siggia, 1988; Bonča *et al.*, 1989; Kane *et al.*, 1989).

It is under intensive study whether superconductivity can result from the purely repulsive Coulomb interactions for the one-band Hubbard model (Hirsch and Lin, 1988; Lin *et al.*, 1988; Hirsch, 1989b). The subsequent work of the Santa Barbara group (Bickers *et al.*, 1989; White *et al.*, 1989) with the use of conserving approximations and the Bethe-Salpeter equation, as well as the quantum Monte Carlo results, strongly suggests that the 2D Hubbard model has a d-wave superconducting ground state for a small range of fillings around $n=1$, but the predicted T_d is low (of order $0.01t$ for $U/4t=1$).

However, an additional attractive interaction (in our case $W<0$) can stabilize the superconducting state.

There are in principle two sources of pairing in Eq. (3.15), one arising from superexchange and the other from charge terms, in particular from $W<0$. The difficulty in constructing a mean-field description of superconductivity and magnetic states is that the Hamiltonian Eq. (3.15) is defined only in the subspace of singly occupied states. A rather simplified picture of superconductivity is obtained upon relaxing the double occupancy condition by linearization $t_{ij}h^{\dagger}_{i\sigma}h_{j\sigma}\rightarrow\delta t_{ij}c^{\dagger}_{i\sigma}c_{j\sigma}$, where $\delta=1-n$ means a deviation from the half-filled-band occupancy. Such a procedure requires a supplementary projection operation to exclude the doubly occupied states. Consequently one simplifies Eq. (3.15) to (Micnas, Ranninger, Robaszkiewicz, and Tabor, 1988)

$$\tilde{H}\cong\sum_{i,j,\sigma}\delta t_{ij}c^{\dagger}_{i\sigma}c_{j\sigma}+\sum_{i,j}J_{ij}\mathbf{S}_i\cdot\mathbf{S}_j+\sum_{i,j}\delta W'_{ij}n_in_j-\mu\sum_i n_i+\text{const}\ , \tag{3.17}$$

where $W'=-\frac{1}{4}J+W$, $n_i=n_{i\uparrow}+n_{i\downarrow}$. Notice that we also scaled the charge couplings by δ in order to get a consistent limit at $\delta=0$. μ is the chemical potential. With the use of Gorkov's-type factorization, the gap equation for the singlet pairing is

$$\Delta_{\mathbf{k}}=\frac{1}{N}\sum_{\mathbf{q}}V_{\mathbf{k},\mathbf{q}}\Delta_{\mathbf{q}}F_{\mathbf{q}}\ , \tag{3.18}$$

where

$$V_{\mathbf{k},\mathbf{q}}=[\tfrac{3}{2}J+\delta(\tfrac{1}{2}J-W)]\gamma_{\mathbf{k}-\mathbf{q}}\ , \tag{3.19a}$$

$$F_{\mathbf{q}}=(2E_{\mathbf{q}})^{-1}\tanh\left[\frac{E_{\mathbf{q}}}{2k_BT}\right],\quad E_{\mathbf{q}}=(\xi_{\mathbf{q}}^2+|\Delta_{\mathbf{q}}|^2)^{1/2}\ . \tag{3.19b}$$

$$\xi_{\mathbf{q}}=-t\delta\gamma_{\mathbf{q}}-\mu\ . \tag{3.19c}$$

For a $d=2$ square lattice the decomposition $\Delta_{\mathbf{k}}=\Delta_\gamma\gamma_{\mathbf{k}}+\Delta_\eta\eta_{\mathbf{k}}$ can be used to determine the critical temperatures for the extended s-wave and d-wave pairings. These equations for T_c are solved together with an equation determining the chemical potential,

$$\delta=\frac{1}{N}\sum_{\mathbf{q}}2\xi_{\mathbf{q}}F_{\mathbf{q}}\ . \tag{3.20}$$

Two facts should be noted. First, had we not scaled charge couplings [by putting $\delta=1$ in Eq. (3.19a)] we would have obtained T_c dependent on W, even in the case of $n=1$, where such coupling terms reduce to a constant. With our scaling, for $\delta=0$, one has $k_BT_c=\frac{3}{8}J$ for both types of pairing. The fact of finite T_c at $\delta=0$ is an artifact of the mean-field approach. The local constraint that every site for $\delta=0$ be singly occupied is not satisfied, and exact SU(2) symmetry is broken.[7] A separate question concerns the neglect of the mixed superconducting-antiferromagnetic solutions.

Secondly, it is easy to demonstrate that the d-wave pairing is the most stable one for $n\approx1$ by making use of the strong-coupling (high-T_c) expansion (Micnas, Ranninger, Robaszkiewicz, and Tabor, 1988). In Figs. 25 and 26 we give the numerical solutions for T_c^s and T_c^d versus δ. The results are presented for both the approach neglecting scaling of charge couplings [like that of Ruckenstein *et al.*, 1987; Figs. 25(a), 26(a)] and the approach performing such a scaling [like that of Micnas, Ranninger, Robaszkiewicz, and Tabor, 1988; Figs. 25(b), 26(b)]. Notice the enlarged temperature scale in Fig. 26(b). For a nearly half-filled band, T_c^s decreases with δ and is very small for δ around 0.1 (Fig. 25). $W>0$ reduces T_c^s and T_c^d, whereas $W<0$ indeed stabilizes both the pairings.

We should like to point out that $W<0$ can be a leading mechanism for pairing even at $J/t=0$ ($U=\infty$ limit). Moreover, s-wave pairing is favored in the low-concentration regime ($\delta\sim1$) and is strongly enhanced by the nearest-neighbor antiferromagnetic exchange (Fig. 26). As concerns p-wave pairing, it also can be realized, but only due to $W<0$, since an equal spin pairing contribution from the J_{ij} term precisely cancels.

We should like to comment critically on the above simplified mean-field approach, which can be only qualitatively correct for large doping concentrations ($\delta t\gg J$) (Ohkawa, 1988). For $\delta t\ll J$, such a Fermi-liquid description is problematic, and the pairing described by Eqs. (3.18) and (3.19) does not necessarily correspond to the original charge excitations; it can be merely the pairing of the spin excitations. This is due to relaxing of the double occupancy constraint. Despite intensive efforts in the last two years (e.g., Fukuyama *et al.*, 1988; Ohkawa, 1988; Suzumura *et al.*, 1988a, 1988b; and references

[7]For $n=1$ the bosonic representation of the strong-correlation limit is appropriate (Arovas and Auerbach, 1988; Kane *et al.*, 1989), since the mean-field version of that model, which treats the occupancy constraint in an average way, gets the physics at half-filling correct.

therein), at present there is no satisfactory mean-field description of superconductivity in the large-U limit of the Hubbard model in terms of constrained fermion operators, which are represented by spin degrees of freedom and constrained spinless boson operators describing the charge degrees of freedom.

Close to the half-filled band ($\delta \approx 0$), one can certainly consider the possibility of formation and Bose condensation of local pairs of holes (see, for example, Huang and Manousakis, 1987; Bonča *et al.*, 1989). Local pair formation is also possible in the low-concentration regime ($\delta \approx 1$) and is favored by an attractive intersite interaction $|W|$. This is the case if the extended Hubbard model with $W<0$ is used effectively to describe the pairing of

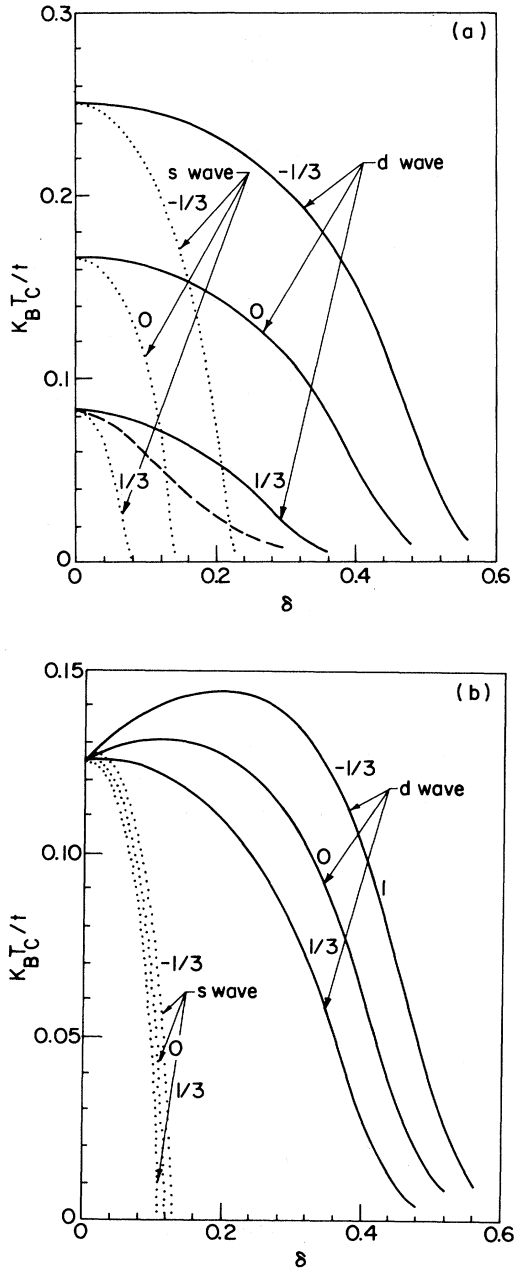

FIG. 25. T_c for s- and d-wave pairings vs doping $\delta = 1-n$ for a $d=2$ square lattice in the $|U \gg t$ limit. T_c^s and T_c^d are plotted by the solid and the dotted lines, respectively: (a) without the scaling of charge couplings, as in Ruckenstein *et al.* (1987); (b) with the scaling of charge couplings, as in Micnas, Ranninger, Robaszkiewicz, and Tabor (1988). $J = 2t^2/U = t/3$. The values of $W/t = -1/3, 0, \frac{1}{3}$ are quoted next to the curves. The T_c for p-wave pairing is indicated by the dashed line for $W/t = -1/3$ in (a), whereas in (b) it is vanishingly small (for this value of W/t).

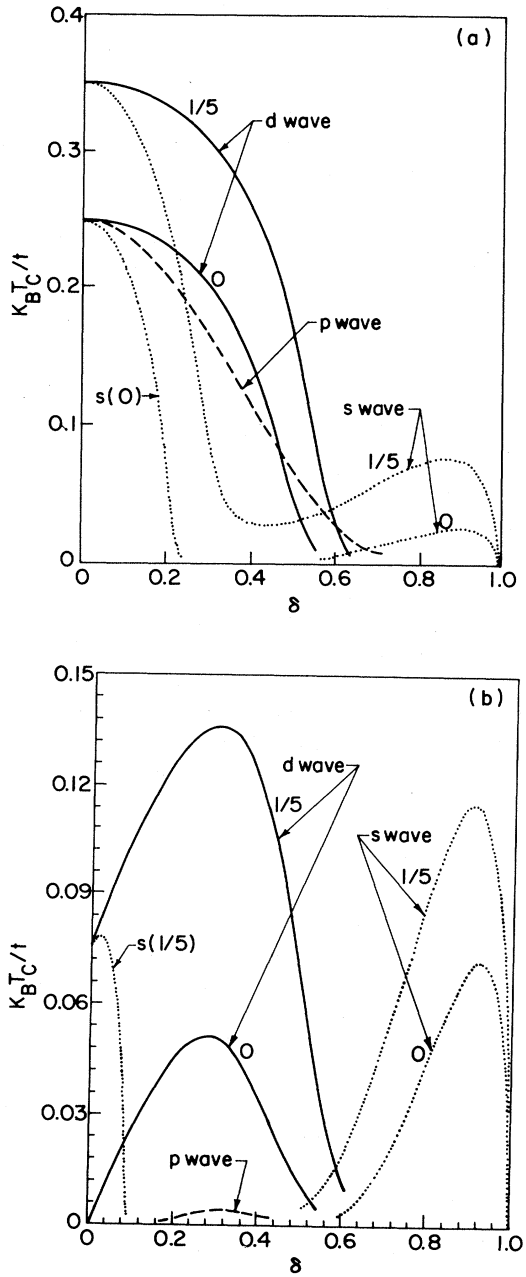

FIG. 26. As in Fig. 25 for $W/t = -1$ and two different values of $J/t = \frac{1}{5}, 0$, quoted next to the curves. The dashed line marks T_c for p-wave pairing independent of J.

oxygen holes in high-T_c materials, and the on-site repulsion is large compared to the hopping integral.

To close this section we stress that combined superexchange and polaronic effects, which could lead to band narrowing and $W<0$, might be relevant to our understanding of the high-T_c superconducting oxides (Kuramoto and Watanabe, 1987; Micnas *et al.*, 1988a; Micnas, Ranninger, Robaszkiewicz, and Tabor, 1988).

IV. MIXTURE OF LOCAL PAIRS AND ITINERANT ELECTRONS

The coexistence of bound pairs and itinerant electrons and the effects resulting from interactions between these two species constitute a crucial problem for real materials concerns. Such a model of a mixture of local pairs and electrons was introduced by us a few years ago (Ranninger and Robaszkiewicz, 1985), and its extended version has been extensively analyzed in a sequence of more recent papers (Micnas *et al.*, 1987a; Ranninger *et al.*, 1987, 1988; Robaszkiewicz *et al.*, 1987). It has been shown that in this type of system a new mechanism of superconductivity can develop. It results from intersubsystem charge-exchange coupling, which can be hybridization induced and/or direct, and leads to a superconducting state involving both types of particles.

In this section we outline the main results concerning this model. As we shall see, the physical properties of such a mixture of interacting charged bosons (bound electron pairs) and electrons can show features that are intermediate between those of pure local pair superconductors and those of classical BCS systems.

Starting from a generalized periodic Anderson model with on-site attraction and eliminating the hybridization between narrow- and wide-band electrons to lowest order by means of a generalized Schrieffer-Wolff transformation (Schrieffer and Wolff, 1966), we were able (Robaszkiewicz *et al.*, 1987) to derive an effective Hamiltonian that, in its simplest form, can be written as

$$\begin{aligned}\hat{H}=&\sum_{\mathbf{k},\sigma}\varepsilon_{\mathbf{k}}c^{\dagger}_{\mathbf{k}\sigma}c_{\mathbf{k}\sigma}+\sum_{i,j,\sigma}t_{ij}d^{\dagger}_{i\sigma}d_{j\sigma}-\tfrac{1}{2}|U|\sum_{i\sigma}d^{\dagger}_{i\sigma}d_{i\sigma}d^{\dagger}_{i-\sigma}d_{i-\sigma}\\&-\mu\left[\sum_{\mathbf{k},\sigma}c^{\dagger}_{\mathbf{k}\sigma}c_{\mathbf{k}\sigma}+\sum_{i,\sigma}d^{\dagger}_{i\sigma}d_{i\sigma}\right]+E_0\sum_{i,\sigma}d^{\dagger}_{i\sigma}d_{i\sigma}-\sum_{i}(I_0d^{\dagger}_{i\uparrow}d^{\dagger}_{i\downarrow}c_{i\downarrow}c_{i\uparrow}+\text{H.c.})\\&-\tfrac{1}{2}\sum_{i\neq j}[I_{ij}d^{\dagger}_{i\uparrow}d^{\dagger}_{i\downarrow}(c_{i\downarrow}c_{j\uparrow}+c_{j\downarrow}c_{i\uparrow})+\text{H.c.}]+C+S\ .\end{aligned}\tag{4.1}$$

Here $c^{(\dagger)}_{\mathbf{k}\sigma}$, $c^{(\dagger)}_{i\sigma}$ denote the electron operators of the wide-band subsystem, $\mathbf{k}$ and i refers to either their momentum or their site, and σ denotes the electron spin. $d^{\dagger}_{i\sigma}$, $d_{i\sigma}$ are the creation and annihilation operators of narrow-band electrons, which sense an effective on-site attractive interaction $|U|$. μ is the chemical potential, which ensures that the total number of particles in the system is constant, i.e.,

$$n=\frac{1}{N}\left[\sum_{\mathbf{k},\sigma}\langle c^{\dagger}_{\mathbf{k}\sigma}c_{\mathbf{k}\sigma}\rangle+\sum_{i,\sigma}\langle d^{\dagger}_{i\sigma}d_{i\sigma}\rangle\right].$$

E_0 denotes the relative position of the d band with respect to the c band. $\varepsilon_{\mathbf{k}}$ refers to the dispersion of the "c" (wide-band) electrons and t_{ij} denotes the effective hopping integral (direct and hybridization-induced) of the "d" (narrow-band) electrons. The terms proportional to I_0 and I_{ij} ($I_0=I_{ii}$) represent the transverse components of the charge-charge coupling between the two subsystems (which is crucial for the superconducting mechanism that we want to discuss). In general, this transverse component has two contributions.

(i) A direct on-site charge-exchange interaction, i.e., a term proportional to the off-diagonal matrix element of the Coulomb interaction

$$\left\langle d\uparrow d\downarrow\left|\frac{1}{r}\right|c\downarrow c\uparrow\right\rangle,$$

in Hubbard's notation (Hubbard, 1963, 1964), which in general has the same order of magnitude (0.1–1.0 eV) as the direct on-site magnetic exchange

$$\left\langle d\uparrow c\downarrow\left|\frac{1}{r}\right|c\uparrow d\downarrow\right\rangle.$$

(ii) An indirect charge-exchange coupling, induced by hybridization (i.e., a Kondo-like coupling):

$$I_{ij}=-\frac{1}{N}\sum_{\mathbf{k}}I_{\mathbf{k}}\exp[i\mathbf{k}\cdot(\mathbf{R}_i-\mathbf{R}_j)],$$

where

$$I_{\mathbf{k}}=V^2\left[\frac{1}{\varepsilon_{\mathbf{k}}-E_0-U}+\frac{1}{E_0-\varepsilon_{\mathbf{k}}}\right],$$

and where V denotes the coupling constant of the hybridization term $\sum_i V(c^{\dagger}_{i\sigma}d_{i\sigma}+\text{H.c.})$.

In Eq. (4.1), C denotes all the density-density interaction terms (except those of $|U|$), both direct and hybridization-induced, which in the present discussion we shall neglect, since we shall focus on the superconducting properties of the Hamiltonian (4.1) rather than on possible CDW or SDW orderings. S in Eq. (4.1) describes the magnetic exchange interactions between the two subsystems. For explicit expressions of the various coupling constants in terms of the parameters of the starting Hamiltonian, we refer the reader to

Robaszkiewicz *et al.* (1987).

Assuming the strong-attraction limit $|U| \gg t, I_{ij}$, one can eliminate (as for the negative-U Hubbard model, see Sec. II.B) any singly occupied d-electron states in $\hat{H}$ [Eq. (4.1)]. This procedure obviously eliminates all the inter-subsystem magnetic interactions. The resulting effective Hamiltonian defined in a subspace where d electrons occur only in the form of pairs is given by

$$\tilde{\mathcal{H}} = \sum_{\mathbf{k},\sigma} \varepsilon_{\mathbf{k}} c^{\dagger}_{\mathbf{k}\sigma} c_{\mathbf{k}\sigma} + \Delta_0 \sum_i (2\rho_i^z + 1) - \sum_{i,j} \tfrac{1}{2} J_{ij} [(\rho_i^+ \rho_j^- + \text{H.c.}) - \rho_i^z \rho_j^z]$$
$$+ \frac{1}{2N} \sum_{i,\mathbf{k},\mathbf{k}'} (I_{\mathbf{k}',-\mathbf{k}} \exp[i(\mathbf{k}+\mathbf{k}')\cdot\mathbf{R}_i] c^{\dagger}_{\mathbf{k}'\uparrow} c^{\dagger}_{-\mathbf{k}\downarrow} \rho_i^- + \text{H.c.}) - \mu \left[\sum_i (2\rho_i^z + 1) + \sum_{\mathbf{k}\sigma} c^{\dagger}_{\mathbf{k}\sigma} c_{\mathbf{k}\sigma} \right] \tag{4.2}$$

where

$$\rho_i^+ = d^{\dagger}_{i\uparrow} d^{\dagger}_{i\downarrow} = (\rho_i^-)^{\dagger} ,$$
$$2\rho_i^z + 1 = \sum_{\sigma} d^{\dagger}_{i\sigma} d_{i\sigma} .$$
$$I_{\mathbf{k}',-\mathbf{k}} = I_{\mathbf{k}} + I_{-\mathbf{k}'} , \tag{4.3}$$
$$I_{\mathbf{k}} = -\sum_j I_{ij} \exp[-i\mathbf{k}\cdot(\mathbf{R}_i - \mathbf{R}_j)] .$$

The charge operators $\{\rho_i\}$ in Eq. (4.2) obey the Pauli spin-$\frac{1}{2}$ commutation rules, i.e.,

$$[\rho_i^+, \rho_j^-] = 2\rho_i^z \delta_{ij} ,$$
$$[\rho_i^{+(-)}, \rho_j^{+(-)}] = 0 ,$$
$$\rho_i^+ \rho_i^- = \rho_i^z + \tfrac{1}{2} .$$

$\Delta_0 = E_0 - \frac{1}{2}|U|$ measures the relative position of the local pair level with respect to the bottom of the wide band of electrons (see Fig. 27), $J_{ij} = 2t_{ij}^2/|U|$.

In the absence of wide-band "c" electrons, the present problem reduces to one of purely on-site pairs and the superconductivity of a charged Bose gas on a lattice, which we discussed at length in Sec. II. Similarly, if $J_{ij} \neq 0$, $I_{ij} = 0$, the "d" electrons forming local pairs will condense to a superfluid state, while the "c" electrons remain in the normal state. Contrary to the case of only "d" electrons, now the superconducting critical temperature *T_c will only implicitly depend on the number of "d" electrons at $T = T_c$*. Moreover, the wide-band electrons can effectively screen the long-range Coulomb interaction between charged pairs of d electrons, favoring local pair superconductivity over a possible dielectric phase.

The case that will interest us here in particular is $J_{ij} = 0$, $I_{ij} \neq 0$. Neither of the two subsystems by itself will be able to become superconducting. Superconductivity is mutually induced in the two subsystems of "c" and "d" electrons via the charge-exchange term $\sim I$. We shall consequently define two order parameters

$$x_0 = \frac{1}{N} \sum_{\mathbf{k}} \langle c^{\dagger}_{\mathbf{k}\uparrow} c^{\dagger}_{-\mathbf{k}\downarrow} \rangle , \quad \rho_0^x = \frac{1}{N} \sum_i \langle d^{\dagger}_{i\uparrow} d^{\dagger}_{i\downarrow} \rangle , \tag{4.4}$$

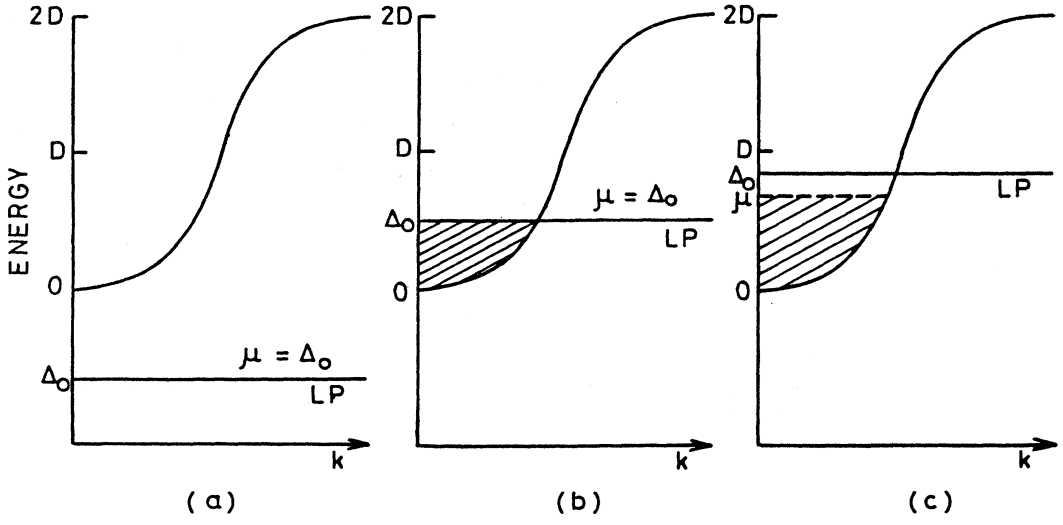

FIG. 27. The relative position of the local pair (LP) level Δ_0 with respect to the bottom of the wide band of electrons in the absence of any interaction effects. μ denotes the chemical potential. (a) $\Delta_0 < 0$. In the ground state only local pair states are occupied. (b) $0 < \Delta_0 = \mu$. In the ground state, both the single-particle states of wide-band electrons and the local pair states are occupied. (c) $\mu = \Delta_0$. In the ground state only the single-particle states of wide-band electrons are occupied.

which have to be determined in conjunction with the average number of "c" and "d" electrons,

$$n^c=\frac{1}{N}\sum_{\mathbf{k},\sigma}\langle c^\dagger_{\mathbf{k}\sigma}c_{\mathbf{k}\sigma}\rangle,\quad n^d=\frac{1}{N}\sum_{i,\sigma}\langle d^\dagger_{i\sigma}d_{i\sigma}\rangle\ , \tag{4.5}$$

as a function of temperature and the total density of carriers $n=n^c+n^d$. For this purpose let us consider the Hamiltonian [Eq. (4.2)] in its corresponding superconducting mean-field approximation, in the absence of any density-density coupling terms. Upon neglecting terms proportional to I_{ij} $(i\neq j)$ that are much smaller than I_0 (Robaszkiewicz *et al.*, 1987), which corresponds to the assumption $I_{\mathbf{k}',-\mathbf{k}}=-I\,(=I_0)$ in Eq. (4.2), we get

$$\begin{aligned}
&\tilde{H}^{MF}=\bar{C}+H_0^c+H_0^d\ ,\\
&\bar{C}/N=J_0(\rho_0^x)^2+2Ix_0\rho_0^x-(\mu-\Delta_0)\ ,\\
&H_0^c=\sum_{\mathbf{k},\sigma}(\varepsilon_{\mathbf{k}}-\mu)c^\dagger_{\mathbf{k}\sigma}c_{\mathbf{k}\sigma}-I\rho_0^x\sum_{\mathbf{k}}(c_{\mathbf{k}\uparrow}c_{-\mathbf{k}\downarrow}+c^\dagger_{-\mathbf{k}\downarrow}c^\dagger_{\mathbf{k}\uparrow})\ ,\\
&H_0^d=-2\sum_i[J_0\rho_0^x+Ix_0]\rho_i^x+2(\Delta_0-\mu)\sum_i\rho_i^z\ ,
\end{aligned} \tag{4.6}$$

where

$$J_0=\sum_{\substack{j\\(i\neq j)}}J_{ij}\ .$$

Upon diagonalization of this Hamiltonian we obtain the following dispersion for single-particle excitations concerning the "c" electron subsystem:

$$\omega_{\mathbf{k}}^{\pm}=\pm[(\varepsilon_{\mathbf{k}}-\mu)^2+(I\rho_0^x)^2]^{1/2}\ . \tag{4.7}$$

For the local pair subsystem of the "d" electrons we obtain (as in the strong-attraction limit of the negative-U Hubbard problem) the two mean-field levels

$$\Delta_{\pm}=\pm[(\mu-\Delta_0)^2+(J_0\rho_0^x+Ix_0)^2]^{1/2}\ , \tag{4.8}$$

where $\Delta_+-\Delta_-$ corresponds to the excitation energy of flopping a pseudospin $\boldsymbol{\rho}$ at any given site. We know that in the case of a purely "d" subsystem (uncoupled to the "c" electrons) these two mean-field levels give the lower and upper bounds of a continuous spectrum of collective excitations, corresponding to the phase fluctuations of the order parameter ρ_0^x; this spectrum is linked to the charge fluctuations of the hard-core charged bosons $b_i^\dagger=d_{i\uparrow}^\dagger d_{i\downarrow}^\dagger$. Although at present we do not know the exact form of this spectrum in the presence of the "c" subsystem, it is clear that the two levels Δ_+ and Δ_- ought to be replaced by a continuous spectrum bounded between Δ_+ and Δ_-.

In order to determine the width of a single-particle gap in the spectrum of the "c" electrons and the width of the bosonic excitations of the "d" subsystem, we must solve the self-consistent equations linking the two order parameters x_0 and ρ_0^x with those for the number of "c" and "d" electrons. These equations are

$$\begin{aligned}
&\rho_0^x=[(J_0\rho_0^x+Ix_0)/2\Delta]\tanh(\beta\Delta)\ ,\\
&x_0=\frac{1}{2N}\sum_{\mathbf{k}}\frac{I\rho_0^x}{\omega_{\mathbf{k}}}\tanh\left[\frac{\beta\omega_{\mathbf{k}}}{2}\right]\ ,\\
&n^c-1=-\frac{1}{N}\sum_{\mathbf{k}}\frac{(\varepsilon_{\mathbf{k}}-\mu)}{\omega_{\mathbf{k}}}\tanh\left[\frac{\beta\omega_{\mathbf{k}}}{2}\right]\ ,\\
&n^d-1=\frac{\mu-\Delta_0}{\Delta}\tanh(\beta\Delta)\ ,
\end{aligned} \tag{4.9}$$

where $\omega_{\mathbf{k}}=\omega_{\mathbf{k}}^+$ and $\Delta=\Delta_+$.

Depending on the relative concentration of "c" and "d" electrons, we distinguish three essentially different physical situations ($0\le n\le 2$; see Fig. 27): (i) $\Delta_0<0$ such that all the available electrons form local pairs of "d" electrons; (ii) $\Delta_0>0$ such that the "c" electron band is filled up to the Fermi level $\mu\equiv\Delta_0$ and the remaining electrons are in the form of local pairs of "d" electrons; (iii) $\Delta_0>0$ such that the Fermi level $\mu<\Delta_0$ and consequently all the available electrons occupy "c" electron states.

Our mean-field analysis can be expected to hold best for case (ii), in which the concentrations of "c" and "d" electrons are both finite. In this case superconductivity comes about by a perpetual interchange between local pairs of "d" electrons and pairs of "c" electrons. In this process "c" electrons become "polarized" into Cooper pairs, and "d" electron pairs increase their mobility by decaying into "c" electron pairs.

In case (i), local pairs of "d" electrons move via virtual excitations into pairs of "c" electrons having opposite momenta and spins. As we shall see below, such a mechanism gives rise to long-range hopping of pairs of "d" electrons with a spatial dependence similar to the Rudermann-Kittel-Kasuya-Yosida (RKKY) interaction for s-d mechanisms in the magnetic equivalent. In case (iii), on the contrary, we find a situation similar to the BCS case: pairs of "c" electrons with opposite momenta and spins are exchanged via virtual transitions into local pair states.

The results for n^c, n^d, ρ_0^x, and x_0 for $T=0$ and $J_0=0$ as a function of Δ_0 are plotted in Fig. 28. In Fig. 29(a) and 29(b) we present $k_BT_c/2D$ as a function of Δ_0/D for different total concentrations of carriers, $n=n^c+n^d=2$, 1.5, 1, and 0.5, as a function of Δ_0/D. D denotes the half-bandwidth of the square DOS for the "c" electrons. The ratio of the single-particle energy gap for wide-band electrons at $T=0$ divided by $2k_BT_c$, $E_g(0)/2k_BT_c$, is given in Fig. 30 for two different values of the charge-exchange coupling, $I/2D=0.5$, 0.1.

Notice that the maximum value of T_c is achieved in case (ii), when $n^c\sim n^d$, in which case it is of order I^2/D. T_c drops to zero when we approach the regions corresponding to cases (i) and (iii). In region (i) the single-particle energy gap is of order Δ_0 and $T_c\sim I^2/\Delta_0$. In region (iii) we recover the BCS value for $E_g(0)/k_BT_c=3.52$. Notice also that the maximum in T_c shifts towards $\Delta_0=0$ as the total carrier concentration is de-

creased. In particular, for systems with low carrier concentration, one expects a sharp and narrow peak in T_c centered on $\Delta_0=0$.

Let us consider now an alternative approach to this model, consisting of eliminating to lowest order the inter-subsystem couplings (the charge exchange and the density-density coupling) through the canonical transformation method (Robaszkiewicz *et al.*, 1987; Ranninger *et al.*, 1988). Such an approach is best substantiated for case (i) of the present model, in which all electrons are condensed into pairs of "d" electrons, and the pairs move via virtual excitations into "c" electron states.

In order to obtain an effective indirect hopping of "d" electron pairs, let us consider the general Hamiltonian including, in addition to charge exchange, the density-density coupling:

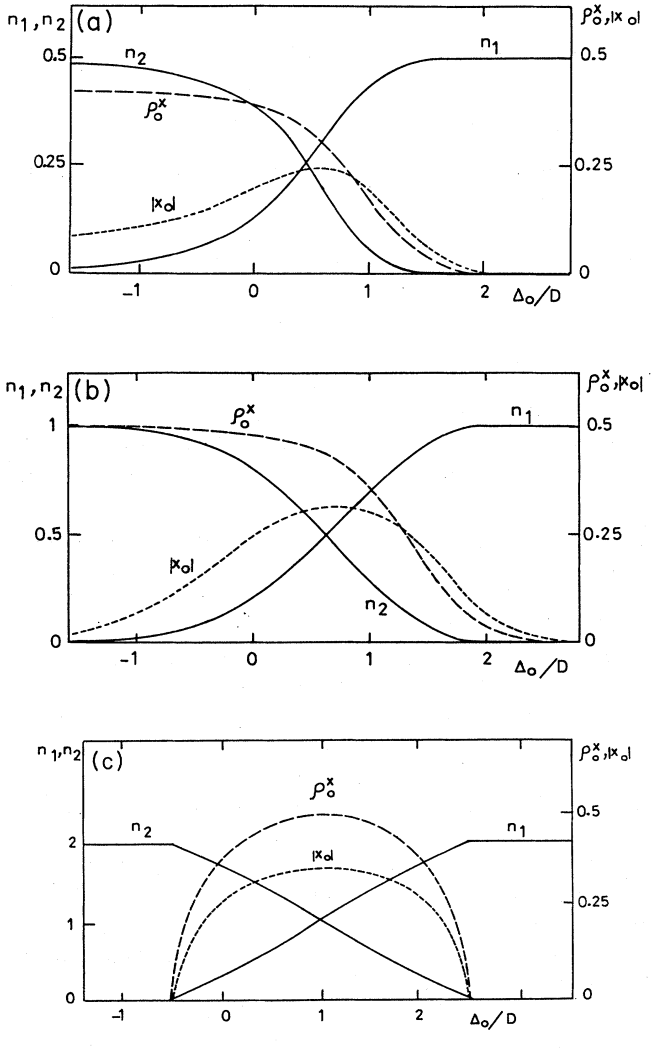

FIG. 28. Variation of the concentration of "c" ($n^c=n_1$) and "d" ($n^d=n_2$) electrons, as well of the two superconducting order parameters x_0 and ρ_0^x, as a function of Δ_0 for $T=0$ and three characteristic values of the total concentration of carriers n: (a) $n(=n_c+n_d)=0.5$; (b) $n=1$; (c) $n=2$.

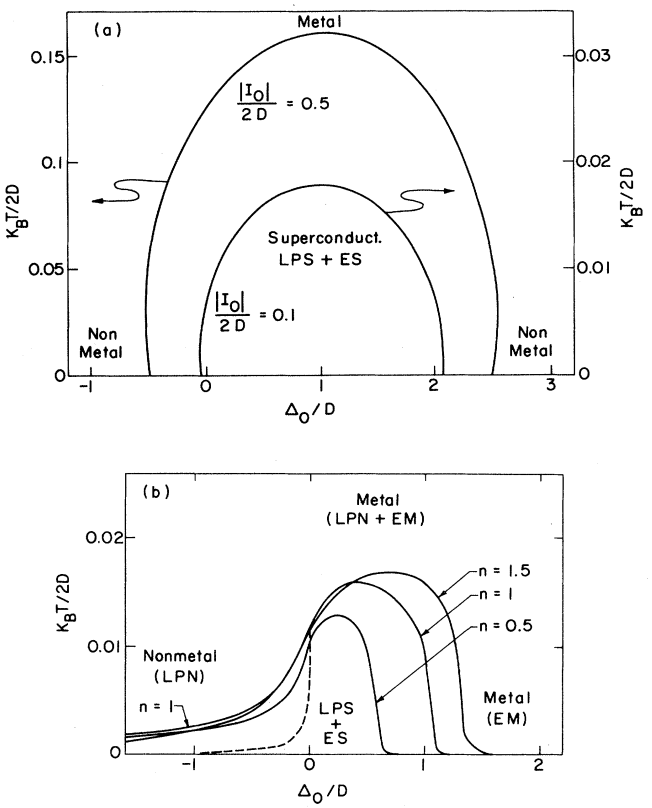

FIG. 29. Finite-temperature phase diagram as a function of Δ_0/D. (a) For two values of $|I|/2D$ (0.5, 0.1), with the total number of particles $n=2$; (b) for $|I|/2D=0.1$ and $n=0.5$, 1, and 1.5. The dashed line (which on the scale presented is indistinguishable for all three cases of n) corresponds to T_c calculated by a perturbational approach for $\Delta \lesssim 0$. LPS+ES denotes the superconducting state involving both local pairs and wide-band electrons. LPN stands for the nonmetallic state of only local pairs, and EM indicates the metallic state of only wide-band electrons.

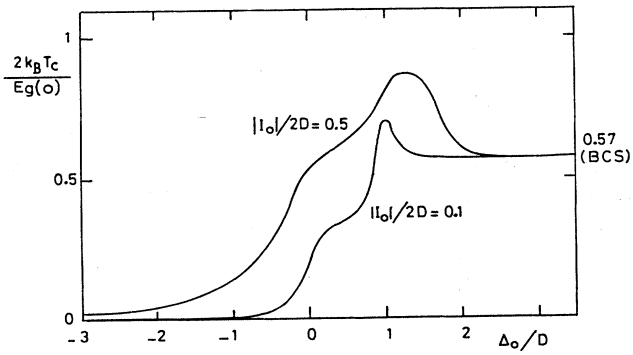

FIG. 30. $2k_BT_c/E_g(0)$ as a function of Δ_0/D for $J_0=0$ and two values of $|I|/2D$ (0.5,0.1) and $n=1$. $E_g(0)$ denotes the gap in the single-particle spectrum of wide-band electrons at zero temperature.

$$H=H_0+H_1\ ,$$

$$H_0=\sum_{\mathbf{k},\sigma}(\varepsilon_{\mathbf{k}}-\mu)c^{\dagger}_{\mathbf{k}\sigma}c_{\mathbf{k}\sigma}+(\Delta_0-\mu)\sum_i(2\rho_i^z+1)\ , \tag{4.10}$$

$$H_1=\frac{1}{2N}\sum_{i,\mathbf{k},\mathbf{k}'}(I_{\mathbf{k}',-\mathbf{k}}e^{i(\mathbf{k}+\mathbf{k}')\cdot\mathbf{R}_i}c^{\dagger}_{\mathbf{k}'\uparrow}c^{\dagger}_{-\mathbf{k}\downarrow}\rho_i^-+\text{H.c.})+\frac{1}{2N}\sum_{i,\mathbf{k},\mathbf{k}',\sigma}V_{\mathbf{k}'\mathbf{k}}e^{-i(\mathbf{k}-\mathbf{k}')\cdot\mathbf{R}_i}c^{\dagger}_{\mathbf{k}'\sigma}c_{\mathbf{k}\sigma}(2\rho_i^z+1)$$

Eliminating the interaction H_1 to first order by unitary transformation $U=\exp(iS)$, where

$$S=\frac{-i}{2N}\sum_{j,\mathbf{k},\mathbf{k}'}\frac{I_{\mathbf{k}',-\mathbf{k}}e^{i(\mathbf{k}+\mathbf{k}')\cdot\mathbf{R}_j}}{\varepsilon_{\mathbf{k}'}+\varepsilon_{\mathbf{k}}-2\Delta_0}c^{\dagger}_{\mathbf{k}'\uparrow}c^{\dagger}_{-\mathbf{k}\downarrow}\rho_i^--\text{H.c.}+\frac{-i}{2N}\sum_{j,\mathbf{k},\mathbf{k}'\sigma}\frac{V_{\mathbf{k}',\mathbf{k}}e^{-i(\mathbf{k}-\mathbf{k}')\cdot\mathbf{R}_j}}{\varepsilon_{\mathbf{k}'}-\varepsilon_{\mathbf{k}}}c^{\dagger}_{\mathbf{k}'\sigma}c_{\mathbf{k}\sigma}(2\rho_i^z+1)\ , \tag{4.11}$$

gives rise to the following Hamiltonian $\bar{H}=UHU^{-1}$ (after averaging over the wide-band electron states):

$$\bar{H}=H_0+\bar{H}_1\ , \tag{4.12}$$

where

$$\begin{aligned}\bar{H}_1&=-\tfrac{1}{2}\sum_{i,j}A(\mathbf{R}_{ij})(\rho_i^+\rho_j^-+\text{H.c.})+\sum_{i,j}B(\mathbf{R}_{ij})(2\rho_i^z+1)(2\rho_j^z+1)+\text{const}\\&=-\tfrac{1}{2}\sum_{i\neq j}A(\mathbf{R}_{ij})(\rho_i^+\rho_j^-+\text{H.c.})+\sum_{i\neq j}B(\mathbf{R}_{ij})(2\rho_i^z+1)(2\rho_j^z+1)-A(0)\sum_i(2\rho_i^z+1)+B(0)\sum_i(2\rho_i^z+1)^2+\text{const}\ ,\end{aligned} \tag{4.13}$$

with

$$A(\mathbf{R}_{ij})=-\frac{1}{N}\sum_{\mathbf{k},\mathbf{k}'}|I_{\mathbf{k}',-\mathbf{k}}|^2\frac{n_{\mathbf{k}}+n_{\mathbf{k}'}-1}{\varepsilon_{\mathbf{k}}+\varepsilon_{\mathbf{k}'}-2\Delta_0}\times e^{-i(\mathbf{k}+\mathbf{k}')\cdot(\mathbf{R}_i-\mathbf{R}_j)}\ ,$$

$$B(\mathbf{R}_{ij})=-\frac{1}{N}\sum_{\mathbf{k},\mathbf{k}'}|V_{\mathbf{k}'\mathbf{k}}|^2\frac{n_{\mathbf{k}}-n_{\mathbf{k}'}}{\varepsilon_{\mathbf{k}}-\varepsilon_{\mathbf{k}'}}\times e^{-i(\mathbf{k}-\mathbf{k}')\cdot(\mathbf{R}_i-\mathbf{R}_j)}\ .$$

where $n_{\mathbf{k}}$ is the Fermi-Dirac distribution function. Clearly $\bar{H}_1$ [Eq. (4.13)] describes an indirect transfer of local pairs via wide-band electron states. $A(\mathbf{R}_{ij})$ is the particle-particle analog of the RKKY-type interaction, whereas $B(\mathbf{R}_{ij})$ is of the RKKY form of the *s-d* mechanism for the particle-hole channel. Both interactions, the pair hopping $A(\mathbf{R}_{ij})$ and the pair interaction $B(\mathbf{R}_{ij})$, can be long ranged, and $B(\mathbf{R}_{ij})$ is an oscillating function of the type $\cos(2k_FR)/(k_FR)^3$.

We should stress that, in contrast to the previous treatment, the Hamiltonian (4.12), (4.13) allowed us to treat properly the self-energy corrections of the bosonic translational motion [i.e., the subtraction of $A(0)$ and $B(0)$ terms], which is always a formidable task for other approaches. Let us now apply these results to the case (i) ($\Delta_0<0$) by putting $I_{\mathbf{k}',-\mathbf{k}}=-I_0$ and $V_{\mathbf{k}',\mathbf{k}}=0$. Carrying out the mean-field analysis on the transformed Hamiltonian (4.12), (4.13), we obtain for T_c (Robaszkiewicz *et al.*, 1987)

$$k_BT_c=-\tilde{J}_0\frac{(n-1)}{\ln\left[\dfrac{n}{2-n}\right]}\ , \tag{4.14}$$

$$\tilde{J}_0=(I_0)^2[A_{\mathbf{k}=0}-A(0)]\ . \tag{4.15}$$

Evaluating $A_{\mathbf{k}=0}$ and $A(0)$ with the use of the square DOS for the wide-band electrons, we obtain

$$A(0)=-\frac{1}{D}\left[\frac{x+1}{x}\ln(1+x)-(1+2/x)\ln(1+x/2)\right]\ ,$$

$$A_{\mathbf{k}=0}=-\frac{1}{4D}\ln(x+1),\quad x=2D/\Delta_0\ . \tag{4.16}$$

A simple numerical analysis of $\tilde{J}_0$ as a function of Δ_0/D shows a sharp drop of $\tilde{J}_0$ as Δ_0/D is lowered below zero, giving values for T_c well below those predicted by the mean-field treatment of the contact interaction. In Fig. 29(b) we plot this result for T_c by a dashed line, which finally leads to a picture for $n<2$ that is, in fact, very similar to that obtained for $n=2$ [compare Fig. 29(a)], i.e., a sharp dropoff of T_c as one approaches values of Δ_0/D where the concentration either of local pairs or of wide-band electrons becomes very small.

To conclude, we notice that the indirect long-range character of charge exchange between local pairs is an essential feature of the mixed model. This should be contrasted with previously considered models of local pair superconductivity in which the pair hopping term resulting from the kinetic exchange mechanism ($\sim t_{ij}^2/|U|$) is obviously short ranged. Thus an indirect charge exchange can be effective even if the local pair centers are well separated in space. The case in which a small number of local pairs are coupled by a long-range interaction resembles an RKKY "spin glass," and it might well exhibit a "superconducting glass" state or a "charge-density-wave glass" state.

Let us summarize the main physical features of the mixture of wide-band electrons and local pairs, discussed in this section. We shall restrict ourselves mainly to case (ii), where both wide-band electrons and local electron

pairs coexist with finite concentrations. As we go from predominantly local pairs to predominantly wide-band electrons, we observe the nonmonotonic behavior of T_c, which passes through a maximum when the two constituents have roughly equal concentrations. The ratio $E_g(0)/k_BT_c$—the energy gap over T_c—varies around the BCS value 3.52 as the relative proportion of local pairs to wide-band electrons is changed. Where T_c is maximal, $E_g(0)/k_BT_c$ has a shallow minimum; it approaches the BCS value for predominantly wide-band electrons and surpasses it as the concentration of local pairs increases above that of wide-band electrons. The specific heat of the system will be determined by a superposition arising from two contributions: single-particle excitations, which will give it a shape like that expected for a BCS superconductor, and collective excitations (lying in the superconducting gap), which will give it a contribution like that in the local pair system: i.e., $c \sim T^d$ for $T \rightarrow 0$ plus a λ-like singularity at T_c.

The coherence length H_{c_2}, the penetration depth, and the Ginzburg-Landau parameter will continuously vary from those characteristic of local pair superconductors (Sec. II) for a predominantly local pair limit to those characteristic of BCS systems.

As far as the normal state above T_c is concerned, we conjecture a depleted density of states near the Fermi energy of the wide-band electron subsystem. This is due to the absorption of electrons into the virtual bound state. As a consequence we also expect rather high values of resistivity. It has been claimed that such a system of local pairs and wide-band electrons could exhibit linear-in-T resistivity in the normal state, where the Fermi level decreases linearly with T (Eliashberg, 1987; Kulik, 1987). The model could possibly apply to the new high-T_c superconductors (Eliashberg, 1987; Kulik, 1987, 1988; Robaszkiewicz *et al.*, 1987; Khomskii and Zvezdin, 1988; Ranninger *et al.*, 1988), as well as to the doped $BaBiO_3$ perovskites (Robaszkiewicz *et al.*, 1987; Sugai, 1989; Sugai, Enomoto, and Murakami, 1989; Micnas *et al.*, 1987a).

V. FINAL REMARKS

A. Summary

In this paper we have reviewed the concept of local pairing and discussed the main differences between local pair superconductivity and standard, weak-coupling BCS superconductivity. We have discussed the thermodynamic and electromagnetic properties of relatively simple models of local pairing, treating the parameters of local interactions as effective ones. An advantage of such simple models is that they permit the exploration of general features of local pairing without resorting to specific microscopic origins of attractive interactions.

The theory presented here is applicable to a variety of materials, which we listed in the Introduction, and as far as particular systems are concerned we refer the reader to the original papers quoted therein (see in particular Ionov *et al.*, 1981; Kulik, 1984; Alexandrov and Elesin, 1985; Eagles, 1985; Alexandrov *et al.*, 1986b; Robaszkiewicz *et al.*, 1987; de Jongh, 1988b; Micnas *et al.*, 1988b).

Let us now summarize the major theoretical results given in this paper. In order to approach the physics of systems with real-space pairing we considered three models, each of which presented particular aspects of this problem.

The first model, which has been studied in greatest detail—the extended Hubbard model with negative U (Sec. II)—permitted us to examine the changeover from weak to strong local attraction, interpolating between two extreme limits: a weak-coupling BCS-like superconductivity and a strong-coupling local pair superconductivity, which is that of a hard-core charged Bose gas on a lattice. The questions of charge ordering and mixed solutions where charge order coexists with superconductivity were also analyzed.

The second model, studied in Sec. III, was an extended Hubbard model with on-site repulsion and intersite attraction. The study of this model (for a square lattice) permitted us to examine the stability of the various anisotropic superconducting states, as well as the spin-density wave state as a function of band filling. In Sec. III we also studied the conditions for pair formation versus dimensionality and the limit of strong correlations ($U \gg t$), as well as the effects of exchange interaction and correlated hopping.

The third model, discussed in Sec. IV, was a mixture of two types of electrons: narrow-band electrons, which exist exclusively in the form of local pairs, and wide-band electrons, which interact with the first type of particles via charge fluctuations. Apart from describing a two-band system, this model may have some relevance to the problem of a single-band system with short-range attraction in the intermediate coupling regime, where pairs are no longer real bound states but rather virtual ones. A mutual exchange between local pairs of narrow-band electrons and pairs of wide-band electrons transforms the latter into Cooper pairs, and thus leads to superconductivity involving condensation of Cooper pairs and local pairs.

B. Superconductors with local pairing versus Bardeen-Cooper-Schrieffer superconductors

1. Tightly bound local pairs

Let us now conclude by listing the main physical features that distinguish a system of tightly bound local pairs (for example, the strong-coupling negative-U Hubbard model) from a standard BCS superconductor. This can serve as a guide for discriminating between superconducting materials that have classical BCS behavior and those which clearly cannot be interpreted on the basis of BCS theory.

(1) *Nature of pairs.* Upon approaching T_c from below in a BCS-like system, the Cooper pairs break up as the coherent quantum state of superconductivity disappears. Above T_c we have a metallic phase of electrons. T_c is controlled by pair breaking (single-electron excitations) and thus increases with the coupling constant and with the density of states at Fermi energy.

In a local pair system, the electron pairs exist above the transition temperature. T_c is determined by the center-of-mass motion of pairs; it increases when the local attraction is decreased and when the bandwidth ($T_c \sim t^2/|U|$ in the case of on-site pairing). Thus the enhancement of T_c with the application of pressure is quite natural for a local pair system. At some temperature $T_p > T_c$ the local pairs finally break up into electrons. Hence there will be in general three temperature regions.

(a) A low-temperature region where the pairs are in the superconducting state with properties analogous to the superfluidity of charged bosons on a lattice. In the high-density limit this phase can simultaneously exhibit CDW ordering (short- or long-range order).

(b) An intermediate-temperature regime with a state of dynamically disordered local pairs.

(c) A high-temperature regime above T_p, around which a dissociation of pairs takes place.

Regions (a) and (b) are separated either by a single λ-type transition (SS$\leftrightarrow$NO) or by a sequence of two (SS-CDW$\leftrightarrow$CDW$\leftrightarrow$NO) or three (SS$\leftrightarrow$SS-CDW$\leftrightarrow$CDW $\leftrightarrow$NO) phase transitions. The type of changeover (showing a phase transition or not) between the region of disordered local pairs and that of quasifree electrons is at present unknown.

It should be pointed out that, since the gap in the single-electron excitation spectrum persists across the SS transition, the *single-electron conductivity* of the normal phase (but below T_p) will be nonmetallic and have an activated character similar to that of a Mott-Hubbard insulator. There could however be a metallic conductivity of the local pairs themselves.

(2) *Energy gap.* A second point, which may be decisive in distinguishing local pair superconductivity from that of the BCS type, concerns the energy gap in the single-particle excitation spectrum Δ, and in particular its temperature variation as T approaches T_c. In the BCS theory, close to T_c we have $\Delta \sim (1-T/T_c)^{1/2}$. In contrast, in a local pair superconductor, Δ is expected to remain almost T independent well into the regime above T_c, where local pairs exist in a nonordered state. The ratio $2\Delta/k_B T_c$ will in general be different from the BCS value 3.52. For the negative-U Hubbard model in the $|U| \gg t$ limit, it behaves as $(U/t)^2$, being much bigger than unity. This ratio, however, can be reduced for lower values of local attraction, particularly in the case of low-dimensional systems (quasi-one-dimensional and two-dimensional), where the minimal energy necessary to bind a pair is diminished.

(3) *Density dependence of T_c.* Usually, the BCS theory applies to materials with sizable band filling, in which the density of states is structureless on the energy scale of T_c. In this case T_c is not related in any obvious way to electron concentration. In local pair systems, which are equivalent to a hard-core Bose gas on a lattice, T_c strongly depends on n for any density. In particular, for the low-density limit, $T_c \sim n^{2/3}$ (n) for $d=3$ ($d=2+\varepsilon$), and such a dependence of T_c on n can be displayed over a wide range of electron densities.

At this point it should be mentioned that for BCS systems with a nearly empty band (such that $\varepsilon_F < \omega_D$), one can get a similar variation of T_c with n, but such a dependence will be restricted to a very narrow range of concentration. In such a limit of parameters, Bose condensation of preexisting pairs should be considered as a real possibility, even in the case of BCS superconductors (Eagles, 1969a, 1969b, 1985).

At higher densities local pair superconductors can display nonmonotonic behavior of T_c versus n, and systems with on-site local pairs invariably show a maximum of T_c near the phase boundary between the SS and CO phases.

(4) *Electromagnetic properties.* The electromagnetic properties of local pair superconductors are qualitatively different from those of BCS systems. The major effect of a magnetic field in a local pair system occurs via its coupling to the orbital motion of the charged local pair. This leads to greatly enhanced values of H_{c_2}, proportionally reduced values for H_{c_1}, no Clogston limit for H_{c_2} as $T \to 0$ [$H_{c_2}(0) \approx E_{\text{binding}} \gg k_B T_c$], and strongly enhanced penetration depth λ_H. Moreover, one obtains an upwards curvature of H_{c_2} near T_c, with $H_{c_2} \sim [1-(T/T_c)^{3/2}]^{3/2}$ in the dilute limit. The temperature dependences of λ_H and H_{c_1} can also be nonstandard (see Secs. II.B.3 and II.B.5; Micnas and Robaszkiewicz, 1988a, 1988b; Wen and Kan, 1988). In particular, for the screened Coulomb interaction, one gets for $T \ll T_c$

$$\lambda_H(T)/\lambda_H(0) - 1 \simeq (T/T_c)^{d+1}$$

and

$$1 - H_{c_1}(T)/H_{c_1}(0) \simeq (T/T_c)^{d+1} .$$

With increasing temperature (beyond the critical region) in the dilute limit, these dependences can change to

$$\lambda_H(T)/\lambda_H(0) = [1-(T/T_c)^{d/2}]^{-1/2}$$

and

$$H_{c_1}(T)/H_{c_1}(0) \approx 1-(T/T_c)^{d/2} .$$

(5) *Short coherence length.* Local pair superconductors are expected to have very short coherence length due to the short-range coupling between pairs and the small radius of a pair. This leads to a relatively weak sensitivity

of the SS phase in the low-concentration limit to the presence of nonmagnetic impurities (except of SS coupled to CDW), in analogy to the relative stability of the superfluid phase of ^{4}He II in the presence of disorder. A more spectacular effect of this small coherence length is the enlarged width of the critical regime, which should be experimentally accessible, making the true critical behavior of the XY, $s=\frac{1}{2}$ model observable. For $d=2$, a Kosterlitz-Thouless-type phase transition is to be expected.

Several other points distinguishing local pair superconductivity from the BCS model were discussed in Sec. II; we list here only the most essential.

(i) The collective excitation spectrum (Sec. II.B.2)—a sound-wave-like excitation branch in the case of a screened Coulomb interaction; a reduced plasma frequency and an energy gap in the two-electron spectrum of the order of the bosonic bandwidth, in the case of an unscreened Coulomb interaction.

(ii) The behavior of the specific heat in the superconducting and normal phases (Sec. II.B.3)—the possibility of power-law T dependence, i.e., $c_v \sim T^3$ (T^2), and a changeover to $c_v \sim T^{3/2}$ (T) with increasing temperature in $d=3$ ($d=2+\varepsilon$).

(iii) The effects of structural disorder (Sec. II.B.6)—the possibility of disorder-induced local pair superconductivity and superconducting glass behavior of a local pair superconductor.

(iv) The weak effect of magnetic impurities for singlet s-type local pairs.

2. Beyond the limit of real-space pair formation

Let us turn now to the properties of models with static, short-range attractive potential in the weak-attraction case, i.e., beyond the limit of real-space pair formation. For high electron concentration this will be the range of $|U|<2zt$ or $|W|<2zt$. The physics now becomes much more similar to that for a BCS superconductor than in the previously discussed case. However, even now, there remain some essential differences. The fact that the attraction is static (without a cutoff in the frequency dependence of the interaction) implies that all the electrons inside the Fermi surface contribute to the pairing. Thus the effective half-bandwidth D (instead of ω_D) will determine the energy scale. The consequences of this are threefold. First, T_c and Δ in the BCS expressions are enhanced, since ω_D is replaced by D. Second, both these quantities are explicitly dependent on the electron density (see below). Third, the ratio $2\Delta/k_B T_c$ can deviate from the BCS value, being a function of lattice structure (DOS), electron concentration, and the strength of the attractive interaction.

It is worthwhile to compare the behavior of T_c versus n in the weak-attraction limit for on-site ($U<0$) and intersite ($W<0$) pairing, respectively.

For on-site pairing (which is of the isotropic s-wave type), if $W=0$, T_c shows a monotonic variation versus n with a maximum at half-filling, for nearest-neighbor hopping. T_c can be strongly enhanced by the presence of the Van Hove singularity for a square lattice. For alternating lattices this pairing can exist for any $U<0$ and arbitrary n. If $W>0$, T_c for on-site pairing becomes nonmonotonic, with a maximum near the border with the CDW state, and above some critical density the superconductivity can coexist with charge-density waves.

Intersite pairing can be of the anisotropic s-, d-, or p-wave type, depending on the symmetry and strength of the pairing potential, the band filling, and the form of the DOS. All these pairings can be driven by the intersite density-density attraction ($W<0$). Antiferromagnetic exchange enhances extended s- and d-wave pairing but suppresses p-wave pairing.

With increasing n (for $U>0$) the system can exhibit either an $s \rightarrow d$ wave transition or a sequence of transitions $s \rightarrow p \rightarrow d$. The correlated hopping term $\propto \tilde{K}$ affects predominantly the s-wave pairing and the repulsive $\tilde{K}$ term ($\tilde{K}>0$) stabilizes the superconductivity of holes in the more than half-filled band case (i.e., for $n_h=2-n<1$) whereas $\tilde{K}<0$ can yield the superconductivity of electrons in the less than half-filled band case (i.e., $n<1$).

At very low densities one can obtain analytic expressions for T_c^s if the pairing potential is restricted either to on-site or to nearest-neighbor attraction: $T_c^s \sim n^{1/3}$ ($n^{1/2}$) for a $d=3$ ($d=2$) lattice. However, if the attractive couplings fall off gradually with distance, $T_c^s \sim n^{2/3}$ (n) for a $d=3$ ($d=2$) lattice, i.e., one gets the same n dependence of T_c as for local pair superconductors. It should also be mentioned that the adequacy of the weak-coupling approximation for the case of low densities is far from clear.

3. Comments on mass renormalization and the (bi)polaronic mechanism

We conclude this subsection with some comments regarding the effective parameters t_{ij}, U, and W_{ij} of the extended Hubbard model and the transfer-matrix element I_{ij} of the model of coexisting local pairs and itinerant electrons, in particular in the context of the polaronic mechanism for pair formation.

If an effective attraction results from electron-boson coupling, these effective model parameters are renormalized from their bare values and dependent on the electron-boson coupling strength and characteristic bosonic frequency ω. The bosonic modes can be phonons or of electronic origin, such as excitons or plasmons.

As is well known from early work on the small-polaron problem by Yamashita and Kurosawa (1958) and Holstein (1959), and on small bipolarons by Alexandrov and Ranninger (1981a), strong-coupling renormalization is rather severe for an effective polaron transfer integral. For example, in strongly coupled electron-phonon (EP) systems, in the inverse adiabatic limit, t_{ij} is renormalized exponentially with the EP coupling strength g, i.e., $t_{ij} \sim t_e \exp(-g^2)$, where t_e is a typical electronic transfer

integral while the phonon-mediated attraction increases typically like $-U \sim 2g^2\omega$. At the coupling strengths required to obtain well-defined self-trapped small bipolarons one might therefore expect to find an enormously enhanced effective bipolaron mass, which in turn would suppress the Bose condensation temperature. Such a picture, which in our opinion is oversimplified (Alexandrov *et al.*, 1986; Nasu, 1987, 1988), leading to an excessive reduction of the bare electronic transfer integral, has caused some authors to believe that either small bipolarons readily localize or their condensation temperature is vanishingly small (Chakraverty, 1979; Rice and Sneddon, 1982; Rice, 1987; Emin, 1989; Emin and Hillery, 1989).

The description of the small-polaron problem is based mainly on the Holstein molecular crystal model, which was initially introduced to describe small-polaron formation showing very strong, local lattice deformation ranging typically over a few lattice constants (Holstein, 1959). What is generally known about this model is its solution in the form of a variational wave function, according to which the electron is surrounded by a local lattice deformation—the so-called Holstein small polaron. The mobility of such a polaron is described by the motion of the electron, which rigidly takes with it the surrounding lattice deformation, and in consequence gives rise to a strong reduction in bare electron hopping. The variational picture of a small polaron serves as a useful guideline but cannot be taken too literally. For instance, Feinberg and Ranninger (1984, 1986) have demonstrated that the mobility of a small polaron consists of a highly nonlinear process between the motion of the charged carrier and the lattice deformation. The vanishingly small polaronic transfer integral is rather a consequence of the Holstein small-polaron variational approximation. Moreover, for the EP coupling constant around a critical value, the electron is dressed by a local lattice deformation showing large zero-point motion between two quite specific configurations. Below this critical value the electron is unable to deform the lattice, whereas above it the formation of a small Holstein polaron can take place. The effective deformation of the lattice, together with its fluctuations, was studied by means of the Feyman path-integral method (de Raedt and Lagendijk, 1983, 1986). The distinction between self-trapping and localization has recently been very clearly discussed by Löwen (1988), who showed that for small polarons in a regular lattice a phonon-induced localization does not occur. Moreover, it has also been demonstrated that an improved treatment of the EP system in strong coupling by means of "squeezed phonon vacuum states" gives an effective small-bipolaron mass of the order of only $\sim 10m_e$, which is sufficient to yield the condensation temperature ~ 100 K, for a 3D lattice (Chakraverty *et al.*, 1987; Zheng, 1988).

A related question concerns the limits of applicability of the Eliashberg-Migdal theory to superconductivity in EP systems with very large values of the EP coupling constant. It seems that the strong-coupling regime may well have to be reconsidered from a theoretical point of view, since Migdal's theorem is expected to be violated (Anderson and Yu, 1985), and hence the Eliashberg formalism might have to be modified to take into account polaronic effects (Alexandrov, Ranninger, and Robaszkiewicz, 1986b; Alexandrov, Grebenev, and Mazur, 1987). The problem is certainly connected with the interpolation between the adiabatic ($t_e \gg \omega$) and inverse adiabatic limits ($t_e \ll \omega$) and a transition between BCS-type behavior and charged-boson superfluidity with increasing coupling strength (Nasu, 1985, 1987, 1988).

For systems in which the bosonic degrees of freedom are not vibronic but of electronic origin, like excitons, or plasmons, a characteristic frequency could be much higher, on the order of 1 eV, and renormalization of the effective transfer integral is not particularly severe. In fact, when ω is of the order of the electronic bandwidth, the situation is almost inverse adiabatic, and the boson can follow the electron without retardation; hence it can cause no mass enhancement. It was shown by Hirsch and Scalapino (1985b) (see also Bari, 1973) that, for excitonic systems, only an algebraic reduction of t_{ij} with coupling strength can be expected.

Strong-coupling renormalization effects are also common for the pair-transfer-matrix element I_{ij} of the mixed model discussed in Sec. IV (Robaszkiewicz *et al.*, 1987; Schüttler and Fedro; 1988; Schüttler *et al.*, 1989). Again, if one considers a coupling of narrow-band electrons to the bosonic modes like excitons, the suppression of I_{ij} will be only algebraic.

Finally, for theories based on the electronic mechanisms of local pairing, such as pairing due to strongly polarizable ions (like oxygens), the effective mass of the carriers is not necessarily dramatically enhanced. In this case the polarizability of the electron cloud gives rise to pair formation of holes on neighboring ions. This was demonstrated by Hüller (1989) for $SrTiO_3$. In such a picture the nuclei of the oxygens do not move, and the relaxation of the polarization is fast compared to the electron hopping rate. This leads to a pairing of charge carriers which does not involve phonons and to an effective mass on the order of two electron masses.

Another local attraction mechanism that is of purely electronic origin has recently been proposed by Hirsch (1989a); it arises from the interaction of a hole with the outer electrons in anions with nearly filled shells. In the simplest version of this model the system is mapped onto the negative-U Hubbard model with the hopping integral of holes renormalized to $\tilde{t}_{ij} = t_{ij} \cos^2\Theta/2$, and Θ is given by the overlap of the outer cloud wave function with and without a hole. Such a system of "small electronic polarons" can give rise to high T_c with an effective mass of carriers m^* on the order of several m_e (Hirsch and Tang, 1989).

C. Local pairing and high-T_c superconductivity

Systems with an effective local attractive electron-electron interaction do exist, and an extensive list of

presently known materials is given in the Introduction. They can exhibit several electronic orderings, mostly charge ordering, but also superconductivity. A large group of these materials does not show superconductivity. The reasons for that are known. Some materials form half-filled bands and hence show a charge-ordered ground state (e.g., Cs_2SbCl_6, $CsAgCl_3$, Ti_4O_7, $Na_xV_2O_5$, etc.) or the SDW ordering, as predicted by the theory. Other reasons for nonoccurrence of superconductivity in local pair systems are their one-dimensional characteristics (for example, KCP), their structural disorder or nonstoichiometry, as in WO_{3-x}, or simply the localization of their electronic pairs on impurity centers, as in chalcogenide glasses.

1. The doped $BaBiO_3$ perovskites

Concerning superconductivity with local pairing, the most interesting systems are $BaPb_{1-x}Bi_xO_3$ perovskites (for a review of experimental work on $BaPb_{1-x}Bi_xO_3$ see Uchida, Kitazawa, and Tanaka, 1987) and their recent high-T_c versions, $Ba_{1-x}K_xBiO_3$ and $Ba_{1-x}Rb_xBiO_3$. The exceptional status of these compounds is due to a very small electronic density of states $N(0)$ at the Fermi level and $T_c/N(0) \gg 1$. The critical temperatures of ~ 13 K in $BaPb_{1-x}Bi_xO_3$ or of ~ 34 K in $Ba_{1-x}K_xBiO_3$ are truly remarkable for the transition-metal-free compounds and are at least 3–5 times higher than in all other superconductors with comparable $N(0)$. Moreover, these high-T_c superconductors based on BiO reveal many features in common with Cu-O based superconductors (discussed below), despite their being non-transition-metal compounds and having truly three-dimensional structure.

In these materials Bi ions can exist in two valence states, $Bi^{3+}(6s^2)$ and $Bi^{5+}(6s^0)$, i.e., one has on-site pairing of electrons in $6s$ states (Sleight, 1989). The extended Hubbard model with on-site attraction and intersite Coulomb repulsion is the simplest model able to describe both the two-sublattice charge order in the diamagnetic and semiconducting (with an energy gap of ~ 0.8 eV) cubic phase of $BaBiO_3$ with $T_{CO} \sim 800$ K and the exotic (s-type) superconductivity occurring upon doping (Robaszkiewicz *et al.*, 1981a, 1981b, 1982), discussed extensively in Sec. II. A more detailed description of the evolution from BCS-type to local pair superconductivity and then to the CDW phase with increasing x in $BaPb_{1-x}Bi_xO_3$ has been presented (Robaszkiewicz *et al.*, 1987) within the framework of the model of coexisting local pairs and wide-band electrons.

The existence of local pairs in $BaPb_{1-x}Bi_xO_3$ and $Ba_{1-x}K_xBiO_3$ is now established in the regime of x, where we have a charge-ordered state (Cox and Sleight, 1979; Tajima *et al.*, 1985, 1987; Uchida *et al.*, 1985; Chaillout *et al.*, 1988). Moreover, there is evidence that local pairs also exist above T_c in the superconducting compositions, as indicated by Mössbauer and positron annihilation studies (Groznov *et al.*, 1984) as well as by optical experiments (Tajima *et al.*, 1985, 1987) and EXAFS spectra (Balzarotti *et al.*, 1984; Menushenkov, 1986).

Let us now enumerate some major experimental findings concerning the BiO-based perovskites, which can be explained by the local pair theory.

(1) The negative magnetic susceptibility observed in the normal state of the superconducting samples and in the CDW phase (Batlogg, Cava, and Stavola, 1988; Batlogg, Cava, Rupp *et al.*, 1988; Cava *et al.*, 1988; Mattheiss *et al.*, 1988).

(2) The persistence of the energy gap in the single-electron excitation spectrum observed in the CDW insulating phase of $BaPb_{1-x}Bi_xO_3$ ($x < 0.35$); this gap persists as a pseudogap in the normal state of the superconducting samples ($0.15 < x < 0.3$). The energy gap is a smooth function of x even in the marginal region of $x \sim 0.3$ (Tajima *et al.*, 1985, 1987).

(3) Semimetallic, or even semiconducting, resistivity behavior above T_c, with very high values of the normal-state resistivity ($\rho \sim 0.1\ \Omega$ cm) and with a negative slope. There is a smooth change in the temperature behavior of the resistivity with x (Thanh *et al.*, 1980; Tajima *et al.*, 1987; Uchida *et al.*, 1987; Dąbrowski *et al.*, 1988; Welp *et al.*, 1988).

(4) A concave upward curvature of H_{c_2} with decreasing T, which can persist over a large temperature range (Welp *et al.*, 1988).

(5) A large penetration depth ($\sim 10^4$ Å; Moiseev *et al.*, 1981; Batlogg, 1984), a rather short coherence length (~ 40–60 Å; Welp *et al.*, 1988; Batlogg, Cava, Rupp, *et al.*, 1988), and strong type-II superconductivity (Kitazawa *et al.*, 1985a, 1985b).

(6) A low density of carriers ($\sim 10^{21}$ cm^{-3}) but high T_c.

(7) The strong nonmonotonic dependence of T_c on carrier concentration (Thanh *et al.*, 1980; Sakudo *et al.*, 1986; Hinks *et al.*, 1988a). $T_c \sim n^{2/3}$ displayed over a wide range of n in $BaPb_{1-x}Bi_xO_3$ (de Jongh, 1988b).

(8) The observation of the highest values of T_c for x close to the boundary with the CDW phase, i.e., near $x \approx 0.25$ in $Ba_{1-x}K_xBiO_3$ and $x \approx 0.27$ in $BaPb_{1-x}Bi_xO_3$.

(9) The enhancement of T_c with the application of pressure in $Ba_{1-x}K_xBiO_3$ with $dT_c/dp \sim 0.1$ K/kbar; this is very similar to the pressure derivatives in the Cu-O perovskites (Schirber *et al.*, 1989).

(10) Noticeable effects of electron-lattice coupling and tendencies toward lattice instabilities. A sizable isotope effect with $\alpha \sim 0.2$–0.25 present in both $BaPb_{1-x}Bi_xO_3$ and $Ba_{1-x}K_xBiO_3$ (Batlogg, Cava, and Stavola, 1988; Batlogg, Cava, Rupp *et al.*, 1988; Hinks *et al.*, 1988b).

Calculations of electron-phonon interactions in BiO-based perovskites lead to a T_c of less than 5 K (Weber, 1988b), which is consistent with the isotope shift measurements (Batlogg, Cava, and Stavola, 1988), but cannot explain the high-T_c superconductivity. The source of the local attractive interaction ($U < 0$) is most likely to be a predominantly atomic mechanism associated with

Bi^{3+}-Bi^{5+} charge disproportionation together with nonlinear screening of the $6s^0$ configuration by charge transfer from the oxygen octahedra to the $6p$ shell, which could be called a chemical mechanism (see Varma, 1988b; Ranninger *et al.*, 1989). Other possibilities to be mentioned are (i) formation of bipolaron states upon doping electrons (holes) to the commensurate CDW insulator and superconductivity arising from the Bose condensation of these bipolarons (Prelovšek *et al.*, 1987); (ii) excitonic local pairing of the oxygen holes added to a disproportionated semiconducting background (Nuñez Regueiro and Aligia, 1988), which in fact is consistent with the concept of coexisting local pairs (on Bi ions) and itinerant holes (on oxygen ions) discussed by us in Sec. IV.

(11) The recent Raman spectroscopy data (Sugai, 1989; Sugai, Enomoto, and Murakami, 1989) indicating the existence of interacting itinerant carriers and small bipolarons in doped $BaBiO_3$.

2. The Cu-O-based perovskites

Let us now concentrate on the new high-T_c superconducting oxides, the cuprate perovskites. They belong to the same family of oxides as $BaBiO_3$:Pb,K,Rb, (see Table I), for which the ideas of local pairing were initially invoked, well before Bednorz and Müller's (1986) discovery.

Before discussing the possible relevance of local pairing concepts for La-Ba-Cu-O and Y-Ba-Cu-O systems, let us list several unusual experimental facts concerning these 3d transition-metal oxides.

(1) They belong to compounds that usually display narrow bands and for which electron correlations are important. Moreover, these new materials are close to the metal-nonmetal transition.

(2) They are oxygen-deficient perovskites exhibiting low-dimensional characteristics such as well-defined CuO_2 planes and Cu-O chains in Y-Ba-Cu-O (Bednorz and Müller, 1988; Rao, 1988; Sleight, 1988). They have generally very low carrier density ($\sim 10^{21}$ cm^3) and show a strong polarization of the structure. There is a tetragonal-to-orthorhombic transition at high temperatures, but this structural transition seems to be unrelated to the occurrence of superconductivity, which usually exists in the orthorhombic phase at zero pressure (Capponi *et al.*, 1987; Cava *et al.*, 1987; Junod *et al.*, 1987; Wu *et al.*, 1987).

(3) The values of T_c exceed the upper limit for conventional BCS superconductors (usually estimated as 30–40 K). They exhibit (anisotropic) superconductivity with a very short coherence length (see, for example, Dinger *et al.*, 1987; Worthington *et al.*, 1987.

(4) The materials are extreme type-II superconductors with the Ginzburg-Landau parameter $\kappa \gg 1$, with H_{c_2} very large while $H_{c_1} \ll H_{c_2}$ H_{c_2} shows a positive slope near T_c (Cava *et al.*, 1987; Dinger *et al.*, 1987; Panson *et al.*, 1987; Worthington *et al.*, 1987; Crabtree *et al.*, 1988; Oh *et al.*, 1988).

(5) There are anomalous changes of the sound velocity at T_c, which could indicate that states far from the Fermi surface are involved in the pairing (D. J. Bishop, Gammel *et al.*, 1987; D. J. Bishop, Ramirez *et al.*, 1987). Anomalously large anisotropic amplitude oscillations of O ions have been observed by neutron scattering (Capponi *et al.*, 1987).

(6) The pairs are presumably strongly coupled, according to different measurements of the superconducting energy gap. (For example, $2\Delta/k_B T_c \cong 8.3$ and 2.4 for Cu(1) and Cu(2), respectively, in $YBa_2CuO_{7-\delta}$ (see Warren *et al.*, 1987; Schlesinger *et al.*, 1987), and $2\Delta/k_B T_c \cong 8 \pm 1.4$ in Bi-Sr-Ca-Cu-O (see Imer *et al.*, 1989). The energy gap shows practically T-independent behavior all the way up to T_c (Geork *et al.*, 1988).

(7) There is a small isotope effect in La-Ba-Cu-O compounds (Batlogg, Kourkoulis *et al.*, 1987; Faltens *et al.*, 1987) and almost none in Y-Ba-Cu-O (Bourne *et al.*, 1987).

(8) The phase diagrams clearly show the appearance of antiferromagnetism in both La-Ba-Cu-O and Y-Ba-Cu-O compounds that are not superconducting (see, for example, Fig. 31), with $T_N \sim 250$ K in La-Ba-Cu-O and $T_N \sim 450$–600 K in Y-Ba-Cu-O (Beille *et al.*, 1987; Freltoft *et al.*, 1987; Johnston *et al.*, 1987; Mitsuda *et al.*, 1987; Uemura *et al.*, 1987; Vaknin *et al.*, 1987; Brewer *et al.*, 1988; Rossat-Mignod *et al.*, 1988; Tranquada *et al.*, 1988). The anitferromagnetism seems to be driven by weak interlayer coupling and quickly disappears upon doping or changing the oxygen stoichiometry. The paramagnetic phase displays a large degree of magnetic correlation and an atypical magnetic form factor (Shirane *et al.*, 1987; Birgenau *et al.*, 1989; Birgenau and Shirane, 1989). It is not clear at present how the super-

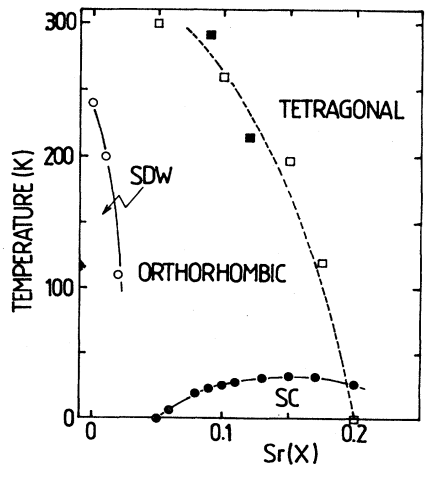

FIG. 31. Phase diagram of $La_{2-x}Sr_xCuO_{4-\delta}$: ●, the superconducting transition; ○, the SDW transition; ■ and □, the orthorhombic-tetragonal phase transition. The dashed lines are guides for the eye. The superconductivity at $x \leq 0$ is not indicated on this diagram, as it concerns only a small fraction of the sample volume in which the carrier concentration does not correspond to "pure" La_2CuO_4 (after Jérome *et al.*, 1988).

conductivity in these materials is connected with the existence of antiferromagnetism observed in the insulating compositions.

(9) Spectroscopic and other measurements indicate mixed valent states of Cu and O ions, practically an absence of Cu^{3+} states, and very low density of states at the Fermi level (Bianconi *et al.*, 1987; Fujimori *et al.*, 1987; Nücker *et al.*, 1987; Steiner *et al.*, 1988; Tournier *et al.*, 1988). Doping seems to create holes preferentially on oxygen sites, with Cu^{2+} unchanged, in agreement with spectroscopic measurements and recent NMR work (Horvatič *et al.*, 1988; Kitaoka *et al.*, 1989).

(10) The normal-state properties of these new superconductors are also unusual. The resistivity exhibits linear-in-T behavior in the a-b plane much below the Debye temperature, and resistivity saturation does not occur at very high temperatures. On the other hand, this almost perfect metallic behavior is in contrast with the values of ρ being close to the Mott-Ioffe-Regel limit (Gurvitch and Fiory, 1987; Kastner *et al.*, 1987; Tozer *et al.*, 1987; Martin *et al.*, 1988).

(11) Superconductivity, antiferromagnetism, and transport properties crucially depend on the oxygen stoichiometry.

The above experimental features and detailed calculations of band structure, together with those based on the conventional Eliashberg-Migdal formalism, indicate that these new materials do not fit in any obvious sense the pattern of ordinary electron-phonon superconductors (Weber and Mattheiss, 1987, 1988). Moreover, the experimentally observed $\Delta c/k_B n \sim 1$ (where Δc is the jump of the specific heat at T_c) would give $T_c \sim T_F/7$ if we applied the BCS relation $\Delta c/k_B n \sim 7T_c/T_F$. It is known that only if $T_c \ll T_F$ will the BCS theory hold.

The small number of carriers, together with short coherence length, leads one therefore naturally to consider the picture of local nonretarded electron pairing in these materials.

3. Observations favoring local pairing

Let us now enumerate several general observations that point to local pairing and local pair formation (virtual or real) as a possibility in the high-T_c superconductors.

(1) The high-T_c superconductors belong to the oxides family (Table I), for which the existence of local pairing has been well established (for instance, Bi^{3+}-Bi^{5+} on-site pairs in $BaBiO_3$ and intersite pairs Ti^{3+}-Ti^{3+} forming bipolaronic charge-density waves in Ti_4O_7).

(2) Their low-dimensional structure certainly favors the bound states. Moreover, simple geometry arguments yield that there can be higher density of only weakly overlapping intersite pairs in one or two dimensions than in three dimensions.

(3) Copper as well as oxygen exist in mixed-valence states (Cu^{1+}, Cu^{2+}, Cu^{3+}-?; O^{2-}, O^{1-}, O^0-?) (Bianconi *et al.*, 1987; Fujimori *et al.*, 1987; Nücker *et al.*, 1987, 1988; Steiner *et al.*, 1987; Tranquada *et al.*, 1987).

(4) The low density of carriers $\sim 10^{21}$ cm^{-3} and strong polarizability of structure favor local pairing over Cooper pairing.

(5) Changing the oxygen content or dopant concentration causes a transition to the dielectric state.

(6) Strong two-dimensional antiferromagnetic correlations with $J_{AF} \sim 500-1500$ K and $J_\perp/J_\parallel \sim 10^{-4}-10^{-5}$ may contribute to the binding energy of intersite pairs.

(7) Their superconductivity is of extreme type II with very short coherence length (~ 16 Å in the CuO_2 planes and ~ 3 Å orthogonal to those planes in a YBaCuO single crystal; see Welp *et al.*, 1989).

(8) The small value of the Fermi energy (Kresin *et al.*, 1988) and $\xi_0 k_F \sim 5-10$ (for $YBa_2Cu_3O_7$) indicate that all carriers can be involved in pairing and that the size of a pair is on the order of the interparticle distance, in contrast to the BCS regime, where $\xi_0 k_F \gg 1$.

In the context of high-T_c superconductors, the concepts of local pairing have been adopted by many authors. Their propositions cover practically all the possible mechanisms of attraction summarized in the Introduction; namely, (i) the polaronic (bipolaronic) mechanism (Chakraverty *et al.*, 1987; Li, 1987; Alexandrov, 1988; de Jongh, 1988a, 1988b; Zheng, 1988; Bussmann-Holder *et al.*, 1989); (ii) the excitonic mechanism (Schüttler *et al.*, 1987; Yu *et al.*, 1987); (iii) the electronic mechanism (Callaway *et al.*, 1987; de Groot *et al.*, 1987; Fedro *et al.*, 1987; Gagliano *et al.*, 1987; Imada, 1987; Balseiro *et al.*, 1988; Hirsch *et al.*, 1988; Weber, 1988a); as well as (iv) "chemical mechanisms" (Wilson, 1987, 1988; Khomskii and Zvezdin, 1988; Micnas *et al.*, 1988b; Ranninger *et al.*, 1988, 1989; Hirsch, 1989a, 1989b; Hirsch and Tang, 1989).

One can consider several types of pairings in these new high-T_c superconductors. (a) on-site pairings, for which we assume that the centers of formation of two holes (electrons) are cation ions (Cu), via reactions $2Cu^{2+} \rightarrow Cu^{1+} + Cu^{3+}$ ($2d^9 \rightarrow d^8 + d^{10}$); or ligand ions (O), via disproportionation $2O^{1-} \rightarrow O^{2-} + O^0$ ($2p^5 \rightarrow p^4 + p^6$); or more probably cation-ligand clusters (CuO_2), i.e., $2K^n \rightarrow K^{n+1} + K^{n-1}$. (b) intersite pairings of different types: a pairing of d holes in the antiferromagnetic background or a pairing of p holes on the neighboring oxygen ions (i.e., p^5-p^5).

4. Relation of models to high-T_c superconductors

There is at present no clear consensus about the mechanism of pairing nor about the type of pairing nor even about the sites on which local pairing occurs. Nevertheless, we can analyze and test various hypotheses regarding pairing in the high-T_c superconductors listed above by making use of the models studied in Secs. II–IV.

For this purpose let us first consider the model of intersite pairing on Cu sites and assume that only d states are partially occupied. Thus a d^9 (Cu^{2+}) configuration corresponds just to the half-filled band case of the model considered in Sec. III (see also Micnas, Ranninger, and Robaszkiewicz, 1988a; Micnas, Ranninger,

Robaszkiewicz, and Tabor, 1988). Such a simplified model can already account for several experimental findings. First, T_c may be high due to the fact that electron (hole) pairing takes place throughout the whole Brillouin zone, in contrast to the BCS model. The short coherence length observed in these materials is consistent with a model assuming local short-range attractive interaction. The phase diagram of the model containing the SDW and superconductivity is reminiscent of that observed in $(La_{1-x}M_x)_2CuO_{4-\delta}$, M =Sr,Ba (compare Fig. 16 and Fig. 31 of Jérome *et al.*, 1988; or Fujita *et al.*, 1987). The rapid disappearance of antiferromagnetism in $La_2CuO_{4-\delta}$ when the oxygen vacancies are changed (Freltoft *et al.*, 1987; Johnston *et al.*, 1987; Mitsuda *et al.*, 1987; Uemura *et al.*, 1987; Vaknin *et al.*, 1987) can be interpreted within our model as a spoiling the Fermi surface nesting. The possibility of anisotropic pairing predicted by the model is supported by recent experimental results, like those concerning the magnetic field penetration depth (Cooper *et al.*, 1988) and the observed anisotropic behavior of H_{c_2} and its positive curvature near T_c (Horn *et al.*, 1987; Worthington *et al.*, 1987). The observed isotope effect in $(La_{1-x}Sr_x)_2CuO_{4-\delta}$ (Batlogg, Kourkoulis *et al.*, 1987; Faltens *et al.*, 1987) indicates that superconductivity is somehow related to electron-lattice coupling and tends to support short-range pairing due to a polaronic mechanism, or at least suggests a contribution from such a mechanism. The linear-in-T behavior of the resistivity in the a-b plane in the normal state can be accounted for by quasi-two-dimensional transport and low carrier (hole) concentration (Micnas *et al.*, 1987b).

All these qualitative conclusions can be derived in the weak-correlation limit ($U<2D$). Recent spectroscopic measurements show that the real situation in these new materials is perhaps the intermediate correlation regime ($U\sim 2D$) (Fujimori *et al.*, 1987; Nücker *et al.*, 1987; Steiner *et al.*, 1987). Within the present model one can approach such a case from the insulating side ($n=1$), assuming $U\gg t$ (see Sec. III.C). Superconductivity would then result from the combined action of "polaronic" intersite attraction and a magnetic superexchange mechanism (kinetic exchange). In this large-U limit, the mechanism of superconductivity is very similar to the resonating-valence-bond approach of Anderson (1987, 1988 and the effective Hamiltonian (3.15) has the form of a generalized t-J model including additionally the intersite attraction term. It should be pointed out that, although everything now happens close to $n=1$, this case corresponds to that of a small number of holes in the nearly half-filled band of the $d=2$ extended Hubbard model. Therefore one expects the formation of charge bosons as pairs of holes and their condensation.

Another quite different concept, which seems to be very well substantiated at present, is the idea that, upon doping, the extra holes go to oxygen ions and that pairing occurs primarily on (neighboring) oxygen ions, i.e., we are dealing with the case of intersite pairing of holes on oxygens (p^5-p^5) (Emery, 1987). Such a picture is strongly supported by spectroscopic data which identify the charge carriers in the normal state as the holes in the oxygen p band, and perhaps peroxide (or superoxide) formation (Rao *et al.*, 1987; Sarma *et al.*, 1987; Sarma and Rao, 1987a, 1987b; Tranquada *et al.*, 1987; Chakraverty *et al.*, 1988; Manthiram *et al.*, 1988; Nücker *et al.*, 1988; Rogers *et al.*, 1988). Recent theoretical studies support the existence of an effective (short-range) attraction just between the p holes on oxygens, induced by (i) coupling to a local magnetic configuration of Cu^{2+} (Emery, 1987, 1988; Emery and Reiter, 1988a); or (ii) the polarization mechanism (Fedro *et al.*, 1987; Varma *et al.*, 1987a, 1987b; Varma, 1988a; Wilson, 1987, 1988); or (iii) electronic correlations (Gagliano *et al.*, 1987; Balseiro *et al.*, 1988; Chakraverty *et al.*, 1988; Emery and Reiter, 1988a; Hirsch *et al.*, 1988; Nuñez Regueiro and Aligia, 1988)—particularly due to Cu-O interaction (Gagliano *et al.*, 1987; Balseiro *et al.*, 1988; Hirsch *et al.*, 1988) or due to the interaction of a hole with outer electrons in oxygen ions with nearly filled shells (Hirsch, 1989a, 1989b; Hirsch and Tang, 1989).

The simplest model of such real-space pairing of oxygen holes could be either the model with on-site attractive interaction defined on effective sites (Sec. II) or the model with intersite attractive interaction (Sec. III), both in the small-density limit. In contrast to the hypothesis of pairing of d holes on Cu sites, which would correspond to the nearly-half-filled band case, we now approach model (1.1) from the opposite limit for electron densities, namely, from the limit of small concentration of holes in a p-like band (i.e., for example, La_2CuO_4, with Cu^{2+} ions, will correspond to $n=0$ in the p-hole representation). In such a case, theory predicts s-wave pairing that is isotropic for $U<0$, and anisotropic-extended s, for $W<0$ (or $J>0$). T_c versus n is nonmonotonic and has a maximum at some n. As a matter of fact the n (or x) dependence of T_c recently observed in $La_{2-x}Sr_xCuO_4$ (Torrance *et al.*, 1988), is very similar to the plots of T_c^s versus n given in Figs. 16 and 18 of Sec. III. (See also Figs. 3–6 in Micnas, Ranninger, Robaszkiewicz, and Tabor, 1988; and Figs. 1 and 4–8 in Micnas *et al.*, 1989). Such a model gives a high T_c and energy gap Δ, which are n dependent, since the pairing takes place over the whole Brillouin zone, as well as a short coherence length due to local attractive interactions. The linear-in-T behavior of the resistivity in the a-b plane can again be accounted for by the low carrier (p-hole) concentration, reinforced by the quasi-2D transport (Micnas *et al.*, 1987b; Xing *et al.*, 1988). As we have shown in Sec. III, in the case of intersite pairing there can be a transition from the extended s-wave to the d-wave (or p-wave) state when n is increased.

We should point out that the nature of the many-body state in the presence of a local attractive interaction will depend on the density of carriers; in the small-density limit the formation of real bound pairs is likely to occur. An additional factor in favor of pairing is the low-dimensional lattice structure of these new materials. As

we demonstrated in Sec. III.B, in two dimensions even weak attraction can produce a real bound state. Therefore, in the low-density limit, superconductivity can result from Bose condensation of pairs of oxygen holes (p^5-p^5), leading to superfluid behavior. In such a dilute limit we expect the thermodynamic and electromagnetic properties of the superconducting state to be well described by the model of a hard-core Bose gas on a lattice, studied in Sec. II. Increasing carrier concentration may well lead to a changeover to the weak-coupling behavior.

In summary, regardless of the specific microscopic pairing mechanism responsible for superconductivity in the 3d transition-metal oxides as well as other oxides listed in Table I, the possible unifying phenomenological concept is *superfluidity of charged bosons* (Micnas *et al.*, 1988b; Ranninger *et al.*, 1989). For the Cu-O based high-T_c superconductors this would be due to the condensation of on-site pairs or intersite pairs of oxygen holes, or pairs of holes in the nearly half-filled Hubbard model in the strong repulsive limit. Such a phenomenological unification clearly covers the BiO-based perovskites discussed in the first part of this subsection and for the Cu-O-based high-T_c superconductors it can be justified by the following findings (compare Sec. II.B and V.B).

(1) The strong dependence of T_c on carrier concentration for both $La_{2-x}Sr_xCuO_{4-\delta}$ and $YBa_2CuO_{7-\delta}$, with the $T_c \sim n$ ($n^{2/3}$) observed over a wide range of n (Shafer *et al.*, 1987; de Jongh, 1988a, 1988b; Uemura *et al.*, 1988, 1989).

(2) The anomalous pressure dependence of T_c, with dT_c/dp positive and of the order of 0.1–0.3 K/kbar for all the Cu-O-based perovskites (Griessen, 1987; Schirber *et al.*, 1989).

(3) The electromagnetic properties that point towards a charged superfluidity rather than to the BCS model; these properties include (see Secs. II.B.4, II.B.5, and V.B) (i) the extreme type-II superconductivity of these materials, with practically all particles involved in pairing, (ii) the positive curvature of H_{c_2} near T_c (Crabtree *et al.*, 1988; Oh *et al.*, 1988; Welp *et al.*, 1989), and (iii) the linear temperature dependence of H_{c_1} from 5 K to $T_c \sim 40$ K in LaSrCuO, with the slopes being independent of doping concentration (Batlogg, Ramirez *et al.*, 1987), which agrees with the theoretical prediction for H_{c_1} in a weakly interacting $2+\varepsilon$ charged Bose gas (Wen and Kan, 1988).

(4) The experimentally measured ratio $\Delta c/k_B n \geq 0.5$, e.g., for $YBa_2Cu_3O_7$ taking $\Delta c \approx 40$–50 mJ/K cm^3 (Inderhees *et al.*, 1987; Nevitt *et al.*, 1987; Butera, 1988; Junod *et al.*, 1988; Millis and Rabe, 1988) and $n = 6\times10^{21}$ cm^{-3}, one gets $\Delta c/k_B n \approx 0.5$–$0.6$; this ratio is in agreement with the theoretical prediction for an interacting Bose gas (Micnas and Robaszkiewicz, 1988a, 1988b; Sobyanin, 1988; Wen and Kan, 1988) and has the same order of magnitude as in superfluid ^{4}He, where $\Delta c/k_B n \approx 2.6$.

(5) The occurrence of superconductivity even in very poor quality samples (in analogy with superfluid helium in porous media).

(6) Small coherence length and other estimated parameters such as the large width of the critical regime, which point to a breakdown of the mean-field behavior and microscopic BCS formulation (Kapitulnik *et al.*, 1988; Lobb, 1987).

(7) Presumably observed critical behavior in H_{c_2} and ξ (Uchida, Takagi *et al.*, 1987; Oh *et al.*, 1988).

(8) Fluctuation contributions to the specific heat near T_c (Inderhees *et al.*, 1988; Salamon, 1989), which cannot be described within a Gaussian approximation (Salamon, 1989), and a λ-type anomaly in the heat capacity (Butera, 1988; Ishikawa *et al.*, 1988; Voronel *et al.*, 1988).

(9) The experimentally observed thermopower with a temperature behavior that does not resemble that of a fermionic system and moreover is independent on an external field up to 30 T (Yu *et al.*, 1988); this behavior suggests spinless particles in the normal state, which could be diamagnetic local pairs.

(10) A superconducting precursor effect seen in the nuclear spin-lattice relaxation time measurements by NQR and NMR techniques in $YBa_2Cu_3O_{6.7}$, suggesting pair formation well above T_c (Warren *et al.*, 1989).

(11) Finally, the existence of local pairs may be reflected in the anomalous dependence of the elastic properties of high-T_c materials. It is known that when the temperature is lowered the lattice becomes stiffer in the superconducting phase, showing a change in slope of the orthorhombic lattice constants $(a-b)/(a+b)$ as well as in the sound velocity measurements (Horn *et al.*, 1988; Saint-Paul *et al.*, 1989). Alexandrov and Ranninger (1989) have recently shown that these phenomena can be explained by assuming that bosons (pairs of electrons) rather than electrons have been coupled to the lattice. Recent photoinduced infrared absorption measurements on La_2CuO_4, $YBa_2Cu_3O_{7-\delta}$ ($\delta = 0.75$) and $TlBa_2Ca_{1-x}Gd_xCu_2O_8$ demonstrate the formation of self-localized polarons (or bipolarons) with a unique local distortion around the photogenerated carriers (Kim *et al.*, 1989; Foster *et al.*, 1989; see also Taliani *et al.*, 1988).

Some of the enumerated points and other arguments quoted before, if taken separately, could have different explanations. For instance, the strong pressure dependence of T_c could also be explicable by magnetic mechanisms, whereas the dependence of T_c upon carrier concentration could also extend beyond the limit of local pair formation (Sec. V.B.2). However, in judging the relevance of the preformed pair concept, one should consider all the evidence together.

In contrast to the conventional BCS theory, the concept of charged-boson superfluidity is able to explain many experimental findings for the whole class of high-T_c superconducting oxides listed in Table I (see Micnas *et al.*, 1988b; Ranninger *et al.*, 1989; and, in particular,

de Jongh, 1988b, for a detailed comparison of the local pair picture and experiments on superconducting oxides).

To close this section let us point out that in comparison to the BiO-based oxides, the cuprate high-T_c superconductors exhibit special features of quasi-two-dimensionality which can be crucial for superfluid behavior and which constitute a challenging problem for the theory. At present, one cannot exclude the possibility that most of the unusual properties of high-T_c superconductors are just manifestations of the *intermediate crossover regime* between BCS superconductivity and superfluidity (Fig. 13), as was extensively discussed in Secs. II.C and IV.

It is also clear that a realistic model of Cu-O-based high-T_c superconductors should include d and p orbitals from the outset, i.e., it has to be at least a two-band extended Hubbard model (Emery, 1987; Varma *et al.*, 1987a, 1987b; Zaanen and Oleś, 1988). An important problem to be solved is to identify the nature of the quasiparticles in such a system and the source of the attractive interaction.

ACKNOWLEDGMENTS

Our work on systems with local pairing was initially developed independently by two groups: Alexandrov and Ranninger in Grenoble and Micnas, Robaszkiewicz, and Chao in Poznań and Linköping. We are very grateful to our early collaborators, A. S. Alexandrov (Moscow) and K. A. Chao (Trondheim), who were instrumental in initiating this work and elaborating the subject in numerous joint publications. We are very grateful to R. Tournier for his continuous interest in the problem of local pair superconductivity, for his encouragement, and for many valuable discussions. A part of this work has been presented by one of us (R.M.) at the Les Houches Workshop "Superconductivity: New Models, New Applications," March 1988. R.M. would like to thank P. Averbuch and M. Avignon for hospitality extended to him in Les Houches. R.M. and J.R. wish to thank the Institute for Scientific Interchange, Torino, for kind hospitality during the completion of this review. R.M. and J.R. benefited from useful discussions at this Institute during the program on High-Temperature Superconductors: Concepts, Models, and Methods. R.M. and S.R. gratefully acknowledge the partial financial support of the Polish Academy of Sciences within the projects RPBP 01.09 (S.R. and R.M.) and CPBP 01.12 (R.M.).

APPENDIX: "ATTRACTION-REPULSION" TRANSFORMATION FOR THE NEGATIVE-U EXTENDED HUBBARD MODEL

Let us assume that the intrasite electron interaction in the Hamiltonian (1.1) is attractive ($U<0$). Since such a term favors the formation of pairs of antiparallel spin electrons on the various sites, and since all other terms in (1.1) are spin independent, the model cannot exhibit any magnetic ordering (for a rigorous proof see Lieb, 1989), i.e., in particular, we have the non-ferromagnetic and non-antiferromagnetic conditions

$$\frac{1}{N}\sum_i \langle \sigma_i^\alpha \rangle = 0 , \tag{A1}$$

$$\frac{1}{N}\sum_i \exp(i\mathbf{Q}\cdot\mathbf{R}_i)\langle \sigma_i^\alpha \rangle = 0 , \tag{A2}$$

where σ_i^α is the $\alpha=+,-,z$ component of the spin operator $\boldsymbol{\sigma}_i$ for an electron at the lattice site $\mathbf{R}_i$. We restrict ourselves to the case of alternate (AB) lattices, and $\mathbf{Q}$ satisfies the condition $\exp(i\mathbf{Q}\cdot\mathbf{R})=-1$ for any translation $\mathbf{R}$ that transforms one sublattice into the other. For such systems with sublattices, the band energies satisfy the perfect nesting condition (for nearest-neighbor hopping) $\varepsilon_{\mathbf{k}}=-\varepsilon_{\mathbf{k}+\mathbf{Q}}$, where

$$\varepsilon_{\mathbf{k}}=\frac{1}{N}\sum_j t_{ij}\exp[i\mathbf{k}\cdot(\mathbf{R}_i-\mathbf{R}_j)] .$$

In order to obtain relations between the cases $U<0$ and $U>0$ let us perform the canonical transformation (Shiba, 1972; Robaszkiewicz *et al.*, 1981a)

$$\begin{aligned} &c_{i\downarrow}^\dagger=\exp(i\mathbf{Q}\cdot\mathbf{R}_i)b_{i\downarrow}, \quad c_{i\uparrow}^\dagger=b_{i\uparrow}^\dagger , \\ &c_{i\downarrow}=\exp(-i\mathbf{Q}\cdot\mathbf{R}_i)b_{i\downarrow}^\dagger, \quad c_{i\uparrow}=b_{i\uparrow} , \end{aligned} \tag{A3}$$

Then the spin operators σ_i^α are transformed to

$$\sigma_i^+=(\sigma_i^-)^\dagger=c_{i\uparrow}^\dagger c_{i\downarrow}=\exp(-i\mathbf{Q}\cdot\mathbf{R}_i)\bar{\rho}_i^+ , \tag{A4a}$$

$$\sigma_i^z=\tfrac{1}{2}(n_{i\uparrow}-n_{i\downarrow})=\bar{\rho}_i^z , \tag{A4b}$$

where

$$\bar{\rho}_i^+=(\bar{\rho}_i^-)^\dagger=b_{i\uparrow}^\dagger b_{i\downarrow}^\dagger ,$$

$$\bar{\rho}_i^z=\tfrac{1}{2}(\bar{n}_{i\uparrow}+\bar{n}_{i\downarrow}-1) ,$$

$$\bar{n}_{i\sigma}=b_{i\sigma}^\dagger b_{i\sigma} .$$

On the other hand, the charge operators are transformed to

$$\rho_i^+=(\rho_i^-)^\dagger=c_{i\uparrow}^\dagger c_{i\downarrow}^\dagger=\exp(i\mathbf{Q}\cdot\mathbf{R}_i)\bar{\sigma}_i^+ , \tag{A5a}$$

$$\rho_i^z=\tfrac{1}{2}(n_{i\uparrow}+n_{i\downarrow}-1)=\bar{\sigma}_i^z , \tag{A5b}$$

where

$$\bar{\sigma}_i^+=b_{i\uparrow}^\dagger b_{i\downarrow}, \quad \bar{\sigma}_i^z=\tfrac{1}{2}(\bar{n}_{i\uparrow}-\bar{n}_{i\downarrow}) ,$$

and

$$n_{i\uparrow}n_{i\downarrow}=\bar{n}_{i\uparrow}-\bar{n}_{i\uparrow}\bar{n}_{i\downarrow} . \tag{A6}$$

Therefore, within a phase factor $\exp(\pm i\mathbf{Q}\cdot\mathbf{R}_i)$, the spin operators $\bar{\sigma}_i^\alpha$ in the new representation (the $\{b_{i\sigma},b_{i\sigma}^\dagger\}$ representation) play the roles of the charge operators ρ_i^α in the old representation (the $\{c_{i\sigma},c_{i\sigma}^\dagger\}$ representation), and vice versa. The operators ρ_i^α, $\bar{\sigma}_i^\alpha$, and $\bar{\rho}_i^\alpha$ all obey the same commutation rules as the spin operators σ_i^α.

The Hamiltonian (1.1) is thus transformed into

$$H=\sum_{i,j,\sigma} t_{ij} b_{i\sigma}^{\dagger} b_{j\sigma} + \tfrac{1}{2}|U| \sum_{i,\sigma} \bar{n}_{i\sigma}\bar{n}_{i-\sigma} + 2\sum_{i,j} W_{ij}\bar{\sigma}_i^z\bar{\sigma}_j^z + 2\sum_i (E_i-\bar{\mu})\bar{\sigma}_i^z - \tfrac{1}{2}|U| \sum_{i\sigma} \bar{n}_{i\sigma} - (\bar{\mu}-\tfrac{1}{2}|U|+\tfrac{1}{2}zW)N \ , \quad \text{(A7)}$$

where

$$\bar{\mu}=\mu+\tfrac{1}{2}|U|-zW \ . \quad \text{(A8)}$$

After the canonical transformation, the electron number condition (2.1) and Eqs. (A1) and (A2) provide the following auxiliary conditions:

$$\frac{2}{N}\sum_i \langle \bar{\sigma}_i^z \rangle = n-1 \ , \quad \text{(A9)}$$

$$\frac{1}{N}\sum_{i,\sigma} \langle \bar{n}_{i\sigma} \rangle = 1 \ ; \quad \text{(A10)}$$

$$\sum_i \langle \bar{\rho}_i^{\pm} \rangle \exp(\mp i\mathbf{Q}\cdot\mathbf{R}_i)=0 \ ,$$

$$\sum_{i\sigma} \langle \bar{n}_{i\sigma} \rangle \exp(i\mathbf{Q}\cdot\mathbf{R}_i)=0 \ , \quad \text{(A11)}$$

$$\sum_i \langle \bar{\rho}_i^{\pm} \rangle = 0 \ .$$

Equations (A7)–(A11) show that the extended Hubbard Hamiltonian (1.1) of N sites and N_e electrons, with intrasite attraction and spin-independent interaction W_{ij}, has been transformed into an extended Hubbard Hamiltonian of one quasiparticle per site ($n=1$), with intrasite repulsion and an Ising-type intersite exchange interaction (antiferromagnetic if $W>0$) in the effective external magnetic field $(E_i-\bar{\mu})$ along the z direction. The magnetization of the transformed system along the z direction has a fixed value given by Eq. (A9). Just as there is no magnetic ordering in the original Hamiltonian (1.1), Eqs. (A10) and (A11) indicate that there is neither on-site s-wave superconducting pairing nor charge ordering in the transformed Hamiltonian (A7).

From Eqs. (A4) and (A5) we readily obtain

$$\frac{1}{N}\sum_i \langle \bar{\sigma}_i^{+} \rangle \exp(i\mathbf{q}\cdot\mathbf{R}_i) = \frac{1}{N}\sum_i \langle \rho_i^{+} \rangle \exp[i(\mathbf{Q}-\mathbf{q})\cdot\mathbf{R}_i] \ , \quad \text{(A12)}$$

$$\frac{1}{N}\sum_i \langle \bar{\sigma}_i^z \rangle \exp(i\mathbf{Q}\cdot\mathbf{R}_i) = \frac{1}{N}\sum_i \langle \rho_i^z \rangle \exp(i\mathbf{Q}\cdot\mathbf{R}_i) \ , \quad \text{(A13)}$$

where $\mathbf{q}=0$ or $\mathbf{Q}$. The quantities at the left-hand side of the above equations measure the magnetic long-range order (LRO) in the canonically transformed Hamiltonian (A7), while those on the right-hand side measure the singlet-superconducting or the charge LRO in the original Hamiltonian (1.1). Equation (A12) indicates that the magnetic order in the XY plane, namely, the off-diagonal LRO (ODRLO) in the transformed Hamiltonian, corresponds to the singlet-superconducting order in the original Hamiltonian. From Eq. (A13) we see that the nonuniform magnetic order along the z axis, i.e., the diagonal LRO (DLRO) in the transformed Hamiltonian corresponds to the charge order in the original Hamiltonian (see Table II).

The consequences of this attraction-repulsion canonical transformation are discussed in Sec. II.

REFERENCES

Aleksandrov, A. Yu., S. P. Ionov, A. M. Pritchard, and V. I. Gol'danskii, 1971, Zh. Eksp. Teor. Fiz. Pis'ma Red. **13**, 13 [JETP Lett. **13**, 8 (1971)].

Alexandrov, A. S., 1988, Phys. Rev. B **38**, 925.

Alexandrov, A. S., and V. F. Elesin, 1982, Fiz. Tverd. Tela (Leningrad) **25**, 456 [Sov. Phys. Solid State **25**, 257 (1983)].

Alexandrov, A. S., and V. F. Elesin, 1985, Izv. Akad. Nauk SSSR **49**, 326.

Alexandrov, A. S., V. N. Grebenev, and E. A. Mazur, 1987, Pis'ma Zh. Eksp. Teor. Fiz. **45**, 357 [JETP Lett. **45**, 455 (1987)].

Alexandrov, A. S., and A. B. Khmelinin, 1986, Fiz. Tverd. Tela (Leningrad) **28**, 3403 [Sov. Phys. Solid State **28**, 1915 (1986)].

Alexandrov, A. S., and J. Ranninger, 1981a, Phys. Rev. B **23**, 1796.

Alexandrov, A. S., and J. Ranninger, 1981b, Phys. Rev. B **24**, 1164.

Alexandrov, A. S., and J. Ranninger, 1989, Physica C **159**, 367.

Alexandrov, A. S., J. Ranninger, and S. Robaszkiewicz, 1986a, Phys. Rev. Lett. **56**, 949.

Alexandrov, A. S., J. Ranninger, and S. Robaszkiewicz, 1986b, Phys. Rev. B **33**, 4526.

Alexandrov, A. S., D. A. Samarchenko, and S. V. Traven, 1987, Zh. Eksp. Teor. Fiz. **93**, 1007 [Sov. Phys. JETP **66**, 567 (1987)].

Anderson, P. W., 1975, Phys. Rev. Lett. **34**, 953.

Anderson, P. W., 1979, in *Ill-Condensed Matter,* Les Houches Session XXXI, edited by R. Balian, R. Maynard, and G. Toulouse (North-Holland, Amsterdam), p. 161.

Anderson, P. W., 1987, Science **235**, 1196.

Anderson, P. W., 1988, in *Frontiers and Borderlines in Many-Particle Physics,* Proceedings of the International School of Physics "Enrico Fermi," Course CIV, edited by R. A. Broglia and J. R. Schrieffer (North-Holland, Amsterdam).

Anderson, P. W., and C. Yu, 1985, in *Highlights of Condensed-Matter Theory,* Proceedings of the International School of Physics "Enrico Fermi," Course No. LXXXIX, edited by F. Bassini and M. P. Tosi (North-Holland, Amsterdam), p. 767.

Arovas, D. P., and A. Auerbach, 1988, Phys. Rev. B **38**, 316.

Atkinson, L., and P. Day, 1969, J. Chem. Soc. A **16**, 2432.

Auerbach, A., and D. P. Arovas, 1988, Phys. Rev. Lett. **61**, 617.

Baeriswyl, D., P. Horsch, and K. Maki, 1988, Phys. Rev. Lett. **60**, 70.

Bahder, T., and F. Woynarovich, 1986, Phys. Rev. B **33**, 2114.

Balseiro, C. A., A. G. Rojo, E. R. Gagliano, and B. Alascio, 1988, Phys. Rev. B **38**, 9315.

Balzarotti, A., A. P. Menushenkov, N. Motta, and J. Purans, 1984, Solid State Commun. **49**, 887.

Bari, R. A., 1973, Phys. Rev. Lett. **30**, 790.

Baskaran, G., Z. Zou, and P. W. Anderson, 1987, Solid State

Commun. **63**, 973.
Bastide, C., and C. Lacroix, 1988a, J. Phys. F **18**, 63.
Bastide, C., and C. Lacroix, 1988b, J. Phys. C **21**, 3557.
Batlogg, B., 1984, Physica B+C **126**, 275.
Batlogg, B., R. J. Cava, L. W. Rupp, Jr., A. M. Mujsce, J. J. Krajewski, J. P. Remeika, W. F. Peck, Jr., A. S. Cooper, and G. P. Espinosa, 1988, Phys. Rev. Lett. **61**, 1670.
Batlogg, B., R. J. Cava, and M. Stavola, 1988, Phys. Rev. Lett. **60**, 754.
Batlogg, B., G. Kourkoulis, W. Weber, R. J. Cava, A. Jayaraman, A. E. White, L. W. Rupp, and E. A. Rietman, 1987, Phys. Rev. Lett. **59**, 912.
Batlogg, B., A. P. Ramirez, R. J. Cava, R. B. van Dover, and E. A. Rietman, 1987, Phys. Rev. B **35**, 5340.
Bednorz, J. G., and K. A. Müller, 1986 Z. Phys. B **64**, 189.
Bednorz, J. G., and K. A. Müller, 1988, Rev. Mod. Phys. **60**, 585.
Beille, J., *et al.*, 1987, Physica B **146**, 307.
Beloborod'ko, S. I., and I. O. Kulik, 1986, Fiz. Nizk. Temp. **12**, 465 [Sov. J. Low Temp. Phys. **12**, 262 (1986)].
Beni, G., P. Pincus, and J. Kanamori, 1974, Phys. Rev. B **10**, 1896.
Bianconi, A., A. C. Castellano, M. de Santis, P. Delgou, A. Gargano, and R. Giorgi, Physica B **146**, 307.
Bickers, N. E., D. J. Scalapino, and S. R. White, 1989, Phys. Rev. Lett. **62**, 961.
Birgenau, R. J., Y. Endoh, K. Kakurai, Y. Hidaka, T. Murakami, M. A. Kastner, T. R. Thurston, G. Shirane, and K. Yamada, 1989, Phys. Rev. B **39**, 2868.
Birgeneau, R. J., and G. Shirane, 1989, in *Physical Properties of High Temperature Superconductors I,* edited by D. M. Ginsberg (World Scientific, Singapore), p. 152.
Bishop, A. R., P. S. Lomdahl, J. R. Schrieffer, and S. A. Trugman, 1988, Phys. Rev. Lett. **61**, 2709.
Bishop, D. J., P. L. Gammel, A. P. Ramirez, R. J. Cava, B. Batlogg, and E. A. Rietman, 1987, Phys. Rev. B **35**, 8788.
Bishop, D. J., A. P. Ramirez, P. L. Gammel, B. Batlogg, E. A. Rietman, R. J. Cava, and A. J. Mills, 1987, Phys. Rev. B **36**, 2408.
Bishop, R. F., 1974, J. Low Temp. Phys. **15**, 601.
Bhattacharya, S., M. J. Higgins, D. C. Johnson, A. J. Jacobson, J. P. Stokes, J. T. Lewandowski, and D. P. Goshorn, 1988, Phys. Rev. B **37**, 5901.
Blatt, J. M., 1964, *Theory of Superconductivity* (Academic, New York).
Bonča, J., P. Prelovšek, and I. Sega, 1989, Phys. Rev. B **39**, 7074.
Bourne, L. C., 1987, A. Zettl, T. W. Barbee III, and M. L. Cohen, Phys. Rev. B **36**, 3990.
Bray, A. J., and M. A. Moore, 1982, J. Phys. C **15**, L765.
Brazovskii, S., N. Kirova, and V. Yakovenko, 1985, Solid State Commun. **55**, 187.
Brewer, J. H., *et al.* 1987, Phys. Rev. Lett. **60**, 1073.
Bruce, A. D., and A. Aharony, 1975, Phys. Rev. B **11**, 478.
Bulaevskii, L. N., A. A. Sobyanin, and D. I. Khomskii, 1984, Zh. Eksp. Teor. Fiz. **87**, 1490 [Sov. Phys. JETP **60**, 856 (1984)].
Bussmann-Holder, A., A. Simon, and H. Büttner, 1989, Phys. Rev. B **39**, 207.
Butera, R. A., 1988, Phys. Rev. B **37**, 5909.
Callaway, J., D. G. Kanhere, and P. K. Misra, 1987, Phys. Rev. B **36**, 7141.
Campbell, D. K., J. Tinka Gammel, and E. Y. Loh, Jr., 1988, Phys. Rev. B **38**, 12043.
Capponi, J. J., C. Chaillout, A. W. Hewat, P. Lejay, P. Marezio, N. Nguyen, B. Raveau, J. L. Souberoux, J. L. Tholence, and R. Tournier, 1987, Europhys. Lett. **3**, 1301.
Cava, R. J., B. Batlogg, R. B. van Dover, D. W. Murphy, S. Sunshine, T. Siegrist, J. P. Remeika, E. A. Rietman, S. Zahurak, and G. P. Espinosa, 1987, Phys. Rev. Lett. **58**, 1676.
Cava, R. J., B. Batlogg, J. J. Krajewski, R. Farrow, L. W. Rupp, A. E. White, K. Shork, W. F. Peck, and K. Kometani, 1988, Nature **332**, 814.
Chaillout, C., A. Santoro, J. P. Remeika, A. S. Cooper, G. P. Espinoza, and M. Marezio, 1988, Solid State Commun. **65**, 1363.
Chakravarty, S., B. I. Halperin, and D. R. Nelson, 1988, Phys. Rev. Lett. **60**, 1057.
Chakraverty, B. K., 1979, J. Phys. (Paris) Lett. **40**, L-99.
Chakraverty, B. K., D. Feinberg, H. Zheng, and M. Avignon, 1987, Solid State Commun. **64**, 1147.
Chakraverty, B. K., and J. Ranninger, 1985, Philos. Mag. B **52**, 669.
Chakraverty, B. K., D. D. Sarma, and C. N. R. Rao, 1988, Physica C **156**, 413.
Chakraverty, B. K., M. J. Sienko, and J. Bonnerot, 1978, Phys. Rev. B **17**, 3781.
Chao, K. A., R. Micnas, and S. Robaszkiewicz, 1979, Phys. Rev. B **20**, 4741.
Chao, K. A., R. Micnas, S. Robaszkiewicz, A. M. Oleś, and B. Oleś, 1983, Phys. Lett. **95A**, 391.
Chao, K. A., J. Spałek, and A. M. Oleś, 1977, J. Phys. C **10**, L271.
Chen, J.-H., T. C. Lubensky, and D. R. Nelson, 1978, Phys. Rev. B **17**, 4274.
Chernik, I. A., S. N. Likhov, and N. I. Grechko, 1982, Fiz. Tverd. Tela (Leningrad) **24**, 2931 [Sov. Phys. Solid State **24**, 1661 (1982)].
Chung, T. C., J. H. Kaufman, A. J. Heeger, and F. Mund, 1984, Phys. Rev. B **30**, 702.
Cohen, M. H., E. N. Economou, and C. M. Soukoulis, 1984a, Phys. Rev. B **29**, 4496.
Cohen, M. H., E. N. Economou, and C. M. Soukoulis, 1984b, Phys. Rev. B **29**, 4500.
Cooper, J. R., C. T. Chu, L. W. Zhou, B. Dunn, and G. Grüner, 1988, Phys. Rev. B **37**, 638.
Cox, D. E., and A. W. Sleight, 1979, Acta Crystallogr. Sec. B **35**, 1.
Crabtree, G. W., W. K. Kwok, and A. Umezawa, 1988, in *Quantum Field Theory as an Interdisciplinary Basis,* Proceedings of the CAP-NSERC Summer Institute in Theoretical Physics, Edmonton, Alberta, 1987, Vol. 1, edited by H. Umezawa, F. C. Khanna *et al.* (World Scientific, Singapore).
Crooker, B. C., B. Hebral, E. N. Smith, Y. Takano, and J. D. Reppy, 1983, Phys. Rev. Lett. **51**, 663.
Dąbrowski, B., D. G. Hinks, J. D. Jorgensen, R. K. Kalia, P. Vashita, D. R. Richards, D. T. Marx, and T. W. Mitchell, 1988, Physica C **156**, 24.
Dasgupta, C., and B. I. Halperin, 1981, Phys. Rev. Lett. **47**, 1556.
Day, P., 1980, in *The Physics and Chemistry of Low Dimensional Solids,* edited by L. Alcacer (Reidel, Dordrecht), p. 305.
de Groot, R. A., H. Gutfreund, and M. Weger, 1987, Solid State Commun. **63**, 451.
de Jongh, L. J., 1988a, Solid State Commun. **65**, 961.
de Jongh, L. J., 1988b, Physica C **152**, 171.
De Marco, R., E. N. Economou, and C. T. White, 1978, Phys. Rev. B **18**, 3968.
De Raedt, H., and A. Lagendijk, 1983, Phys. Rev. B **27**, 6097.

De Raedt, H., and A. Lagendijk, 1986, Z. Phys. B **65**, 43.
Dinger, T. R., T. K. Worthington, W. J. Gallagher, and R. L. Sandstrom, 1987, Phys. Rev. Lett. **58**, 2687.
Doniach, S., 1984, in *Percolation, Localization and Superconductivity,* NATO Advanced Study Institute Series B, Vol. 109, edited by A. M. Goldman and S. A. Wolf (Plenum, New York), p. 401.
Eagles, D. M., 1969a, Phys. Rev. **178**, 668.
Eagles, D. M., 1969b, Phys. Rev. **186**, 456.
Eagles, D. M., 1985, Solid State Commun. **60**, 521.
Economou, E. N., C. T. White, and R. De Marco, 1978, Phys. Rev. B **18**, 3946.
Efetov, K. B., and A. I. Larkin, 1975, Zh. Eksp. Teor. Fiz. **69**, 75 [Sov. Phys. JETP **42**, 390 (1976)].
Eliashberg, G. M., 1987, Pisma Zh. Eksp. Teor. Fiz. **46**, 94.
Emery, V. J., 1976, Phys. Rev. B **14**, 2989.
Emery, V. J., 1977, in *Chemistry and Physics of One-Dimensional Metals,* edited by H. J. Keller (Plenum, New York), p. 1.
Emery, V. J., 1987, Phys. Rev. Lett. **58**, 2794.
Emery, V. J., 1988, talk given at the IBM Workshop on High-Temperature Superconductivity in Oberlech, Austria, unpublished, and IBM J. Res. Dev. **33**, 246 (1989).
Emery, V. J., and G. Reiter, 1988a, Phys. Rev. B **38**, 4547.
Emery, V. J., and G. Reiter, 1988b, Phys. Rev. B **38**, 11938.
Emin, D., 1989, Phys. Rev. Lett. **62**, 1544.
Emin, D., and M. S. Hillery, 1989, Phys. Rev. B **39**, 6575.
Erata, T., and H. Nagasawa, 1983, J. Phys. Soc. Jpn. **52**, 3652.
Faltens, T. A., *et al.*, 1987, Phys. Rev. Lett. **59**, 915.
Fedro, A. J., H. B. Schüttler, and S. K. Sinha, 1987, Physica B **148**, 250.
Feinberg, D., and J. Ranninger, 1984, Phys. Rev. A **30**, 3339.
Feinberg, D., and J. Ranninger, 1986, Phys. Rev. A **33**, 3436.
Fetter, A. L., 1970, Ann. Phys. (N.Y.) **60**, 464.
Fetter, A. L., 1971, Ann. Phys. (N.Y.) **64**, 1.
Fisher, D. S., and M. P. A. Fisher, 1988, Phys. Rev. Lett. **61**, 1847.
Fisher, M. E., and D. R. Nelson, 1974, Phys. Rev. Lett. **32**, 1350.
Foldy, L. L., 1961, Phys. Rev. **124**, 649.
Foldy, L. L., 1962, Phys. Rev. **125**, 2208.
Foster, C. M., A. J. Heeger, G. Stucky, and N. Herron, 1989, Solid State Commun. **71**, 945.
Fradkin, E., and J. E. Hirsch, 1983, Phys. Rev. B **27**, 1680.
Freltoft, T., J. E. Fischer, G. Shirane, D. E. Moncton, S. K. Sinha, D. Vaknin, J. P. Remeika, A. S. Cooper, and D. Harshman, 1987, Phys. Rev. B **36**, 826.
Fujimori, A., E. Takayama-Muromachi, Y. Uchida, and B. Okai, 1987, Phys. Rev. B **35**, 8814.
Fujita, T., *et al.*, 1987, Jpn. J. Appl. Phys. Suppl. **26-3**, 1041.
Fukuyama, H., Y. Hasegawa, and Y. Suzumura, 1988, Physica C **153-155**, 1630.
Gagliano, A. R., A. G. Rojo, C. A. Balseiro, and B. Alascio, 1987, Solid State Commun. **64**, 901.
Gammel, J. T., and D. K. Campbell, 1988, Phys. Rev. Lett. **60**, 71.
Ganguli, B. N., U. N. Upadhyaya, and K. P. Sinha, 1966, Phys. Rev. **146**, 317.
Geerk, J., X. X. Xi, and G. Linker, 1988, Z. Phys. B **73**, 329.
Ginzburg, V. L., 1964, Zh. Eksp. Teor. Fiz. **47**, 2318 [Sov. Phys. JETP **20**, 1549 (1965)].
Ginzburg, V. L., 1976, Usp. Fiz. Nauk **118**, 315 [Sov. Phys. Usp. **19**, 174 (1976)].
Griessen, R., 1987, Phys. Rev. B **36**, 5284.
Groznov, I. N., S. P. Ionova, I. B. Kevedina, V. S. Lubimov, E. F. Makarov, O. V. Marchenko, N. N. Mikhailov, V. A. Onishchuk, and V. P. Shantarovich, 1984, Phys. Status Solidi B **123**, 183.
Guinea, F., 1983, J. Phys. C **16**, 405.
Gurvitch, M., and A. T. Fiory, 1987, Phys. Rev. Lett. **59**, 1337.
Gusmão, M. A., 1987, Phys. Rev. B **35**, 1682.
Haldane, F. D. M., 1980, Phys. Rev. Lett. **45**, 1358.
Halperin, B. I., T. C. Lubensky, and S.-K. Ma, 1974, Phys. Rev. Lett. **32**, 292.
Harris, A. B., and R. V. Lange, 1967, Phys. Rev. **157**, 295.
Harrison, M. R., P. P. Edwards, and J. B. Goodenough, 1985, Philos. Mag. B **52**, 679.
Hasegawa, Y., and H. Fukuyama, 1986, J. Phys. Soc. Jpn. **55**, 3978.
Hertz, J. A., L. Fleishman, and P. W. Anderson, 1979, Phys. Rev. Lett. **43**, 942.
Hines, D. F., and N. E. Frankel, 1979, Phys. Rev. B **20**, 972.
Hinks, D. G., B. Dąbrowski, J. D. Jorgensen, A. W. Mitchell, D. R. Richards, S. Pei, and D. Shi, 1988a, Nature **333**, 836.
Hinks, D. G., D. R. Richards, B. Dabrowski, D. T. Marx, and A. W. Mitchell, 1988b, Nature **335**, 419; **336**, 604(E).
Hirsch, J. E., 1985a, Phys. Rev. B **31**, 4403.
Hirsch, J. E., 1985b, Phys. Rev. Lett. **54**, 1317.
Hirsch, J. E., 1987a, Phys. Rev. B **35**, 1851.
Hirsch, J. E., 1987b, Phys. Rev. B **35**, 8726.
Hirsch, J. E., 1989a, Phys. Lett. **134**, 451.
Hirsch, J. E., 1989b, Phys. Lett. **136**, 163.
Hirsch, J. E., and E. Fradkin, 1983, Phys. Rev. B **27**, 4302.
Hirsch, J. E., and H. Q. Lin, 1988, Phys. Rev. B **37**, 5070.
Hirsch, J. E., and F. Marsiglio, 1989, Phys. Rev. B **39**, 11 515.
Hirsch, J. E., and D. J. Scalapino, 1985a, Phys. Rev. B **32**, 117.
Hirsch, J. E., and D. J. Scalapino, 1985b, Phys. Rev. B **32**, 5639.
Hirsch, J. E., and D. J. Scalapino, 1986, Phys. Rev. Lett. **56**, 2732.
Hirsch, J. E., and S. Tang, 1989, Solid State Commun. **69**, 987.
Hirsch, J. E., S. Tang, E. Loh, Jr., and D. J. Scalapino, 1988, Phys. Rev. Lett. **60**, 1668.
Hohenberg, P. C., 1967, Phys. Rev. **158**, 383.
Holstein, T., 1959, Ann. Phys. (N.Y.) **8**, 343.
Hore, S. R., and N. E. Frankel, 1975, Phys. Rev. B **12**, 2619.
Hore, S. R., and N. E. Frankel, 1976, Phys. Rev. B **14**, 1952.
Horn, P. M., D. T. Keane, G. A. Held, J. L. Jordan-Sweet, D. L. Kaiser, F. Holtzberg, and T. M. Rice, 1987, Phys. Rev. Lett. **59**, 2772.
Horvatič, M., P. Sérgansan, C. Berthier, P. Butaud, J. Y. Henry, M. Couach, and J. P. Chaminade, 1989, Phys. Rev. B **39**, 7332.
Huang, K., and E. Manousakis, 1987, Phys. Rev. B **36**, 8302.
Hubbard, J., 1963, Proc. R. Soc. London Ser. A **276**, 238.
Hubbard, J., 1964, Proc. R. Soc. London Ser. A **277**, 237.
Hüller, A., 1989, Z. Phys. B **76**, 445.
Imada, M., 1987, J. Phys. Soc. Jpn. **56**, 3793.
Imada, M., and D. J. Scalapino, 1986, Phys. Rev. B **34**, 3480.
Imer, J.-M., F. Patthey, B. Dardel, W.-D. Schneider, Y. Baer, Y. Petroff, and A. Zettl, 1989, Phys. Rev. Lett. **62**, 336.
Inderhees, S. E., M. B. Salamon, T. A. Friedmann, and D. M. Ginsberg, 1987, Phys. Rev. B **36**, 2401.
Inderhees, S. E., M. B. Salamon, N. Goldenfeld, J. P. Rice, B. G. Pazol, D. M. Ginsberg, J. Z. Liu, and G. W. Crabtree, 1988, Phys. Rev. Lett. **60**, 1178.
Ionov, S. P., G. V. Ionova, V. S. Lubimov, and E. F. Makarov, 1975, Phys. Status Solidi B **71**, 11.
Ionov, S. P., G. V. Ionova, A. I. Maiybaev, L. A. Manakova,

and G. K. Semin, 1981, Izv. Akad. Nauk SSSR **45**, 589.
Ionov, S. P., G. V. Ionova, A. I. Maiybaev, L. A. Manakova, and G. K. Semin, 1985, Izv. Akad. Nauk SSSR **49**, 310.
Ionova, G. V., E. F. Makarov, and S. P. Ionov, 1977, Phys. Status Solidi B **81**, 671.
Ishikawa, M., Y. Nakazawa, T. Takabate, A. Kishi, and A. Maesono, 1988, Solid State Commun. **66**, 201.
Jérome, D., W. Kang, and S. S. P. Parkin, 1988, J. Appl. Phys. **63**, 4005.
Johnston, D. C., J. P. Stokes, D. P. Goshorn, and J. T. Lewandowski, 1987, Phys. Rev. B **36**, 4007.
Junod, A., *et al.*, 1987, Europhys. Lett. **4**, 247.
Junod, A., A. Bezinge, and J. Muller, 1988, Physica C **152**, 50.
Kac, M., and J. Luttinger, 1973, J. Math. Phys. **14**, 1626.
Kac, M., and J. Luttinger, 1974, J. Math. Phys. **15**, 183.
Kanai, Y., S. Kagoshima, and H. Nagasawa, 1980, Synth. Metals **9**, 369.
Kane, C. L., P. A. Lee, and N. Read, 1989, Phys. Rev. B **39**, 6880.
Kapitulnik, A., M. R. Beasley, C. Di Castro, and C. Castellani, 1988, Phys. Rev. B **37**, 537.
Kapitulnik, A., and G. Kotliar, 1985, Phys. Rev. Lett. **54**, 473.
Kastner, M. A., *et al.*, 1988, Phys. Rev. B **37**, 111.
Keller, H. J., 1981, in *Extended Linear Chain Compounds,* edited by J. S. Miller (Plenum, New York), Vol. 1, p. 357.
Khomskii, D. I., and A. K. Zvezdin, 1988, Solid State Commun. **66**, 651.
Kim, Y. H., C. M. Foster, A. J. Heeger, S.Cox, L. Acedo, and G. Stucky, 1989, Phys. Scr. **27**, 19.
Kitaoka, Y., K. Ishida, K. Fujiwara, and K. Asayama, 1988, talk given at the IBM Workshop on High-T_c Superconductivity, Oberlech, Austria, unpublished.
Kitazawa, K., M. Naito, T. Itoh, and S. Tanaka, 1985, J. Phys. Soc. Jpn. **54**, 2682.
Kitazawa, K., S. Uchida, and S. Tanaka, 1985, Physica B **135**, 505.
Kivelson, S., W. P. Su, J. R. Schrieffer, and A. J. Heeger, 1987, Phys. Rev. Lett. **58**, 1889.
Kivelson, S., W. P. Su, J. R. Schrieffer, and A. J. Heeger, 1988, Phys. Rev. Lett. **60**, 72.
Klinger, M. I., 1985, Usp. Fiz. Nauk **146**, 105 [Sov. Phys. Usp. **28**, 391 (1985)].
Kosterlitz, J. M., D. R. Nelson, and M. E. Fisher, 1976, Phys. Rev. B **13**, 412.
Kostyrko, T., 1987, Phys. Status Solidi B **143**, 149.
Kotliar, G., and A. Kapitulnik, 1986, Phys. Rev. B **33**, 3146.
Kresin, V. Z., G. Deutscher, and S. A. Wolf, 1988, J. Supercond. **1**, 327.
Krivnov, V. Ya., and A. A. Ovchinnikov, 1974, Zh. Eksp. Teor. Fiz. **67**, 1568 [Sov. Phys. JETP **40**, 781 (1984)].
Kubo, K., and S. Takada, 1983, J. Phys. Soc. Jpn. **52**, 2108.
Kulik, I. O., 1984, Physica B **126**, 280.
Kulik, I. O., 1987, Fiz. Nizk. Temp. **13**, 879 [Sov. J. Low Temp. Phys. **13**, 505 (1987)].
Kulik, I. O., 1988, Fiz. Nizk. Temp. **14**, 209 [Sov. J. Low Temp. Phys. **14**, 116 (1988)].
Kulik, I. O., and A. G. Pedan, 1980, Zh. Eksp. Teor. Fiz. **79**, 1469 [Sov. Phys. JETP **52**, 742 (1980)].
Kuramoto, Y., and T. Watanabe, 1987, Solid State Commun. **63**, 821.
Lakkis, S., C. Schlenker, B. K. Chakraverty, R. Buder, and M. Marezio, 1976, Phys. Rev. B **14**, 1429.
Leggett, A. J., 1980a, in *Modern Trends in the Theory of Condensed Matter,* edited by A. Pekalski and J. Przystawa (Springer, Berlin/New York), p. 13.
Leggett, A. J., 1980b, J. Phys. (Paris) **41**, C7, 19.
Li, Y. M., 1987, Solid State Commun. **62**, 677.
Lieb, E., and F. Wu, 1968, Phys. Rev. Lett. **20**, 1445.
Lieb, E. H., 1989, Phys. Rev. Lett. **62**, 1201.
Lin, H. Q., J. E. Hirsch, and D. J. Scalapino, 1988, Phys. Rev. B **37**, 7359.
Little, W. A., 1964, Phys. Rev. A **134**, 1416.
Little, W. A., 1981, Int. J. Quantum Chem. **15**, 545.
Liu, K. S., and M. E. Fisher, 1973, J. Low Temp. Phys. **10**, 655.
Lobb, J., 1987, Phys. Rev. B **36**, 3930.
Loh, E. Y., Jr., T. Martin, P. Prelovšek, and D. K. Campbell, 1988, Phys. Rev. B **38**, 2494.
Löwen, H., 1988, Phys. Rev. B **37**, 8661.
Ma, M. B., B. I. Halperin, and P. A. Lee, 1986, Phys. Rev. B **34**, 3136.
Ma, M., and P. A. Lee, 1985, Phys. Rev. B **32**, 5658.
Ma, S.-K., 1972, Phys. Rev. Lett. **29**, 1311.
Manthiram, A., X. X. Tang, and J. B. Goodenough, 1988, Phys. Rev. B **37**, 3734.
Marsiglio, F., and J. F. Hirsch, 1989, Physica C **139**, 157.
Martin, S., A. T. Fiory, R. M. Fleming, L. F. Schneemeyer, and J. V. Waszczak, 1988, Phys. Rev. Lett. **60**, 2194.
Matsubara, T., and H. Matsuda, 1956, Prog. Theor. Phys. **16**, 569.
Matsubara, T., and H. Matsuda, 1957, Prog. Theor. Phys. **17**, 19.
Matsuda, H., and T. Tsuneto, 1970, Prog. Theor. Phys. Suppl. **46**, 411.
Mattheiss, L. F., E. M. Gyorgy, and D. W. Johnston, Jr., 1988, Phys. Rev. B **37**, 3745.
Mazumdar, S., 1988, Solid State Commun. **66**, 427.
Menushenkov, A. P., 1986, "Structure of x ray spectra of $BaPb_{1-x}Bi_xO_3$," preprint, Moscow Physics and Engineering Institute, Moscow (in Russian).
Micnas, R., 1988a (unpublished).
Micnas, R., 1988b (unpublished).
Micnas, R., 1988c (unpublished).
Micnas, R., J. Ranninger, and S. Robaszkiewicz, 1987a, J. Magn. Magn. Mater. **63-64**, 420.
Micnas, R., J. Ranninger, and S. Robaszkiewicz, 1987b, Phys. Rev. B **36**, 4051.
Micnas, R., J. Ranninger, and S. Robaszkiewicz, 1988a, J. Phys. C **21**, L145.
Micnas, R., J. Ranninger, and S. Robaszkiewicz, 1988b, J. Phys. (Paris) Suppl. **49**, C8-2221.
Micnas, R., J. Ranninger, and S. Robaszkiewicz, 1989, Phys. Rev. B **39**, 11653.
Micnas, R., J. Ranninger, S. Robaszkiewicz, and S. Tabor 1988, Phys. Rev. B **37**, 9410.
Micnas, R., and S. Robaszkiewicz, 1988a, "Thermodynamics of local pair superconductors with anisotropic lattice structures," preprint, Adam Mickiewicz University, Poznań, Poland.
Micnas, R., and S. Robaszkiewicz, 1988b, "Thermodynamic and electrodynamic properties of local pair superconductors: Effects of long range Coulomb interaction," preprint, Adam Mickiewicz University, Poznań, Poland.
Micnas, R., S. Robaszkiewicz, and K. A. Chao, 1983, J. Magn. Magn. Mater. **31-34**, 365.
Micnas, R., S. Robaszkiewicz, and K. A. Chao, 1984, Phys. Rev. B **29**, 2784.
Micnas, R., S. Robaszkiewicz, and K. A. Chao, 1985a, Physica A **131**, 393.
Micnas, R., S. Robaszkiewicz, and K. A. Chao, 1985b, Physica

A **132**, 504.
Miller, J. S., and A. J. Epstein, 1976, Prog. Inorg. Chem. **20**, 2.
Millis, A. J., and K. M. Rabe, 1988, Phys. Rev. B **38**, 8908.
Mitsuda, S., G. Shirane, S. K. Sinha, D. C. Johnston, M. S. Alvarez, D. Vaknin, and D. E. Moncton, 1987, Phys. Rev. B **36**, 822.
Miyake, K., 1983, Prog. Theor. Phys. **69**, 1794.
Miyake, K., T. Matsuura, H. Jichu, and Y. Nagaoka, 1984, Prog. Theor. Phys. **72**, 1063.
Miyake, K., S. Schmitt-Rink, and C. V. Varma, 1986, Phys. Rev. B **34**, 6554.
Moiseev, D. P., S. K. Uvarova, and M. B. Fenik, 1981, Fiz. Tverd. Tela (Leningrad) **23**, 2347 [Sov. Phys. Solid State **23**, 1371 (1981)].
Mozihes, B. Ya., and I. A. Drabkin, 1983, Fiz. Tverd. Tela (Leningrad) **25**, 1974 [Sov. Phys. Solid State **25**, 1139 (1983)].
Mullin, W. J., 1971a, Phys. Rev. Lett. **26**, 611.
Mullin, W. J., 1971b, Phys. Rev. A **4**, 1247.
Nagosa, N., 1989, Phys. Rev. B **39**, 2188.
Nagasawa, S., and K. Hida, 1988, J. Phys. Soc. Jpn. **57**, 3506.
Nasu, K., 1985, J. Phys. Soc. Jpn. **54**, 1933.
Nasu, K., 1987, Phys. Rev. B **35**, 1748.
Nasu, K., 1988, Phys. Rev. B **37**, 5075.
Nevitt, M. F., G. W. Crabtree, and T. E. Klipper, 1987, Phys. Rev. B **36**, 2398.
Ng, K. W., R. N. Shelton, and E. L. Wolf, 1985, Phys. Lett. **110A**, 423.
Nozières, Ph., and S. Schmitt-Rink, 1985, J. Low Temp. Phys. **59**, 195.
Nücker, N., J. Fink, J. C. Fuggle, J. P. Durham, and W. M. Temmerman, 1988, Phys. Rev. B **37**, 5158.
Nücker, N., J. Fink, B. Renker, D. Ewert, C. Politis, J. W. P. Wejis, and J. C. Fuggle, 1987, Z. Phys. B **67**, 9.
Nuñez Regueiro, M. D., and A. A. Aligia, 1988, Phys. Rev. Lett. **61**, 1889.
Oh, B., K. Char, A. D. Kent, M. Naito, M. R. Beasley, T. H. Geballe, R. H. Hammond, A. Kapitulnik, and J. M. Graybeal, 1988, Phys. Rev. B **37**, 7861.
Ohkawa, F. J., 1984, J. Phys. Soc. Jpn. **53**, 3568.
Ohkawa, F. J., 1988, J. Phys. Soc. Jpn. **57**, 3920.
Ohkawa, F. J., and H. Fukuyama, 1984, J. Phys. Soc. Jpn. **53**, 4344.
Oleś, A. M., R. Micnas, K. A. Chao, and S. Robaszkiewicz, 1984, Phys. Lett. **102A**, 323.
Onoda, M., and H. Nagasawa, 1983, J. Phys. Soc. Jpn. **52**, 2231.
Onoda, M., T. Takahashi, and H. Nagasawa, 1982, J. Phys. Soc. Jpn. **51**, 3868.
Panson, A. J., A. I. Braginski, J. R. Gavaler, J. K. Hulm, M. A. Janocko, H. C. Pohl, A. M. Stewart, J. Talvacchio, and G. R. Wagner, 1987, Phys. Rev. B **35**, 8774.
Pedan, A. G., and I. O. Kulik, 1982, Fiz. Nizk. Temp. **8**, 236 [Sov. J. Low Temp. Phys. **8**, 118 (1982)].
Pincus, P., P. Chaikin, and C. F. Coll III, 1973, Solid State Commun. **12**, 1265.
Prelovšek, P., T. M. Rice, and F.-C. Zhang, 1987, J. Phys. C **20**, L229.
Que, W. M., and G. Kirczenov, 1987, Solid State Commun. **64**, 1053.
Randeira, M., J. M. Duan, and L. Y. Shieh, 1989, Phys. Rev. Lett. **62**, 981.
Ranninger, J., R. Micnas, and S. Robaszkiewicz, 1988, Ann. Phys. (Paris) **13**, 455.
Ranninger, J., R. Micnas, and S. Robaszkiewicz, 1989, in *High T_c Superconductors Electronic Structure,* edited by A. Bianconi and A. Marcelli (Pergamon, New York), p. 51.
Ranninger, J., and S. Robaszkiewicz, 1985, Physica B **135**, 468.
Ranninger, J., S. Robaszkiewicz, A. Sulpice, and R. Tournier, 1987, Europhys. Lett. **3**, 347.
Ranninger, J., and W. Thirring, 1963, Z. Phys. **171**, 312.
Rao, C. N. R., 1988, Ann. Phys. (Paris) **13**, 327.
Rao, C. N. R., P. Ganguly, M. S. Hedge, and D. D. Sarma, 1987, J. Am. Chem. Soc. **109**, 6893.
Reger, J. D., and A. P. Young, 1988, Phys. Rev. B **37**, 5978.
Rice, T. M., 1987, Z. Phys. **67**, 141.
Rice, T. M., and L. Sneddon, 1981, Phys. Rev. Lett. **47**, 689.
Robaszkiewicz, S., 1979, Acta Phys. Pol. A **45**, 75.
Robaszkiewicz, S., 1984, Physica B+C **125**, 150.
Robaszkiewicz, S., R. Micnas, and K. A. Chao, 1981a, Phys. Rev. B **23**, 1447.
Robaszkiewicz, S., R. Micnas, and K. A. Chao, 1981b, Phys. Rev. B **24**, 1579.
Robaszkiewicz, S., R. Micnas, and K. A. Chao, 1981c, Solid State Commun. **40**, 403.
Robaszkiewicz, S., R. Micnas, and K. A. Chao, 1981d, Phys. Rev. B **24**, 4018.
Robaszkiewicz, S., R. Micnas, and K. A. Chao, 1982, Phys. Rev. B **26**, 3915.
Robaszkiewicz, S., R. Micnas, and J. Ranninger, 1987, Phys. Rev. B **37**, 180.
Robin, M. R., and P. Day, 1967, Adv. Radiochem. **10**, 247.
Rogers, J. W., Jr., N. D. Shinn, J. E. Schirber, E. L. Venturini, D. S. Ginley, and B. Morosin, 1988, Phys. Rev. B **38**, 5021.
Rossa-Mignod, J., P. Burlet, M. J. G. M. Jurgens, and J. Y. Henry, 1988, Physica C **152**, 19.
Ruckenstein, A. E., P. J. Hirschfeld, and J. Appel, 1987, Phys. Rev. B **36**, 857.
Saint-Paul, M., J. L. Tholence, H. Noel, J. C. Levet, M. Poten,and P. Gougeon, 1989, Solid State Commun. **69**, 1161.
Sakudo, T., H. Uwe, T. Suzuki, J. Fujita, J. Shiozawa, and M. Isobe, 1986, J. Phys. Soc. Jpn. **55**, 314.
Salamon, M. B., 1989, in *Physical Properties of High Temperature Superconductors I,* edited by D. M. Ginsberg (World Scientific, Singapore), p. 40.
Salje, E., and B. Güttler, 1984, Philos. Mag. B **50**, 607.
Sarma, D. D., K. Sredhar, P. Ganguly, and C. N. R. Rao, 1987, Phys. Rev. B **36**, 2371.
Sarma, D. D., and C. N. R. Rao, 1987a, J. Phys. C **20**, L659.
Sarma, D. D., and C. N. R. Rao, 1987b, Solid State Commun. **65**, 47.
Savransky, S. D., 1986, J. Non-Cryst. Solids **83**, 235.
Scalapino, D. J., E. Loh, Jr., and J. E. Hirsch, 1986, Phys. Rev. B **34**, 8190.
Scalapino, D. J., E. Loh, Jr., and J. E. Hirsch, 1987, Phys. Rev. B **35**, 6694.
Scalettar, R. T., E. Y. Loh, J. E. Gubernatis, A. Moreo, S. R. White, D. J. Scalapino, R. L. Sugar, and E. Dagotto, 1989, Phys. Rev. Lett. **62**, 1407.
Scalettar, R. T., D. J. Scalapino, R. L. Sugar, and D. Toussaint, 1989, Phys. Rev. B **39**, 4711.
Schafroth, R. M., 1955, Phys. Rev. **100**, 463.
Schafroth, R. M., J. M. Blatt, and S. T. Butler, 1957, Helv. Phys. Acta **30**, 93.
Schirber, J. E., B. Morosin, and D. S. Ginley, 1989, Physica C **157**, 237.
Schirmer, O. F., and E. Salje, 1980, J. Phys. C **13**, L1067.
Schlenker, C., 1985, in *Physics of Disordered Materials,* edited by D. Adler, H. Fritzsche, and S. Ovshinsky (Plenum, New York), p. 369.

Schlenker, C., S. Ahmed, and M. Gourmula, 1979, J. Phys. C **12**, 3503.
Schlenker, C., and M. Marezio, 1980, Philos. Mag. **42**, 453.
Schlesinger, Z., R. T. Collins, D. L. Kaiser, and F. Holtzberg, 1987, Phys. Rev. Lett. **59**, 1958.
Schmitt-Rink, S., C. M. Varma, and A. E. Ruckenstein, 1988, Phys. Rev. Lett. **60**, 2793.
Schmitt-Rink, S., C. M. Varma, and A. E. Ruckenstein, 1989, Phys. Rev. Lett. **63**, 445.
Schneider, T., and A. Politi, 1987, J. Appl. Phys. **61**, 3959.
Schrieffer, J. R., and P. A. Wolff, 1966, Phys. Rev. **149**, 491.
Schrieffer, J. R., X.-G. Wen, and S.-C. Zhang, 1988, Phys. Rev. Lett. **60**, 944.
Schüttler, H.-B., and A. J. Fedro, 1988, Phys. Rev. B **38**, 9063.
Schüttler, H.-B., M. Jarrell, and D. J. Scalapino, 1987, Phys. Rev. Lett. **58**, 1147.
Schüttler, H.-B., M. Jarrell, and D. J. Scalapino, 1989, Phys. Rev. B **39**, 6501.
Scott, J., J. L. Bredas, J. H. Kaufman, P. Pfluger, G. B. Street, and K. Yakushi, 1983, Mol. Cryst. Liq. Cryst. **118**, 163.
Shafer, M. W., T. Penney, and B. L. Olsen, 1987, Phys. Rev. B **36**, 4047.
Shiba, H., 1972, Prog. Theor. Phys. **48**, 2171.
Shirane, G., Y. Endoh, R. J. Birgenau, M. A. Kastner, Y. Hidaka, M. Oda, M. Suzuki, and T. Murakami, 1987, Phys. Rev. Lett. **59**, 1613.
Shraiman, B. I., and E. D. Siggia, 1988, Phys. Rev. Lett. **60**, 740
Šimanek, E., 1979, Solid State Commun. **32**, 731.
Sleight, A. W., 1988, Lecture given at Les Houches Workshop, "Superconductivity: New Models, New Applications," March, 1988, unpublished.
Sleight, A., 1989, Proceedings of the Robert Welch Foundation, Conferences on Chemical Research XXXII, in press.
Sleight, A. W., J. L. Gillson, and P. E. Bierstedt, 1975, Solid State Commun. **17**, 27.
Sobyanin, A. A., 1988, Physica C **15-155**, 1203.
Stechel, E. B., and D. R. Jennison, 1988, Phys. Rev. B **38**, 4632.
Steiner, P., V. Kinsinger, I. Sander, B. Siegwant, S. Hufner, and C. Politis, 1987, Z. Phys. B **67**, 19.
Steiner, P., *et al.*, 1988, Z. Phys. B **69**, 449.
Sugai, S., 1989, Solid State Commun., in press.
Sugai, S., Y. Enomoto, and T. Murakami, 1989, Solid State Commun., in press.
Suzumura, Y., Y. Hasegawa, and H. Fukuyama, 1988a, J. Phys. Soc. Jpn. **57**, 401.
Suzumura, Y., Y. Hasegawa, and H. Fukuyama, 1988b, J. Phys. Soc. Jpn. **57**, 2768.
Tajima, S., S. Uchida, A. Masaki, H. Takagi, K. Kitazawa, S. Tanaka, and A. Katsui, 1985, Phys. Rev. B **32**, 6305.
Tajima, S., S. Uchida, A. Masaki, H. Takagi, S. Tanaka, and S. Sugai, 1987, Phys. Rev. B **35**, 696.
Takahashi, M., 1969, Prog. Theor. Phys. **42**, 1098.
Taliani, C., R. Zamboni, G. Ruani, F. C. Matacotta, and K. I. Pokhodnya, 1988, Solid State Commun. **66**, 487.
Thanh, T. D., A. Koma, and S. Tanaka, 1980, Appl. Phys. **22**, 205.
Thouless, D. J., 1960, Ann. Phys. (N.Y.) **10**, 553.
Ting, C. S., K. L. Nagai, and C. T. White, 1980, Phys. Rev. B **22**, 2318.
Torrance, J. B., Y. Tokura, A. I. Nazzal, A. Bezinge, T. C. Huang, and S. S. P. Parkin, 1988, Phys. Rev. Lett. **61**, 1127.
Tournier, R., A. Sulpice, P. Lejay, O. Laborde, and J. Beille, 1988, J. Magn. Magn. Mater. **76-77**, 552.
Tozer, S. W., A. W. Kleinsasser, T. Penney, D. Kaiser, and F. Holtzberg, 1987, Phys. Rev. Lett. **59**, 1768.
Tranquada, J. M., S. M. Heald, and A. R. Moodenbaugh, 1987, Phys. Rev. B **36**, 5263.
Tranquada, J. M., *et al.*, 1988, Phys. Rev. Lett. **60**, 156.
Tricker, M. J., I. Adams, and J. M. Thomas, 1972, Inorg. Nucl. Chem. Lett. **8**, 633.
Uchida, S., K. Kitazawa, and S. Tanaka, 1987, Phase Transitions **8**, 95.
Uchida, S., S. Tajima, A. Masaki, S. Sugai, K. Kitazawa, and S. Tanaka, 1985, J. Phys. Soc. Jpn. **54**, 4395.
Uchida, S., H. Takagi, S. Tanaka, K. Nakano, N. Miura, K. Kishio, K. Kitazawa, and K. Fueki, 1987, Jpn. J. Appl. Phys. **26**, L196.
Uemura, Y. J., W. J. Kossler, X.H. Yu, J. R. Kempton, H. E. Schone, D. Opie, C. E. Stronach, D. C. Johnston, M. S. Alvarez, and D. P. Goshorn, 1987, Phys. Rev. Lett. **59**, 1045.
Uemura, Y. J., *et al.*, 1988, Phys. Rev. B **38**, 909.
Uemura, Y. J., *et al.*, 1989, Phys. Rev. Lett. **62**, 2317.
Vaknin, D., S. K. Sinha, D. E. Moncton, D. C. Johnston, J. M. Newsam, C. R. Safinya, and H. E. King, Jr., 1987, Phys. Rev. Lett. **58**, 2802.
Varma, C. M., 1988a, in *High-T_c Superconductors,* Proceedings of an International Discussion Meeting, Schloss Mauterndorf, Austria, edited by H. W. Weber (Plenum, New York).
Varma, C. M., 1988b, Phys. Rev. Lett. **61**, 2713.
Varma, C. M., S. Schmitt-Rink, and E. Abrahams, 1987a, in *Novel Superconductivity,* edited by S. A. Wolf and V. Z. Kresin (Plenum, New York), p. 355.
Varma, C. M., S. Schmitt-Rink, and E. Abrahams, 1987b, Solid State Commun. **62**, 681.
Vidal, F., J. A. Veira, J. Maza, F. García-Alvarado, E. Morán, and M. A. Alario, 1988, J. Phys. C **21**, L599.
Voronel, A. V., O. Linsky, A. Kislink, and S. Drislikh, 1988, Physica C **153**, 1068.
Warren, W. W., Jr., R. E. Walstedt, G. F. Brennert, G. P. Espinoza, and J. P. Remeika, 1987, Phys. Rev. Lett. **60**, 1860.
Warren, W. W., Jr., R. E. Walstedt, G. F. Brennert, R. J. Cava, R. Tycko, R. F. Bell, and G. Dabbagh, 1989, Phys. Rev. Lett. **62**, 1193.
Watkins, G. D., 1984, in *Festkörperprobleme, (Advances in Solid State Physics),* Vol. 24, edited by H. J. Queisser (Pergamon/Vieweg, Braunschweig), p. 163.
Weber, W., 1988a, in *Festkörperprobleme (Advances in Solid State Physics),* Vol. 28, edited by U. Rössler (Vieweg, Braunschweig), p. 141.
Weber, W., 1988b, quoted in Varma (1988b), p. 2716.
Weber, W., and L. F. Mattheiss, 1987, Physica B **148**, 271.
Weber, W., and L. F. Mattheiss, 1988, Phys. Rev. B **37**, 599.
Weichmann, P. B., and M. E. Fisher, 1986, Phys. Rev. B **34**, 7652.
Weichmann, P. B., M. Rasolt, M. E. Fisher, and M. J. Stephen, 1986, Phys. Rev. B **33**, 4632.
Welp, U., W. K. Kwok, G. W. Crabtree, H. Claus, K. G. Vandervoort, B. Dąbrowski, A. W. Mitchell, D. R. Richards, D. T. Marx, and D. G. Hinks, 1988, Physica C **156**, 27.
Welp, U., W. K. Kwok, G. W. Crabtree, K. G. Vandervoort, and J. Z. Liu, 1989, Phys. Rev. Lett. **62**, 1908.
Wen, X. G., and R. Kan, 1988, Phys. Rev. B **37**, 595.
Wheatley, J. M., T. C. Hsu, and P. W. Anderson, 1988, Phys. Rev. B **37**, 5897.
White, C. T., and E. N. Economou, 1978, Phys. Rev. B **18**, 3959.
White, S. R., D. J. Scalapino, N. E. Bickers, and R. T. Scalettar, 1989, Phys. Rev. B **39**, 839.
Whitlock, R. T., and P. R. Zilsel, 1963, Phys. Rev. **131**, 2409.

Wilson, J. A., 1987, J. Phys. C **20**, L911.
Wilson, J. A., 1988, J. Phys. C **21**, 2067.
Worthington, T. K. W. J. Gallagher, and T. R. Dinger, 1987, Phys. Rev. Lett. **59**, 1160.
Wu, M. K., J. R. Ashburn, C. J. Tong, P. H. Hor, R. L. Meng, L. Gao, E. J. Huang, Y. Q. Wang, and C. W. Chu, 1987, Phys. Rev. Lett. **58**, 908.
Xing, D. Y., M. Liu, and C. S. Ting, 1988, Phys. Rev. B **37**, 9769.
Yamashita, J., and T. Kurosawa, 1958, J. Phys. Chem. Solids **5**, 34.
Yu, C. C., and P. W. Anderson, 1984, Phys. Rev. B **29**, 6165.
Yu, J., S. Massida, A. J. Freeman, and D. D. Koeling, 1987, Phys. Lett. A **122**, 203.
Yu, R. C., M. J. Naughton, X. Yan, P.M. Chaikin, F. Holtzberg, R. L. Greene, J. Stuart, and P. Davies, 1988, Phys. Rev. B **37**, 7963.
Zaanen, J., and A. M. Oleś, 1988, Phys. Rev. B **37**, 9423.
Zhang, F. C., 1989, Phys. Rev. B **39**, 7375.
Zhang, F. C., and T. M. Rice, 1988, Phys. Rev. B **37**, 3759.
Zhang, F. C., and T. M. Rice, 1989, "On the validity of the *t-J* model," preprint, ETH, Zürich.
Zheng, H., 1988, Phys. Rev. B **38**, 11865.